SYNTHESIS OF LOW MOLECULAR WEIGHT OLEFINS OVER COPRECIPITATED IRON-MANGANESE CATALYSTS. VOLUME 8. FINAL REPORT

UTAH UNIV., SALT LAKE CITY. DEPT. OF FUELS ENGIEERING

15 JUN 1985

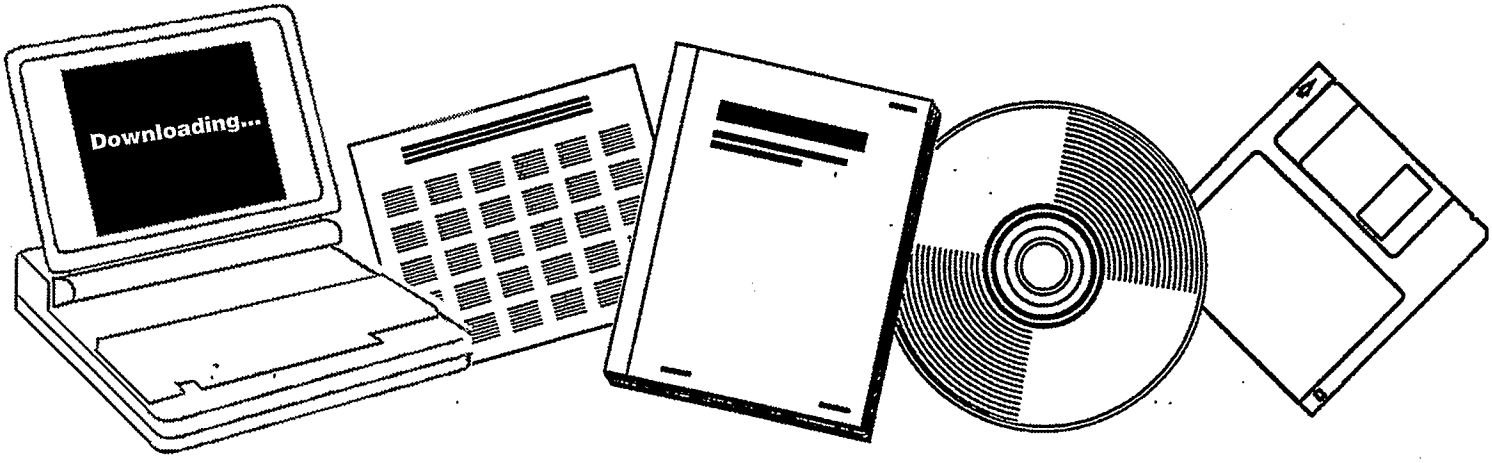

DE85014173

DOE/ET/14700-T1(Vol.8)
(DE85014173)
Distribution Category UC-90d

CHEMISTRY AND CATALYSIS OF COAL LIQUEFACTION: CATALYTIC AND THERMAL UPGRADING OF COAL LIQUIDS: AND HYDROGENATION OF CO TO PRODUCE FUELS

FINAL REPORT

DOE Contract No. DE-AC22-79ET14700

Wendell H. Wiser, Principal Investigator

Volume VIII

Investigator: Francis V. Hanson
Alex G. Oblad

Department of Fuels Engineering
University of Utah
Salt Lake City, Utah 84112

June 15, 1985

CONTENTS

ABSTRACT

The synthesis of low molecular weight olefins ($C_2 - C_4$) from hydrogen and carbon monoxide has been investigated over unsupported iron-manganese catalysts. Nine iron-manganese catalysts with different atomic ratios were prepared by coprecipitation of Mn/Fe iron and manganese nitrates. Atomic absorption (AA) spectroscopy was used to determine the catalyst compositions. The catalyst preparation procedure which involved the addition of concentrated ammonium hydroxide to a homogeneous mixture of iron and manganese nitrates produced catalysts with reproducible atomic Mn/Fe ratios.

The major bulk phase of the calcined iron-manganese catalysts was hematite ($\alpha - Fe_2O_3$). No manganese oxide was observed due to the low concentration of manganese in the catalysts. The average particle size of hematite in the catalysts decreased as the atomic ratio of Mn/Fe increased. In addition, the range of the crystallite size of the α-Fe_2O_3 for these catalysts with Mn/Fe atomic ratios ranging from 0 to 11.8/100 was 15 - 24 nm.

The catalysts were evaluated in a conventional bench-scale fixed bed reactor system. A period of 12 hours was generally required to stabilize the activity and selectivity of the iron-manganese catalysts at the operating conditions investigated: 473 - 483 K temperature, 1465 kPa pressure, 2/1:H_2/CO ratio, and 1.08 $cm^3 g^{-1} s^{-1}$ reactant gas space velocity. No evidence of catalyst

deactivation was detected during the deactivation experiments up to forty hours on stream.

A catalyst reduction study with these iron-manganese catalysts was carried out in a thermogravimetric analysis (TGA) system. A reduction in flowing hydrogen at 673 K and at the ambient pressure for 8 hours was found to be sufficient to activate the catalyst for the carbon monoxide hydrogenation reaction. The tests for the effects of the catalyst bed dilution on the catalyst activity and the product selectivity were also conducted in the fixed-bed reactor by using inert Denstone 57 as the diluent material. The experimental results indicated that a volumetric dilution ratio of Denstone 57/catalyst of 4/1 was effective in decreasing the heat effect in the catalyst bed and modifying the $C_2 - C_4$ olefin production for the catalyst in the CO hydrogenation. The experiments on the influence of the catalyst pretreatment on the catalyst activity and selectivity were carried out in the same reactor with flowing hydrogen, carbon monoxide, and synthesis gas (H_2/CO ratios of 1, 2, and 3) at 673 K for 8 hours. The data indicated that the hydrogen pretreatment resulted in a relatively more stable pattern of catalyst activity, higher selectivity for $C_2 - C_4$ hydrocarbons with olefin content (i.e., 70 mole percent) and lower total production of carbon dioxide and methane.

The experimental results of the carbon monoxide hydrogenation at the standard catalyst evaluation conditions (i.e., 2/1:H_2/CO, 1465 kPa, 1.0 $cm^3 g^{-1} s^{-1}$ and 483 - 504 K) over a series of iron-manganese catalysts indicated that the catalyst activity generally

decreased as the manganese concentration of the catalyst increased; however, the $C_2 - C_4$ olefin selectivity was significantly enhanced in the presence of a small amount of manganese in the catalyst (i.e., 2.5 Mn/100 Fe). The data on selective chemisorption of hydrogen and carbon monoxide at 292 K for these iron-manganese catalysts indicated that the CO uptake for the catalyst was much higher than the H_2 uptake. In addition, the increase in the manganese concentration of the catalyst generally resulted in lower hydrogen uptake and higher carbon monoxide to hydrogen atom ratio for these iron-manganese catalysts. The ensemble effect and the electronic influence of manganese oxide on iron were proposed to explain the variations in the catalyst activity and selectivity.

The Synthesis of Low Molecular Weight Olefins over Coprecipitated Iron-Manganese Catalysts

Francis V. Hanson
Alex G. Oblad

Introduction

The catalytic hydrogenation of carbon monoxide for the production of liquid hydrocarbons and oxygenated organic chemicals has been extensively investigated since the pioneering work of Fischer and Tropsch.[1] Storch, et al.[2] and Anderson[3] have published extensive reviews of the early work. The Fischer-Tropscy synthesis provided a significant portion of the essential liquid motor fuels, gasoline, and diesel fuel required by the German war machine during the Second World War. The primary commercial catalysts used in the German refineries were iron and cobalt. After the war a number of domestic research laboratories initiated research projects on the Fischer-Tropsch synthesis processes. The increasing availability of inexpensive petroleum crude in the early 1950s dissipated interest in the Fischer-Tropsch synthesis due to its lack of economic viability for the production of liquid fuels and chemicals from coal resources. At present, the only commercial application of Fischer-Tropsch synthesis technology is the Sasol plant in the Republic of South Africa.[4,5]

The 1973 OPEC oil embargo, the subsequent escalating costs of crude petroleum, and the uncertainty of stable foreign petroleum supplies brought about a renewal of interest in developing alternative fossil energy resources. This renewed interest embraced research and development activities aimed at producing the

technology required for the utilization of oil shale, tar sands, and coal.

Coal utilization studies included combustion, liquefaction, and gasification. The gasification of coal in the presence of steam and oxygen produces a process gas stream containing high concentrations of water, carbon dioxide, carbon monoxide, and hydrogen. The hydrogen to carbon monoixide ratio of this stream can be adjusted by the water-gas shift reaction to provide a suitable feedstock for Fischer-Tropsch synthesis reactions to produce liquid motor fuels and/or chemical feedstocks.[3] Thus the Fischer-Tropsch synthesis provides an effective processing scheme for the utilization of coal as an alternative to petroleum.

Low molecular weight olefins, such as ethylene, propylene, and butylene, are some of the basic feedstocks for the petrochemical industry.[6] These feedstocks are primarily produced from petroleum sources; therefore the production of these olefins from coal via the Fischer-Tropsch synthesis route would significantly impact the demand for imported petroleum crude and would improve the availability of domestic crude oil for conversion into liquid motor fuels. Several recent investigations have focused on the hydrogenation of carbon monoxide to produce low molecular weight olefins.[7-14] Manganese promoted iron catalysts have been shown to be highly selective for the production of low molecular weight olefins[10,11,15-22] and numerous investigations have reported on the iron-manganese catalyst system.[23-29]

The objectives of this investigation were to determine the influence of catalyst preparation, catalyst pretreatment/activation,

and process operating variables on the activity and selectivity of the catalyst for the production of low molecular weight olefins and to attempt to define the role of manganese in promoting the synthesis of low molecular weight olefins. Hydrogen and carbon monoxide chemisorption isotherms were used to correlate catalyst activity and selectivity.

EXPERIMENTAL

Preparation of Iron-Manganese Catalysts

The unsupported iron-manganese catalysts used in the investigation of the hydrogenation of carbon monoxide to produce low molecular weight olefins ($C_2 - C_4$) were prepared by the coprecipitation technique. Two series of catalysts were prepared to study the effects of the preparation on the catalyst activity and the product distribution.

Individual quantities of $Fe(NO_3)_3 \cdot 9\,H_2O$ and $Mn(NO_3)_2$ solution were measured out in the appropriate proportions to give the desired Fe/Mn atomic ratio in the final catalyst. The iron salt was dissolved in one liter of distilled water. The manganese nitrate solution was then added to the aqueous iron nitrate solution to form a homogeneous mixture. The precipitated catalyst was formed by adding the mixture slowly to one liter of ammonium hydroxide at 353 K. The solution was continuously stirred during the precipitation and the pH value was maintained above 9 to insure the complete precipitation of the metals. The chemicals used were $Fe(NO_3)_3 \cdot 9\,H_2O$, $Mn(NO_3)_2$ solution (fifty volume percent), and concentrated ammonium hydroxide (all purchased from J. T. Baker Chemicals Corporation).

After precipitation the catalyst was recovered by filtration. The wet cake was washed with hot distilled water at 363 K and filtered again. The wet cake was repeatedly washed until no trace of

nitrate ions was found in the filtrate. The nitrate ion test procedures were reported by Sorum, et al.[41] The wet cake obtained in the final filtration was oven dried in air at 393 K for 16 hours. The dried catalyst was then crushed to 24 - 32 mesh size before loading into the reactor.

Generally the YST series of Fe-Mn catalysts was prepared according to the procedure outlined above. Catalyst YST-1 (pure iron) was obtained starting from only iron nitrate. An atomic ratio of Mn/Fe of 3.0/100 was used to prepare catalysts YST-2 through YST-4. However for catalyst YST-3 the iron nitrate solution was added to the ammonium hydroxide solution first and the manganese nitrate solution was then added during the precipitation. The precipitation procedures for catalyst YST-4 were just the reverse of those for catalyst YST-3. The FT series of catalysts were prepared by slowly adding the ammonium hydroxide solution to the solution of iron nitrate and manganese nitrate at 353 K to precipitate the catalyst. The addition of ammonium hydroxide was stopped when the pH value was above 9. The procedures employed for the filtration, washing, and drying steps were the same for all of the catalysts.

The actual compositions of the iron-manganese catalysts were determined by using atomic absorption (AA) spectroscopy. An Instrumentation Laboratory Model 351 AA Spectrophotometer was employed for the analysis. The atomic absorption analysis included (1) the instrument calibration with standard solutions; (2) the determination of absorption data for the catalyst samples; and (3) the interpretation of the experimental data to obtain the catalyst compositions. A detailed description of the operating procedures for

the instrumentation was reported by Tai.[19]

Apparatus and Procedures

Fixed-bed Reactor System

A high pressure reactor system was used for the investigation of the hydrogenation of carbon monoxide over iron-manganese catalysts. The system was designed to operate at pressures up to 6.9 MPa and reaction temperatures up to 973 K. A schematic of the bench-scale fixed-bed reactor system is presented in Figure 1.

The high pressure regulators (E) were used to adjust the upstream reactant gas pressures. All of the reactant gases were passed through a Hoke 6 HD-500 sampling cylinder (G) filled with 6 - 8 mesh activated charcoal pellets to remove metal carbonyl contaminants. The activated charcoal was regenerated periodically in flowing hydrogen at ambient pressure and 423 K for 4 hours. Reactant gases for the catalyst pretreatment were further passed through two Matheson purifiers (H) (Models 64-1010 and 450) to remove oxygen and water from the gas stream.

The flowrate of the synthesis gas was measured with a high pressure Hoke rotameter (K). A Union Carbide Model 4311-1 low pressure flowmeter (I) (maximum operating pressure 1.4 MPa) was used to adjust the flowrate of the reactant gas at ambient pressure for the catalyst pretreatment. All of the flowrates were also controlled with a Union Carbide Model FM 4550-12 C mass flowmeter (V) (maximum operating pressure 10.4 MPa). The mass flowmeter was calibrated at different flowrates for a variety of H_2/CO ratios and pressures. The reactor was heated by a Lindberg Model 54331 single-zone tube

Figure 1

The Fixed-bed Reactor System

A: Hydrogen Gas

B: Carbon Monoxide Gas

C: Helium Gas

D: CO/H_2 Synthesis Gas

E: Pressure Regulator

F: Shut-Off Valve

G: Activated Carbon Purifier

H: Oxygen Removal Purifier

I: Flowmeter

J: In-Line Filter

K: High Pressure Rotameter

L: Metering Valve

M: Temperature Control Device

N: Reactor and Furnace

O: Grove Loader

P: Pressure Gauge

Q: Liquid Trap

R: Cold Trap

S: Sampling Point

T: Wet Testmeter

U: Heating Tape

V: Mass Flowmeter

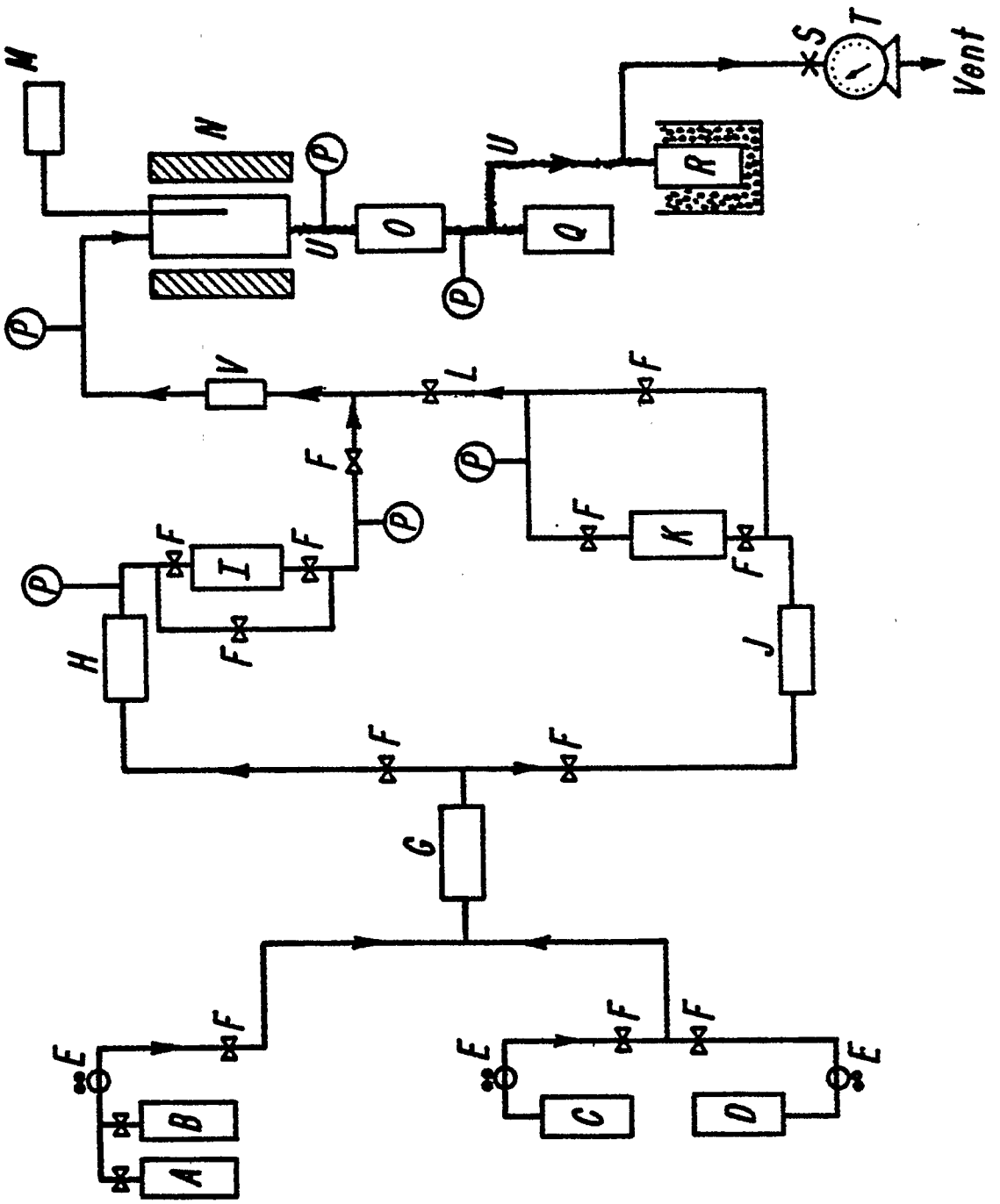
M
N
P
U
O
Q
R
S
T
Vent
V
L
F
I
K
H
J
G
E
A
B
C
D

furnace (N) with an inside diameter of 6.25 cm and a length of 30.48 cm. The maximum power of the furnace was 1600 watts and its maximum operating temperature was 1273 K. A Love Model 522 Temperature Controller (M) was used to adjust the furnace temperature. The effluent from the reactor was depressurized to ambient pressure through a Grove Loader Model S-91-W back pressure regulator (O). The product stream was passed through a liquid trap (Q) and a cold trap (R) at ambient pressure to collect the liquid products and water. Each trap was fabricated from a Whitey Model HDF4-150 sampling cylinder. Heavy duty Briskeat heating tapes (U) were wrapped around the tubing between the reactor and the cold trap to prevent the condensation of liquid product and water on the tubing wall. The flow-rate of the condensable-vapor-free gas stream was measured by a wet test meter (T). The helium gas (C) at 6.9 MPa was used to perform the leak-free test for the system. The premixed synthesis gases (D) and carbon monoxide (B) were purchased from the Linde Specialty Gas Division of the Union Carbide Corporation. Helium, hydrogen, and nitrogen that was used to supply the reference gas pressure for the Grove Loader back pressure regulator were obtained from the Stores and Receiving Department of the University of Utah.

The fixed-bed reactor assembly (an axial side view) is presented in Figure 2. The reactor was made of a 39.4 centimeter-long 316 stainless steel tube with an outside diameter of 2.54 cm and an inside diameter of 1.27 cm. A 2.54 cm-thick aluminum shield was placed around the reactor tube to maintain the even temperature distribution. The dense-packed catalyst bed was arranged approximately in the center region of the reactor. Inert Denstone 57 ceramic

Figure 2

Axial Cross Section of the Fixed-bed Reactor

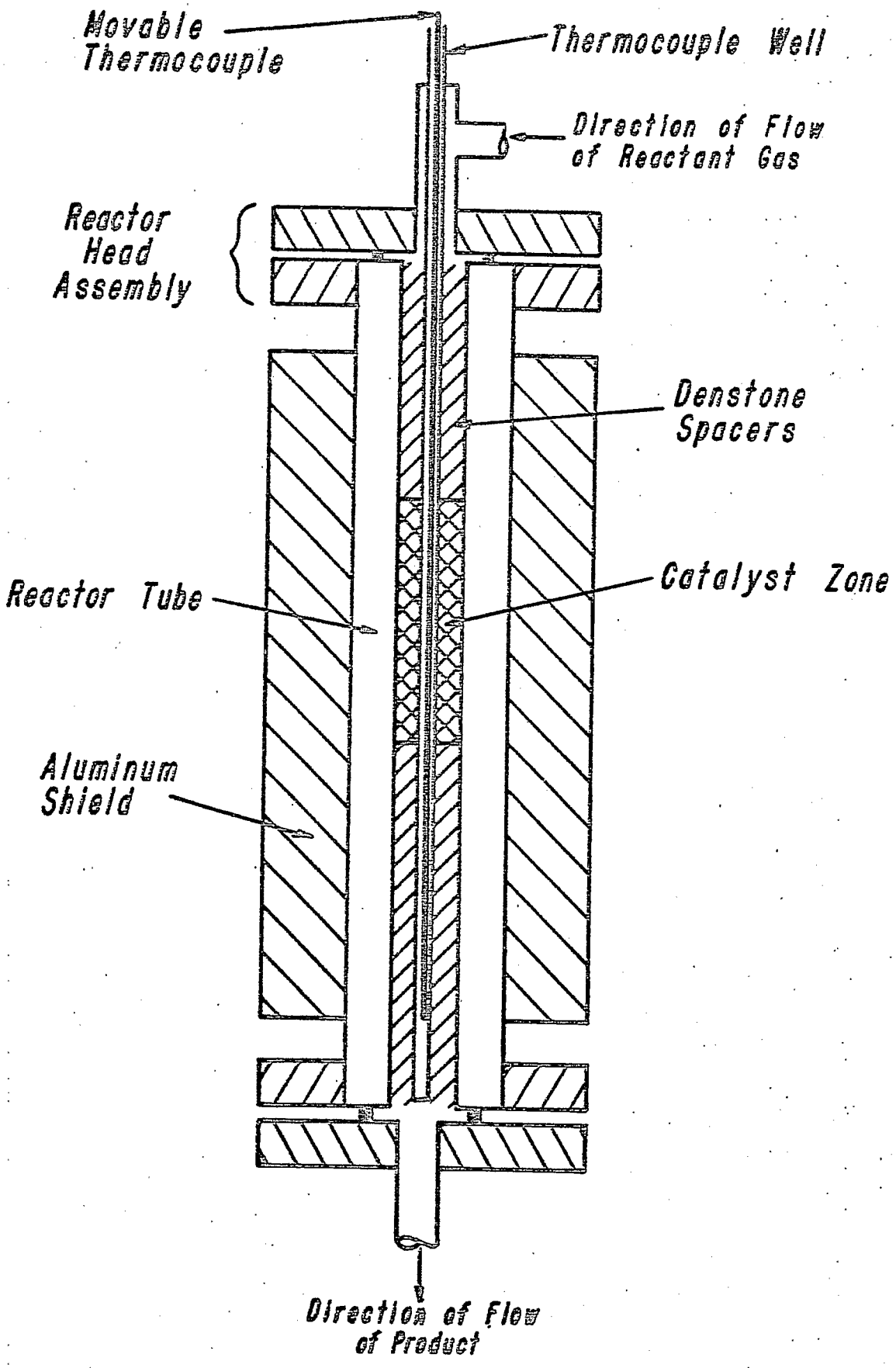
Movable Thermocouple
Thermocouple Well
Direction of Flow of Reactant Gas
Reactor Head Assembly
Denstone Spacers
Catalyst Zone
Reactor Tube
Aluminum Shield
Direction of Flow of Product

spacers with sizes larger than 24 - 32 mesh were placed above and below the catalyst zone and served as the preheater and the support material for the catalyst bed. Premixed catalyst and Denstone 57 particles of 23 - 24 mesh size were loaded into the reactor for the diluted bed experiments. The loading technique was capable of providing a well mixed bed of the two components. A 304 stainless steel tubing with an outside diameter of 0.32 cm was placed along the axis of the reactor as a thermocouple well. A movable J-type thermocouple with a length of 60.96 cm and a sheath diameter of 0.102 cm was used to measure the temperatures at different axial positions in the reactor. The reactor temperature readings were indicated by an Omega Model 199 temperature readout. A J-type thermocouple attached to the aluminum shield was also used as the control thermocouple. The inert Denstone 57 ceramic particles were purchased from Norton Chemicals Company.

The iron-manganese catalysts were activated prior to the activity and selectivity tests. In the initial stages of this investigation the catalyst was pretreated in flowing hydrogen at 773 K and ambient pressure and at a hydrogen space velocity of 0.3 $cm^3g^{-1}s^{-1}$ for 20 hours. However the in-situ hydrogen reduction at 673 K for 8 hours was later adopted and the standard reduction procedure due to the results of the catalyst reduction study. In the experiments to determine the effects of the catalyst pretreatment carbon monoxide and synthesis gases of H_2/CO of 1, 2, and 3 were also used. The pretreatment gas flow was set on the mass flowmeter after the reactor system was assembled. The system was raised to the desired pretreatment temperature (i.e., 673 K or 773 K) in about 60 minutes. After the flowrate of the pretreatment gas and the

pretreatment temperature were established the catalyst was activated for the desired period of time (i.e., 20 hours or 8 hours). After the pretreatment was completed the catalyst was cooled to the reaction temperature (e.g., 483 K) in the flowing pretreatment gas.

When the desired reaction temperature was reached the pretreatment gas flow was discontinued. The nitrogen pressure in the Grove Loader back pressure regulator was set at the value slightly lower (i.e., 68.9 kPa lower) than the desired system pressure. The reactant synthesis gas was passed through the system and the flowrate was set on the mass flowmeter. The system pressure was then slowly increased to the desired value. The temperature for the heating tapes was adjusted at 393 K. The system was allowed to stabilize for 30 minutes before the product analysis. In the event of changing the set value of process variables (i.e., flowrate, pressure, and temperature) the corresponding control devices were adjusted accordingly and the system was then stabilized for thirty minutes before the product analysis. After the catalyst evaluation was completed the pressure of the reactant gas was released slowly and the reactor was cooled to room temperature.

The analysis of gas samples from the experiment was performed by using a Hewlett-Packard 5830A Gas Chromatograph with helium as the carrier gas. Two stainless steel columns of 6.1 m x 0.3175 cm with Chromsorb 102 80/100 mesh powder were used. The flowrates of the helium gas in both columns were set at 45 $cm^3 min^{-1}$. A thermal conductivity detector (TCD) and a flame ionization detector (FID) in series were used alternately for the analysis of hydrogen, nitrogen, carbon monoxide, carbon dioxide, water (by TCD), and hydrocarbons (by

FID). A time/temperature program was developed for the analysis in this study. Appendix A lists this program with the operating conditions for the gas chromatograph.

Two conversions and selectivities were calculated with a computer program based on a carbon atom balance. A BASIC computer program "YST" was developed for this investigation. This program is currently stored in the computer system of the University of Utah Computer Center. The computer program and a typical data printout are presented in Appendix B.

The carbon monoxide conversion and the selectivities for the different products were calculated as follows; that is, (all components are on a molar basis)

$$X_o = CO + CO_2 + \sum_{i=1}^{10} iC_iH_{2i+2} + \sum_{i=1}^{10} iC_iH_{2i} + \Sigma \text{ Alcohols} \quad (6)$$

(all in the product gas)

$$Y = CO_2 + \sum_{i=1}^{10} iC_iH_{2i+2} + \sum_{i=1}^{10} iC_iH_{2i} + \Sigma \text{ Alcohols} \quad (7)$$

(all in the product gas)

$$\text{CO Conversion (input - output basis, \%)} = \frac{X_I - (X_o - Y)}{X_I} \cdot 100 \quad (8)$$

$$\text{CO Conversion (output basis, \%)} = (Y/X_o) \cdot 100 \quad (9)$$

$$\text{Carbon Atom Material Balance} = \frac{X_I - X_o}{X_I} \cdot 100 \quad (10)$$

$$CO_2\ \% = \frac{CO_2 \text{ in the product gas}}{Y} \cdot 100 \qquad (11)$$

$$CH_4\ \% = \frac{CH_4 \text{ in the product gas}}{Y} \cdot 100 \qquad (12)$$

$$C_2 - C_4\ \% = \frac{C_2 - C_4 \text{ in the product gas}}{Y} \cdot 100 \qquad (13)$$

$$C_5^+\ \% = \frac{C_5^+ \text{ in the product gas}}{Y} \cdot 100 \qquad (14)$$

$$ROH\ \% = \frac{ROH \text{ in the product gas}}{Y} \cdot 100 \qquad (15)$$

$$\frac{\text{Olefin}}{\text{Paraffin}}\ (O/P) =$$

$$\frac{C_2H_4\,\% \times 2 + C_3H_6\,\% \times 3 + (1C_4H_8\,\% + 2C_4H_8\,\%) \times 4}{C_2H_6\,\% \times 2 + C_3H_8\,\% \times 3 + (nC_4H_{10}\,\% + iC_4H_{10}\,\%) \times 4} \qquad (16)$$

In the above equations, X_I is the total amount of carbon monoxide that flowed into the system per unit time, Y is the total carbon product yield in the exit gas per unit time, and X_o is the summation of the total carbon in the products and the uncreacted carbon monoxide in the exit gas per unit time. The C_5^+ fraction is the yield of hydrocarbon products containing five carbon atoms or more in the exit gas. The olefin/paraffin ratio is O/P in the $C_2 - C_4$ hydrocarbon fraction.

The response areas of one cubic centimeter of nitrogen, carbon monoxide, carbon dioxide, and the hydrocarbon products from the reaction were calibrated with standard gases. The relative

response factors were obtained for the computer program. Pure carbon monoxide and methane were used as the calibration standards for the TCD and FID detectors, respectively. The response areas from 1 cubic centimeter CO and 1 cubic centimeter CH_4 were fed to the computer program for the calculations of all of the response areas of the products.

X-ray Diffraction Crystallography (XRD)

The X-ray diffraction technique was used to identify the major phases and to estimate the average particle size in the precipitated iron-manganese catalysts. The unreduced catalysts were calcined at 573 K in a muffle furnace for 16 hours prior to the experiments. A Phillips Norelco Electronic Instrument X-ray Diffractometer was used in the study.

The calcined catalyst was ground to a fine powder (smaller than 200 mesh) using a mortar and pestle. The finely powdered catalyst samples were placed in an aluminum sample holder. The top of the holder was smoothed with a spatula to obtain an even surface. The incident beam was CuKα X-ray radiation with a wavelength (λ) of 0.15405 nm. The diffracted X-rays were detected by an ionization chamber which could be rotated to determine the angle for constructive interference and the Bragg equation was used to determine the atomic innert layer spacing. The intensity of the diffraction X-rays were indicated on a chart recorder as the goniometer was rotated. The chart speed was synchronized with the rotation of the goniometer so that a plot of intensity versus angle could be obtained. The catalyst sample was examined from 20° to 80° (2θ) using a scan

speed of $2\theta = 2°min^{-1}$. Pure hematite (α-Fe_2O_3) was also scanned to provide as a standard for the identification of the peaks. Peak positions for the sample were compared to spectra for pure hematite and the interplanar spacings listed in the ASTM diffraction files.

X-ray line broadening was used to estimate the crystallite size of α-Fe_2O_3. This technique is applicable to the crystallites in the size range 3.0 - 50 nm. The estimation was made according to the Scherrer's equation as follows:[58]

$$B_d^2 = B_{exp}^2 - B_{Inst}^2 \qquad (17)$$

$$\bar{d}_B = k\lambda/(B_d \cos\theta) \qquad (18)$$

where

B_d is the true line width due to particle size broadening at one half maximum intensity, 1/2 I_{max} (radian),

B_{exp} is the experimental line width at 1/2 I_{max} for the sample,

B_{Inst} is the instrumental line width,

k is shape factor, equal to 0.9,

θ is diffraction angle (radian),

λ is wavelength of X-ray (nm),

$\bar{d}_B$ is the average crystallite size (nm).

B_{Inst} was obtained by measuring the line width at 1/2 I_{max} for pure hematite.

Thermogravimetric Analysis (TGA) System

A thermogravimetric analysis system was used for the catalyst reduction study to determine an optimum reduction temperature for the Fe-Mn catalysts. A flow diagram of the system is shown in Figure 3. A DuPont Model 951 TGA (E) and a DuPont Model 990 Chart Recorder (G) were used for the analysis. The hydrogen and helium gases were purified by a Matheson Model 8362 hydrogen purifier (B) and a Matheson Model 8301 Hydroxpurifier (C), respectively. All of the gases used were initially passed through a 5A molecular sieve trap for moisture removal. The helium gas was obtained from the Stores and Receiving Department of the University of Utah. The ultra high purity (99.995 % purity) hydrogen gas was purchased from the Linde Specialty Gas Division of Union Carbide Corporation. Air, nitrogen, and oxygen gases of ultra high purity (99.995 %) were obtained from Matheson Gas Company.

The catalyst weight used was generally between 25 to 45 mg. The catalyst sample was loaded into the boat of the TGA. The flow-rate of the purified reactant gas was adjusted at 50 $cm^3 min^{-1}$ with a bubble flowmeter (F). The chart paper and pens in the recorder were set up and the catalyst weight was measured according to the TGA manual. The desired temperatures for the initial state (usually 298 K) and the final state were selected and heating rate was chosen. Either the isothermal mode or the programmed mode was used depending upon the purpose of the test. The furnace was heated at the programmed rate and the weight loss of the sample was recorded on the chart. A plot of catalyst weight loss versus temperature (or time) was obtained. When purified hydrogen was used, the hydrogen

Figure 3

Thermogravimetric Analysis (TGA) System

A: Vacuum Pump

B: Hydrogen Purifier

C: Hydrox Purifier

D: Valve

E: DuPont TGA

F: Flowmeter

G: Recorder

K: Trap

M: Bubble Flowmeter

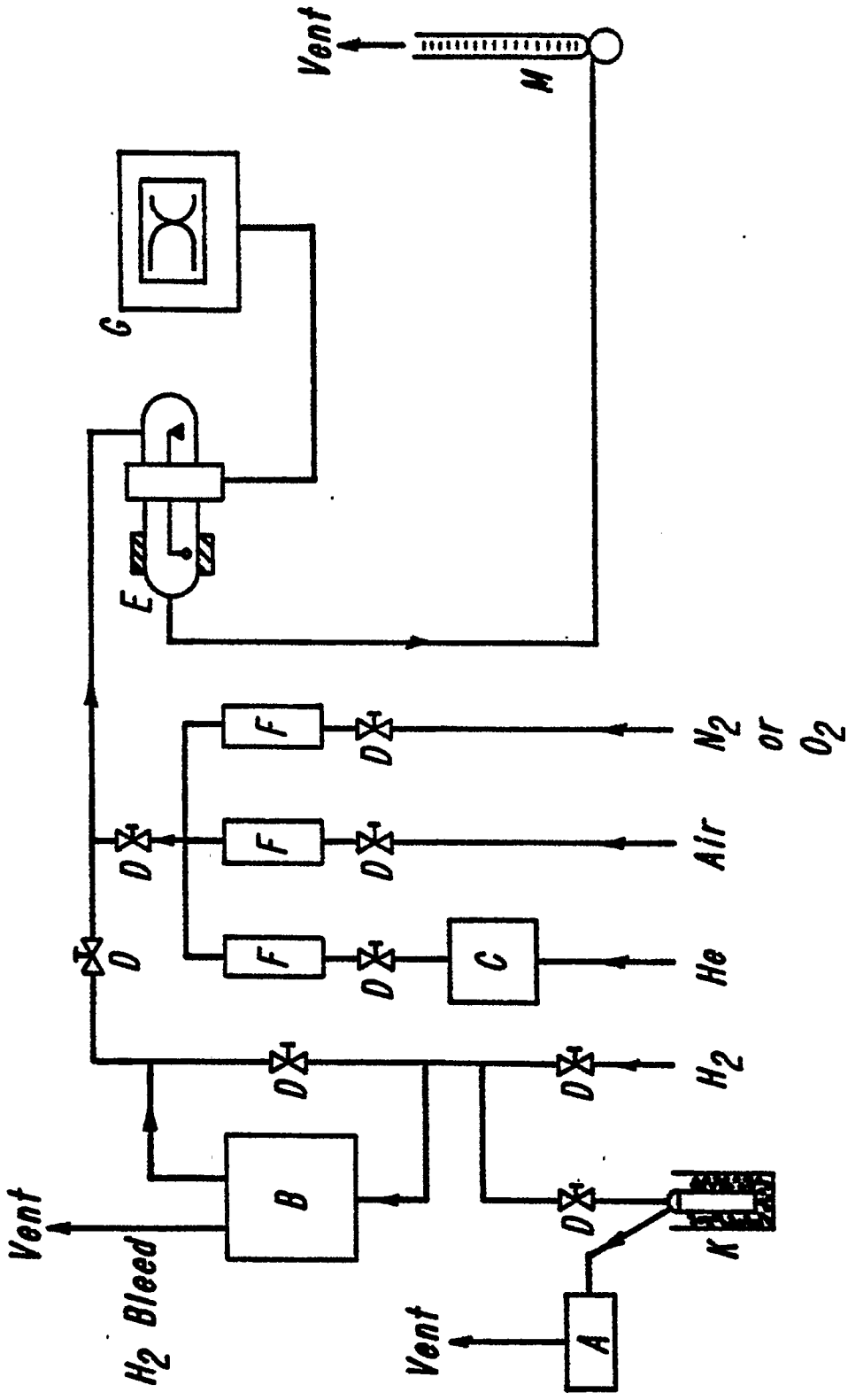
Vent
M
G
E
F
D
N_2 or O_2
Air
He
H_2
C
B
A
K
Vent
H_2 Bleed
Vent

tubing was evacuated with a mechanical vacuum pump (A) for 5 minutes to remove any residual air from the system before the Matheson hydrogen purifier was turned on.

Selective Chemisorption

A constant volume gas adsorption system was used to study the chemisorption isotherms over unsupported iron-manganese catalysts. A schematic of the adsorption system is presented in Figure 4. Two gas manifolds (C) and a vacuum manifold (D) were made of 25 mm OD Pyrex glass tubing. Six 5 liter gas storage bulbs (B) were connected to the gas manifolds by 4 mm stopcocks. Each of the vacuum manifolds was connected to the gas manifolds by a 6 mm stopcock. Two CVC Model GTC-004 thermocouple gauges (I_1, I_2) (vacuum measurement up to 10^{-3} Torr) and a CVC Model GIC-028-2 ionization gauge (G) (vacuum measurement up to 10^{-10} Torr) were connected to these different positions in the system to provide the measurements of the system pressure. A Precision Scientific Model 25 mechanical vacuum pump (L) was used for the initial stage of the system evacuation up to 10^{-2} Torr. A CVC Model PMCS-2C oil diffusion pump (K) was also used along with the mechanical pump to provide a system vacuum less than 10^{-6} Torr. A 40/50 vacuum cold trap was connected to isolate the mechanical pump for the prevention of gaseous contamination. A 50/50 vacuum cold trap was also connected between a 15 mm high vacuum stopcock (H) and the diffusion pump for the condensation of the adsorbent contamination. These two cold traps were immersed in the liquid nitrogen bath. During the experiment the system pressure measurements were read with a CVC GIC-300A ionization

Figure 4

Volumetric Gas Adsorption System

A: Texas Instruments Precision Pressure Gauge

B: 5-liter Gas Storage Bulb

C: Gas Handling Manifold

D: Vacuum Manifold

E: Adsorption Cell

F: Calibrated Bulb

G: Ionization Vacuum Gauge

H: 3-way High Vacuum Stopcock

I_1,I_2: Thermocouple Vacuum Gauge

J: Hydrogen Purifier

K: Oil Diffusion Pump

L: Mechanical Vacuum Pump

M: Bubble Flowmeter

N: Measuring Port

O: Reference Port

P: Furnace

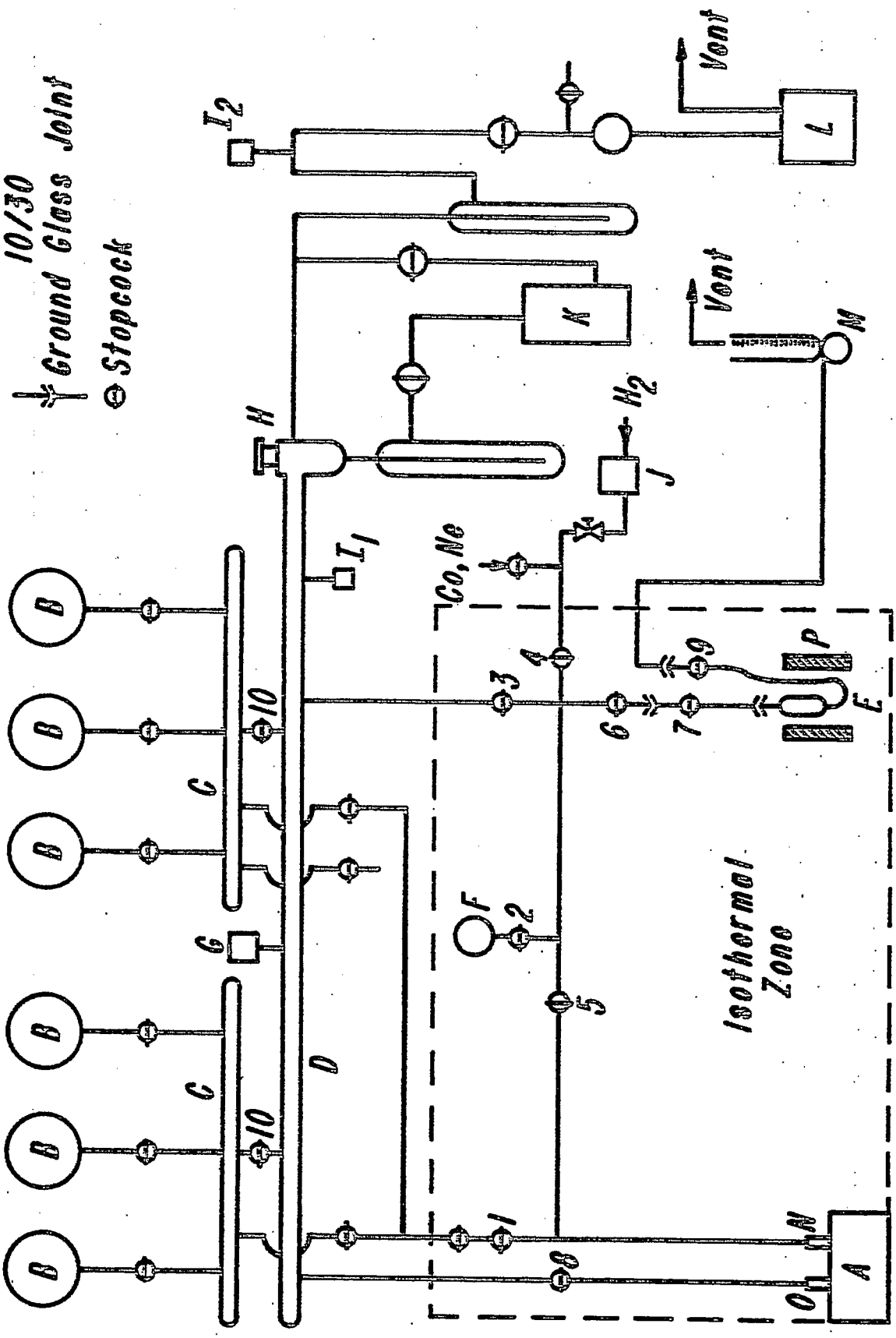
10/30
Ground Glass Joint
Stopcock
I_2
Vent
L
K
Vent
M
H
H_2
J
I_1
Co, Ne
B
C
10
G
F
2
5
D
1
8
A
N
O
3
4
6
7
9
P
E
Isothermal Zone

gauge controller. General Electric high vacuum grease was used to lubricate the stopcocks of high vacuum type in the system.

The section enclosed by dotted lines indicated in Figure 4 is the isothermal zone. This isothermal adsorption zone in the system was enclosed in a Plexiglass box to maintain a constant ambient temperature during the experiment. This box was fabricated with the screws and the front of the box could be removed easily for the operation of the system. Three sliding doors were also constructed in the front of the box so that the stopcocks in the isothermal zone were accessible for the operation. The differential pressure in the isothermal zone was measured with a Texas Instruments Model 145 precision gauge (A). The pressure sensing device was a type 5, fused quartz Bourdon capsule. The measuring side of the capsule (N) was connected to the doser volume by a graded glass seal and the reference side (O) was connected to the vacuum manifold via a stopcock. The doser section in the isothermal zone was made of Pyrex capillary tubing. A detailed diagram of the adsorption section is presented in Figure 5. The doser volume was connected to the gas manifolds and the vacuum manifold with several 4 mm stopcocks. A calibrated bulb (F) with a volume of 52.797 cm^3 was connected to the doser section with a 4 mm stopcock to calibrate the dead volume in the isothermal zone. The catalyst sample was placed in the adsorption cell (E). A furnace (P) fabricated in the laboratory was used to heat up the cell during the experiment. The heating zone of the furnace was made from two semicylindrical heating elements. The zone had an inside diameter of 3.81 cm and a length of 15.24 cm. It could provide a maximum power of 800 watts. The temperature of the furnace was

Figure 5

Doser Section of the Adsorption System

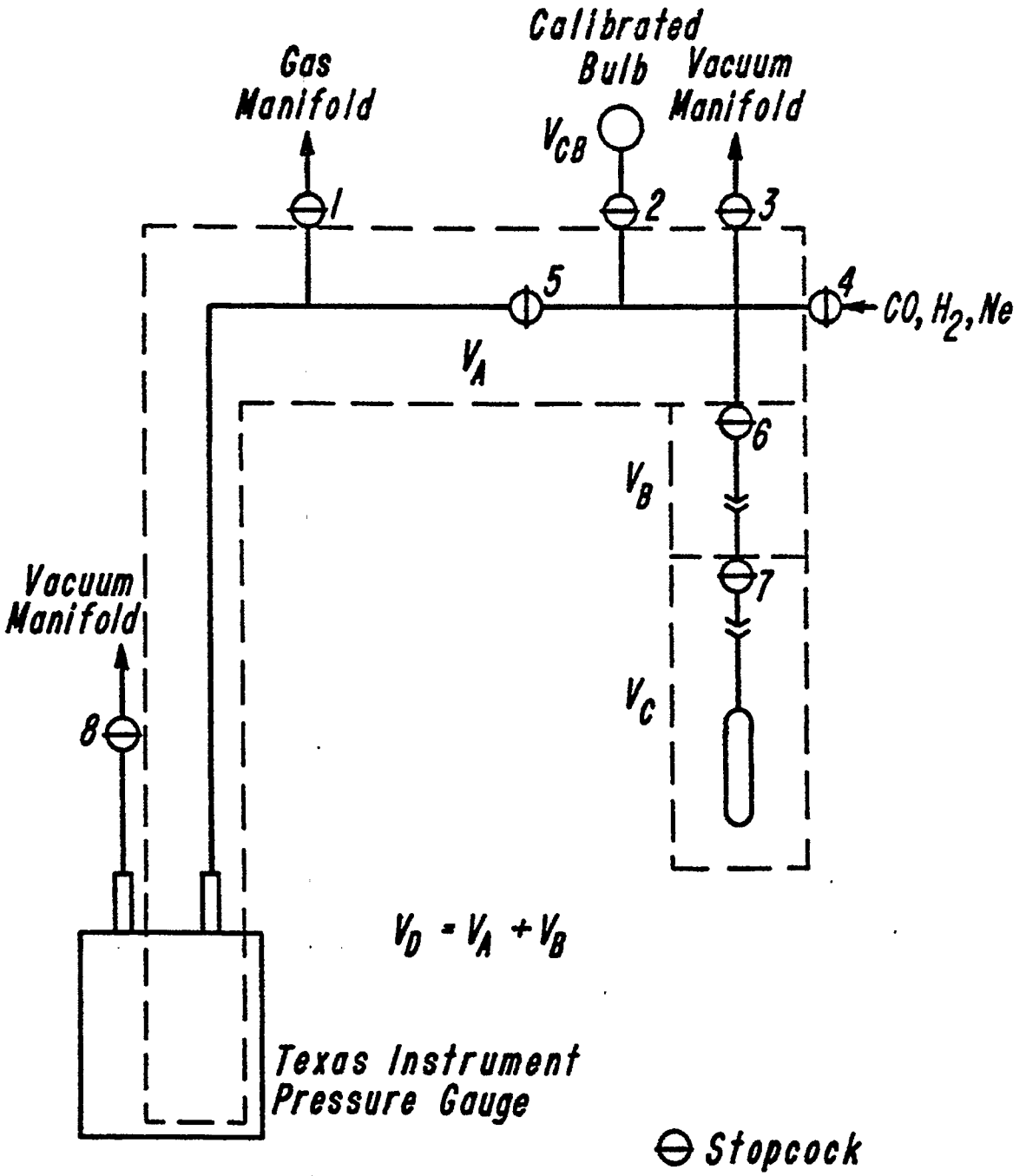
Calibrated
Bulb
Gas
Manifold
Vacuum
Manifold
V_{CB}
1
2
3
5
4
CO, H_2, Ne
V_A
6
V_B
7
Vacuum
Manifold
8
V_C
$V_D = V_A + V_B$
Texas Instrument
Pressure Gauge
Stopcock

controlled with a Love Model 522 temperature controller. The J-type thermocouples were used to measure the temperatures of the isothermal zone, the adsorption cell, and the furnace.

All of the adsorptives were introduced via stopcock (4) into the storage bulbs. Hydrogen, carbon monoxide, and neon (all ultra high purity, 99.995 %) were purchased from the Linde Specialty Gas Division of Union Carbide Corporation. Carbon monoxide and neon were stored without further purification; however, hydrogen was purified by a Matheson hydrogen purifier (J) before loading into the bulbs.

A detailed diagram of the adsorption cell is presented in Figure 6. The catalyst chamber in the cell was made of 8 mm OD Pyrex glass tubing and was 60 mm long. The inlet line was fabricated from 6 mm OD Pyrex glass tubing with a length of 170 mm and it was terminated in an inner 10/30 ground glass joint. The exhaust line was made of Pyrex capillary tubing with a 2 mm capillary tubing with a 2 mm capillary stopcock (9) and it was connected to the vent line with an inner 10/30 ground glass joint. A bubble flowmeter (M) was attached to the end of the vent line to measure the gas flowrate during the catalyst pretreatment. The cell was connected to the doser section with a 2 mm capillary stopcock (6) which had outer 10/30 ground glass joints on both ends. The joint between the cell and the stopcock (7) was sealed with Apiezon black wax and the joint between the assembled cell and the doser section was sealed with GE high vacuum grease. A similar gas adsorption system was also reported by Hanson.[42]

The following catalyst reduction procedures were used in the experiment. The unreduced catalyst (about 1.0 g) was weighed and

Figure 6

Diagram of Adsorption Cell

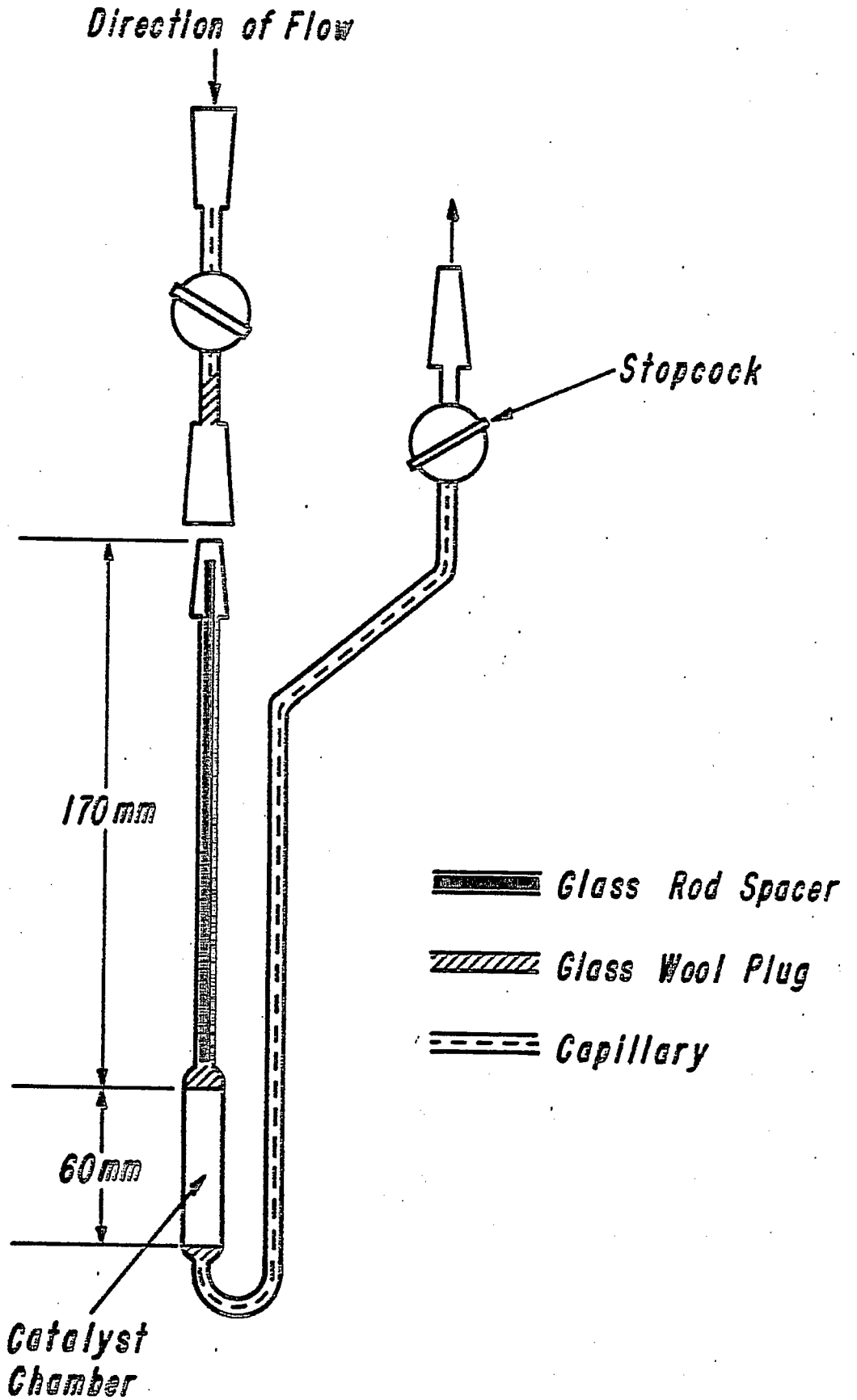
Direction of Flow
Stopcock
170 mm
60 mm
Catalyst Chamber
Glass Rod Spacer
Glass Wool Plug
Capillary

loaded into the catalyst chamber in the adsorption cell. The cell was then assembled according to the diagram in Figure 6 and connected to the doser section via the stopcock (6). The whole system was first evacuated with the mechanical pump. When the pressure indicated by the gauge (I_1) was about 30 - 40 x 10^{-3} Torr, the diffusion pump was used to evacuate the system. The whole system was evacuated for 1 hour at room temperature. The catalyst cell was then evacuated at 423 K for 2 hours. The cell was cooled to the room temperature under evacuation. Stopcocks (2), (3), and (5) were closed to isolate the cell from the system. Purified hydrogen gas flow at a pressure slightly higher than the ambient pressure (i.e., 35 kPa higher) was established via stopcocks (4), (6), (7), and (9). The gas flowrate was measured with the bubble flowmeter at the end of the vent line. The space velocity for the hydrogen reduction was generally 1.5 - 3.0 $cm^3g^{-1}s^{-1}$. When the hydrogen flowrate was established the furnace was then heated to 673 K and the catalyst sample was reduced in flowing hydrogen at 673 K for 8 hours. The catalyst cell was cooled to the room temperature in flowing hydrogen. The hydrogen flow was turned off and stopcocks (4) and (9) were closed to isolate the cell from the hydrogen flow and the vent line. Stopcocks (3) and (5) were then opened to the vacuum manifold and the catalyst cell was evacuated at 723 K for 2 hours. When the cell was cooled to the room temperature under evacuation, the furnace was removed from the isothermal zone. The isothermal zone was established by assembling the Plexiglass box and the catalyst cell was placed in a constant temperature bath. The whole system was evacuated to a pressure of less than

10^{-5} Torr.

The procedures for the adsorption isotherm included (1) the determination of the dead volume in the adsorption cell with neon, and (2) the determination of the adsorption isotherm with the adsorptives (i.e., hydrogen and carbon monoxide). The details of the calculations for each experiment of the isotherm are listed in Appendix C. It includes the doser volume calibration, the calculations of the cell volume, and the adsorption isotherm calculations.

The procedures for the determination of the dead volume are described as follows:

(a) neon gas from the storage bulb was introduced into the doser section via stopcock (1) and the gas handling manifold while stopcocks (3), (6), and (7) were closed;

(b) the pressure of neon in the doser section was adjusted at 600 - 700 Torr;

(c) stopcock (1) was closed and the ambient temperature and pressure were recorded;

(d) stopcock (6) was opened to expand neon into the connecting stopcock volume and the pressure and temperature were recorded again;

(e) stopcock (7) was opened to expand neon into the catalyst cell and the final temperature and pressure were recorded;

(f) neon was evacualted via stopcocks (3) and (7) and the system was evacuated to a pressure less than 10^{-5} Torr.

The procedures outlined above were generally repeated 3 to 6 times to determine the dead volume for each experiment of the adsorption isotherm. It usually took 300 seconds to equilibrate the

temperature and pressure for each recording; however, a longer period of time was also needed for the equilibration in some cases.

The procedures for the determination of the adsorption isotherm are described as follows:

(a) the neon gas was evacuated from the system by opening stopcocks (3) and (10);

(b) stopcocks (1), (3), (7), and (10) were closed when the system pressure was less than 10^{-5} Torr;

(c) the adsorptive gas was expanded from the storage bulb into the gas manifold;

(d) the adsorptive gas was introduced to the doser section via stopcock (1) and the glass transfer line very slowly;

(e) stopcock (1) was closed and the pressure and temperature were then recorded;

(f) stopcock (7) was opened to expand the adsorptive gas into the catalyst cell;

(g) the temperature and pressure were recorded after the equilibration in the system was completed and stopcock (7) was closed;

(h) the adsorptive gas from the gas handling manifold was introduced via stopcock (1) to increase the pressure in the doser section and the pressure and temperature were recorded;

(i) the adsorptive gas was expanded into the cell by opening stopcock (7) and the pressure and temperature were recorded. The procedures outlined above were generally repeated 5 to 6 times to complete the adsorption isotherm. For each isotherm point ninety minutes were allowed to equilibrate the adsorption system

because of the slow process of the adsorption for the coprecipitated iron-manganese catalysts. In the event that the determination of physically adsorbed CO was needed, a second isotherm was further obtained in the following manner. When the first carbon monoxide isotherm was completed, stopcock (5) was closed and the cell was evacuated for 120 seconds via stopcock (3). Stopcocks (3) and (7) were then closed and the second isotherm was determined according to the procedures outlined previously.

RESULTS

Compositions of Iron-Manganese Catalysts

Four YST series catalysts and five FT series catalysts were prepared by the coprecipitation method. The details of the preparation were described in the Experimental section. The compositions of these iron-manganese catalysts were determined by using atomic absorption spectroscopy. Table 1 lists the atomic ratios of Mn/100 Fe for these catalysts.

TABLE 1
COMPOSITION OF IRON-MANGANESE CATALYSTS

Catalyst	Atomic Ratios (Mn/100 Fe)	
	Calculated	Measured
YST-1	0	0
YST-2	3.0	3.6
YST-3	3.0	3.5
YST-4	3.0	3.5
FT-1	0	0
FT-2	2.5	2.5
FT-3	5.0	5.1
FT-4	8.1	8.2
FT-5	12.2	11.8

Catalyst YST-1 was a pure iron and the other catalysts in the YST series were prepared from solutions calculated to give an atomic ratio of Mn/Fe of 3.0/100. The actual compositions for YST-2, YST-3, and YST-4 were 3.6 Mn/100 Fe, 3.5 Mn/100 Fe, and 3.5 Mn/100 Fe, respectively. Five catalysts were prepared in the FT series with the atomic ratios of Mn/Fe ranging from 0 to 12.2/100. The actual compositions for these catalysts were all almost identical to the calculated values. The differences between the rwo ratios for catalysts FT-4 and FT-5 were very small (i.e., less than 5%).

X-Ray Diffraction Analysis of Iron-Manganese Catalysts

The identification of the major phase and the determination of the average particle size for the unreduced iron-manganese catalysts were accomplished by x-ray diffraction. Pure research grade α-Fe_2O_3 was used for the comparison spectra and tested as a standard for the line-broadening experiments. ASTM files were also used to identify the peeks and Scherrer's equation was used to calculate the average hematite particle sizes in the catalysts. The major phase, the primary peak position, and the average particle size for the calcined catalysts are presented in Table 2.

The primary peak for hematite (α-Fe_2O_3) was identified at a 2θ of 33.1° and its line width of 0.2° at the one half maximum intensity was used as the instrumental line width. The other peaks for hematite were also identified at the following values of 2θ: 35.6°, 40,8°, 49.5°, 54.1", 57.6°, 62.4°, 63.9°, and 71.8°. The data for the six catalysts tested indicated that all the peaks were identified at the same values of 2θ as those for α-Fe . No peak other

TABLE 2

X-RAY DIFFRACTION DATA FOR CALCINED IRON-MANGANESE CATALYSTS

Catalyst	Mn/100 Fe Atomic Ratio	2θ	B_{exp}	B_{inst}	$\bar{d}_B$(nm)
α-Fe_2O_3	--	33.1°	--	0.2°	--
YST-1	0	33.1°	0.40°	--	23.9
YST-2	3.6	33.1°	0.43°	--	21.8
FT-1	0	33.3°	0.40°	--	23.9
FT-2	2.5	33.3°	0.42°	--	22.4
FT-3	5.4	33.3°	0.50°	--	18.1
FT-4	8.2	33.3°	0.60°	--	14.6

than those for hematite was found in the x-ray diffraction spectra for these catalysts. These results showed that hematite was the only major phase in the bulk structure and no manganese oxide peak was identified in these calcined catalysts. The average crystallite sizes of hematites for catalysts YST-1 and FT-1 were 23.9 nm; however, those for other catalysts were in the range of 15 - 22 nm. Catalyst FT-5 was tested but the x-ray spectra did not show any peak. These data also indicated that the particle size of hematite became smaller as the manganese content in the catalyst increased.

Catalyst Stability Tests

Catalyst stability experiments were performed to determine the effects of time on stram on the catalyst activity and the product selectivity for YST series Fe-Mn catalysts. These four catalysts were

reduced in-situ in flowing hydrogen at a space velocity of 0.3 $cm^3g^{-1}s^{-1}$ at the abmient pressure and 773 K for 20 hours. The standard operating conditions used for the experiment were a pressure of 1465 kPa, a H_2/CO ratio of 2, a space velocity of 1.08 $cm^3g^{-1}s^{-1}$, and a temperature of 473 - 483 K. The reaction temperature was chosen to maintain a carbon monoxide conversion of approximately 5 - 6%. Therefore, for catalyst YST-1 the experiment was undertaken at 473 K and those for other YST catalysts were studied at 483 K. The duration of the experiment was generally 35 - 40 hours.

The effect of stream time on the activity for carbon monoxide conversion, olefin selectivity, and product distribution through 33 hours on stream are presented in Figures 7 and 8 and Table 3. The CO conversion increased gradually from 2.3 percent at 3 hours on stream to 5 percent at approximately 12 - 15 hours. The carbon monoxide conversion remained constant at 5 percent throughout the course of the run. During the test the C_2-C_4 yield was constant in the range of 42 - 45 percent and the yields for CO_2 and ROH, that is, 5 and 7 percent, respectively, were also independent of the time on stream. Methane production declined initially from 34 percent at 3 hours to 25 percent at 12 hours and remained at that level for the balance of the experiment. The C_5^+ yield increased gradually from 12 percent at 3 hours to a constant level of 18 percent after 12 hours on stream. The O/P ratio in the C_2-C_4 hydrocarbon fraction was constant at 1.30 during the run. The olefin selectivity ratios for C_2, C_3 and C_4 were also constant, that is, 0.6, 2.0, and 1.6, respectively, during the test. Generally speaking, catalyst YST-1 stabilized approximately at 12 hours on stream in terms of the

Figure 7

Catalyst Stability Test; Dense Bed Catalyst Loading;

Carbon Monoxide Conversion and Olefin Selectivity

Versus Time on Stream; Temperature = 473 K;

Space Velocity = 1.08 $cm^3g^{-1}s^{-1}$;

Pressure = 1465 kPa; H_2/CO = 2/1;

YST-1

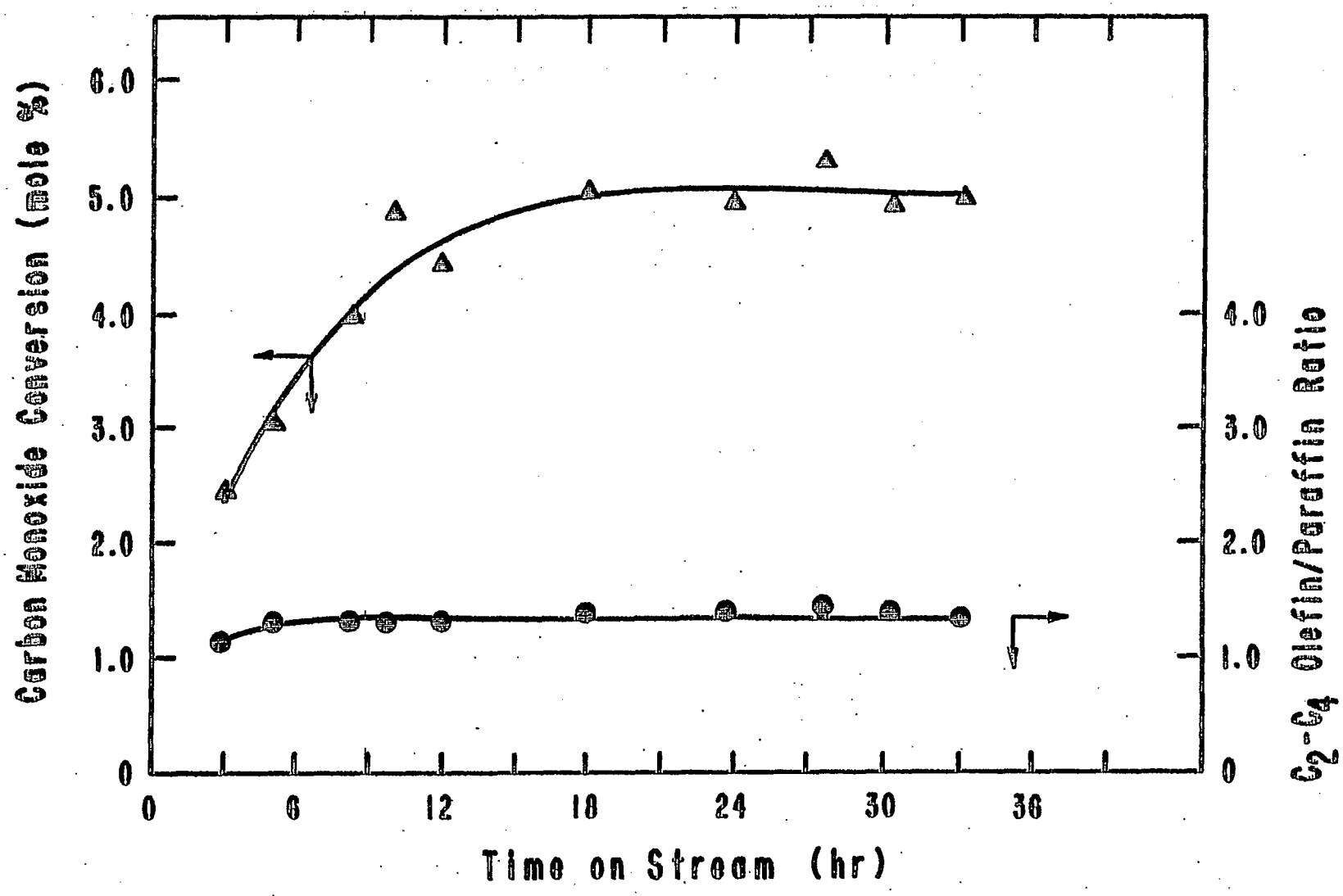
Carbon Monoxide Conversion (mole %)
6.0
5.0
4.0
3.0
2.0
1.0
0
0
6
12
18
24
30
36
Time on Stream (hr)
4.0
3.0
2.0
1.0
0
C_2-C_4 Olefin/Paraffin Ratio

Figure 8

Catalyst Stability Test; Dense Bed Catalyst Loading;

Product Distribution Versus Time on Stream;

Temperature = 473 K; Pressure = 1465 kPa;

Space Velocity = 1.08 $cm^3 g^{-1} s^{-1}$;

H_2/CO = 2/1; YST-1

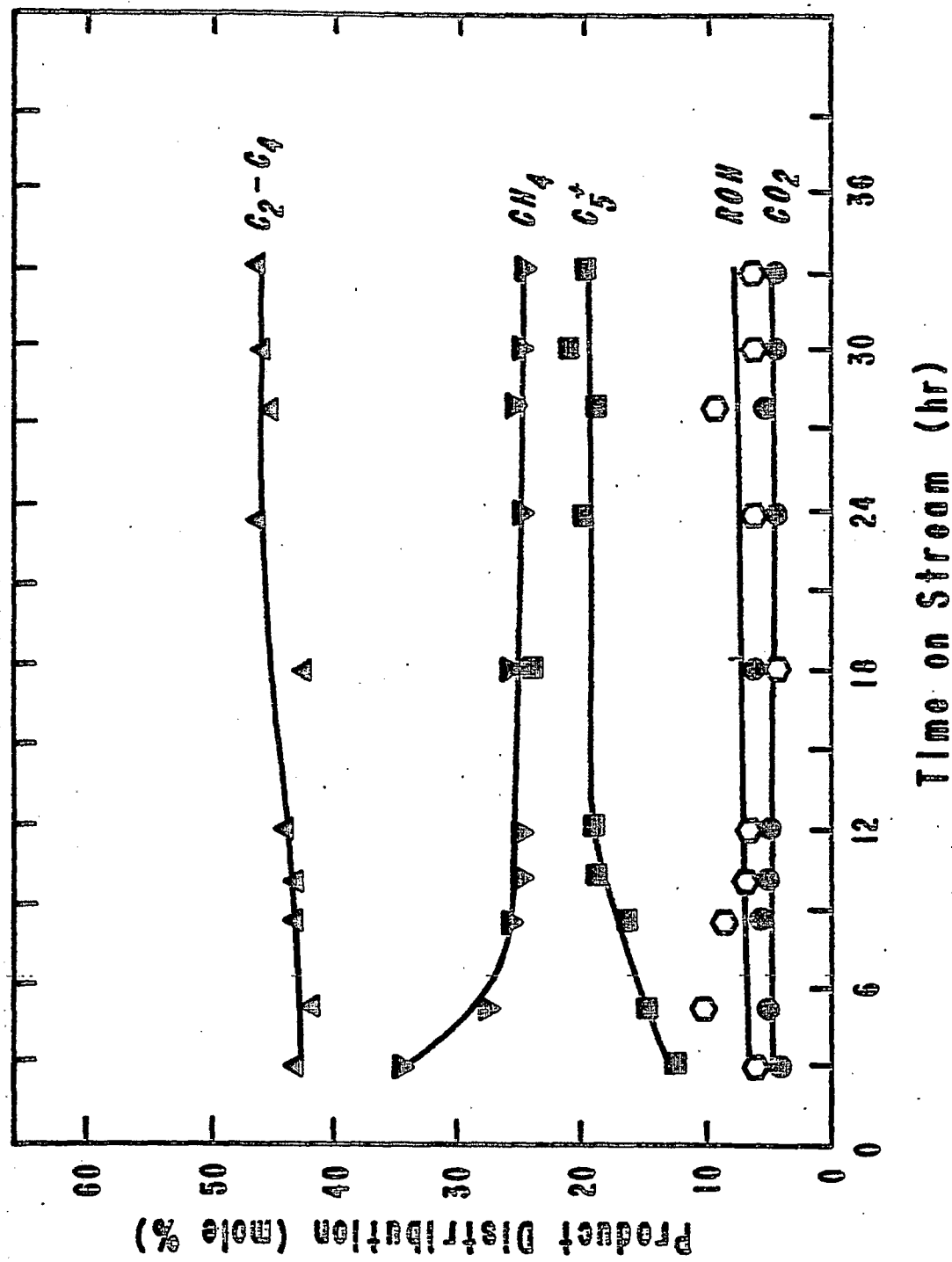
Product Distribution (mole %)
0
10
20
30
40
50
60
Time on Stream (hr)
0
6
12
18
24
30
36
C_2-C_4
CH_4
C_5^+
ROH
CO_2

TABLE 3

LOW MOLECULAR WEIGHT OLEFIN SELECTIVITY RATIO VERSUS TIME ON STREAM IN CATALYST STABILITY TEST[a]

Olefin/Paraffin Ratio	Time on Stream (hours)								
	3.0	8.5	11.5	18.0	20.0	23.5	28.0	30.0	33.0
$C_2^=/C_2$	0.6	0.6	0.6	0.7	0.6	0.6	0.5	0.6	0.5
$C_3^=/C_3$	1.9	2.0	2.0	1.9	2.0	2.0	2.0	2.0	2.0
$C_4^=/C_4$	1.3	1.6	1.6	1.8	1.7	1.7	1.6	1.6	1.6

[a]Dense Bed Catalyst Loading; Temperature = 473 K; Pressure = 1465 kPa; Space Velocity = 1.08 $cm^3g^{-1}s^{-1}$; H_2/CO = 2/1; YST-1.

activity, olefin selectivity, and product distribution. In addition, there was no sign of catalyst deactivation during the course of the experiment.

The effects of time on stream on the activity, olefin selectivity and the product distriubtion for catalyst YST-2 up to 40 hours on stream are presented in Figures 9 and 10 and Table 4. The carbon monoxide conversion increased slightly from 5.0 to 5.4 percent over the initial period up to 9 hours on stream and remained constant at 5.4 percent through 40 hours on stream. The yields of C_2-C_4, C_5^+ and CO_2 and the O/P ratio in C_2-C_4 also increased over an initial period of 9 - 10 hours and then stabilized at 50, 21, and 10 percent and 2.6, respectively, up to the end of the test. The ROH yield was relatigely small, that is, 2 percent and independent of the time on stream. The methane production declined during the initial 9 hour period and remained constant at 17 percent through the end of the run. The olefin selectivity ratios for C_2, C_3, and C_4 increased over the initial period of 9 - 10 hours and then stabilized at 1.5, 4.2, and 3.2, respectively, throughout the experiment. A period of about 10 hours was needed to stabilize the activity and the product distribution for catalyst YST-2. No indication of catalyst deactivation was observed during the test.

The stability test on stream with catalyst YST-3 was conducted for 38 hours. The effects of time on stream on carbon monoxide conversion, olefin selectivity, and product distribution are presented in Figures 11 and 12 and Table 5. The carbon monoxide conversion declined from 7.5 percent at 2 hours on stream to 5.5 percent at 15 hours. The carbon monoxide conversion stabilized at 5.3 percent up to

Figure 9

Catalyst Stability Test; Dense Bed Catalyst Loading;
Carbon Monoxide Conversion and Olefin Selectivity
Versus Time on Stream; Temperature = 483 K;
Pressure = 1465 kPa; Space Velocity =
1.08 $cm^3 g^{-1} s^{-1}$; H_2/CO = 2/1; YST-2

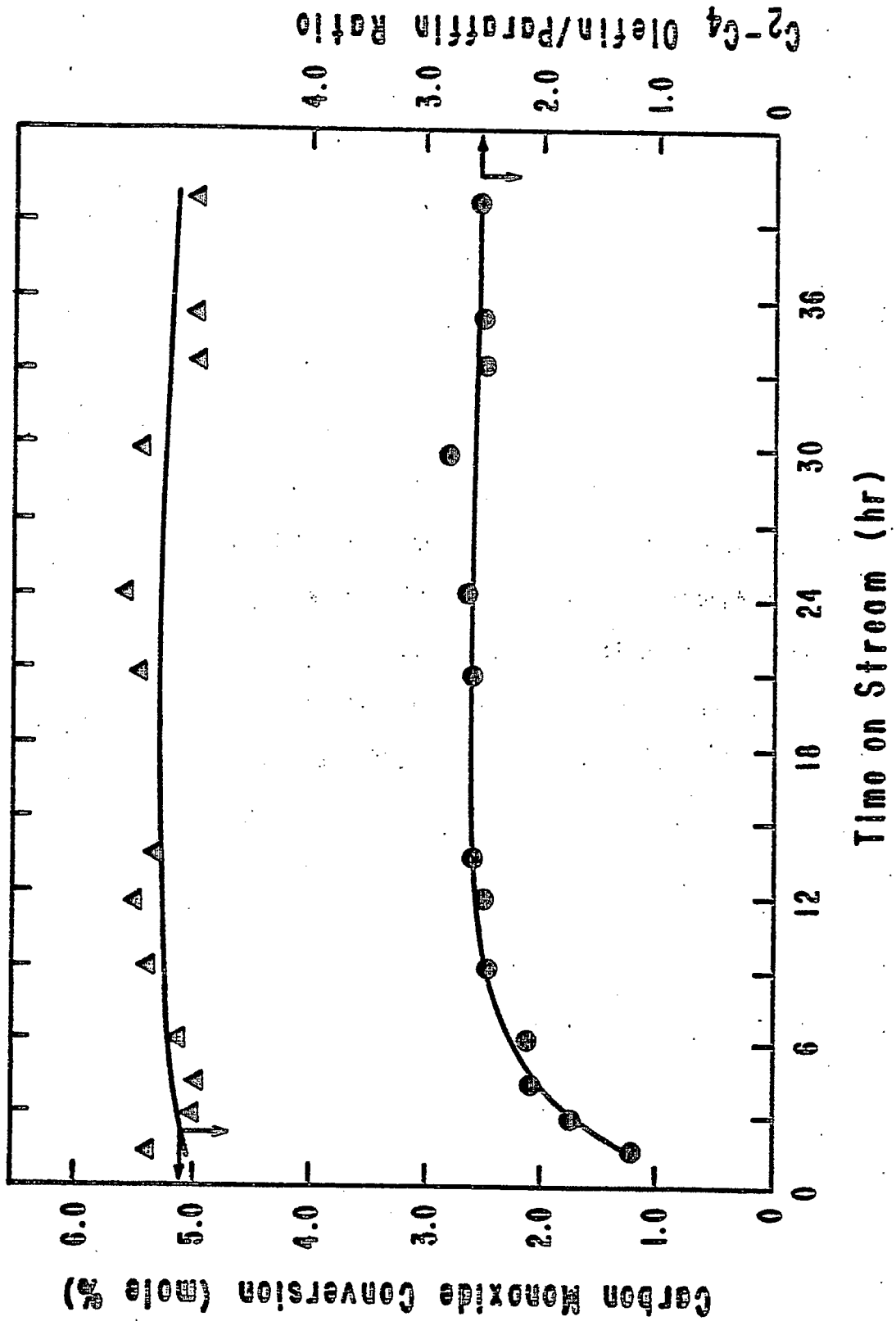
Carbon Monoxide Conversion (Mole %)
6.0
5.0
4.0
3.0
2.0
1.0
0
6
12
18
24
30
36
Time on Stream (hr)
C_2-C_4 Olefin/Paraffin Ratio
4.0
3.0
2.0
1.0
0

Figure 10

Catalyst Stability Test; Dense Bed Catalyst Loading;
Product Distribution Versus Time on Stream;
Temperature = 483 K; Pressure = 1465
kPa; Space Velocity = 1.08 $cm^3g^{-1}s^{-1}$;
H_2/CO = 2/1; YST-2

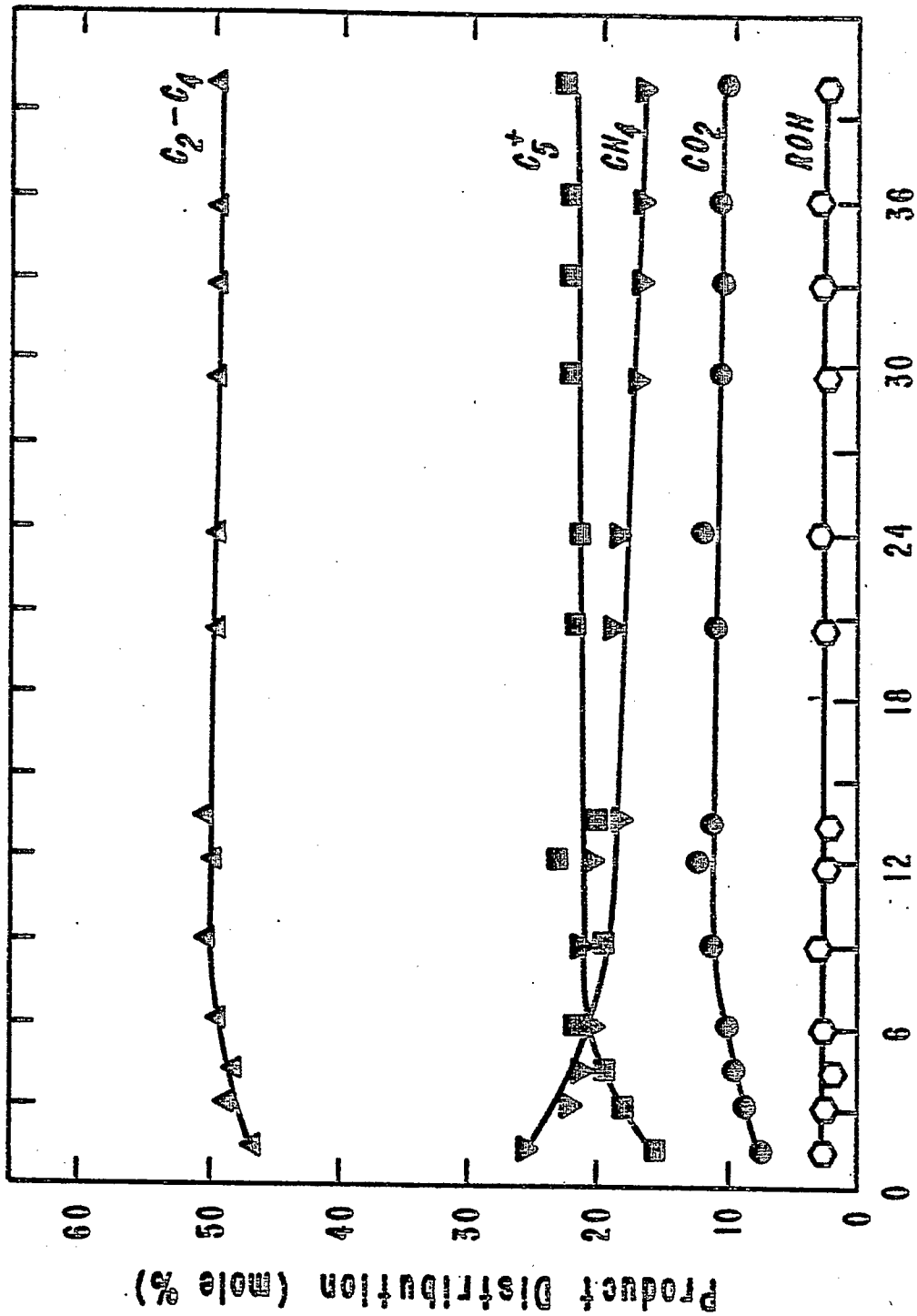
Product Distribution (mole %)
60
50
40
30
20
10
0
0
6
12
18
24
30
36
Time on Stream (hr)
$C_2 - C_4$
C_5^+
CH_4
CO_2
ROH

TABLE 4

LOW MOLECULAR WEIGHT OLEFIN SELECTIVITY RATIO VERSUS TIME ON STREAM IN CATALYST STABILITY TEST[a]

Olefin/Paraffin Ratio	Time on Stream (hours)								
	1.5	4.5	9.0	13.0	20.0	24.0	29.0	33.0	39.0
$C_2^=/C_2$	0.4	0.9	1.3	1.4	1.6	1.5	1.6	1.5	1.5
$C_3^=/C_3$	2.3	3.6	4.0	4.1	4.3	4.2	4.3	4.1	4.1
$C_4^=/C_4$	1.6	2.7	3.0	3.1	3.3	3.2	3.1	3.0	3.2

[a]Dense Bed Catalyst Loading; Temperature = 483 K; Pressure = 1465 kPa; Space Velocity = 1.08 $cm^3g^{-1}s^{-1}$; H_2/CO = 2/1; YST-2.

Figure 11

Catalyst Stability Test; Dense Bed Catalyst Loading; Carbon Monoxide Conversion and Olefin Selectivity Versus Time on Stream; Temperature = 483 K; Pressure = 1465 kPa; Space Velocity = 1.08 $cm^3 g^{-1} s^{-1}$; H_2/CO = 2/1; YST-3

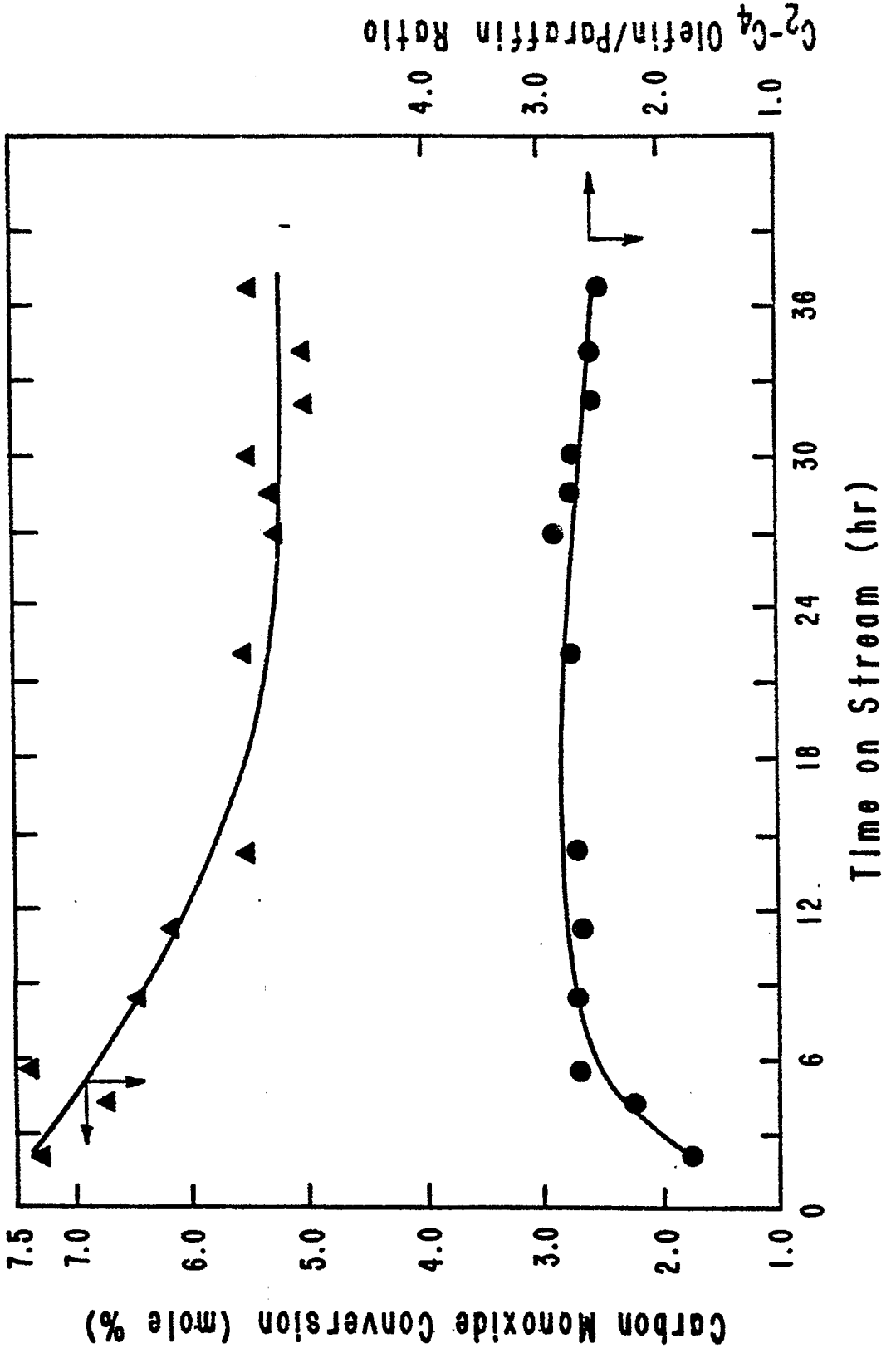
Carbon Monoxide Conversion (mole %)
7.5
7.0
6.0
5.0
4.0
3.0
2.0
1.0
0
6
12
18
24
30
36
Time on Stream (hr)
C2-C4 Olefin/Paraffin Ratio
4.0
3.0
2.0
1.0

Figure 12

Catalyst Stability Test; Dense Bed Catalyst Loading;

Product Distribution Versus Time on Stream;

Temperature = 483 K; Pressure = 1465 kPa;

Space Velocity = 1.08 $cm^3 g^{-1} s^{-1}$;

H_2/CO = 2/1; YST-3

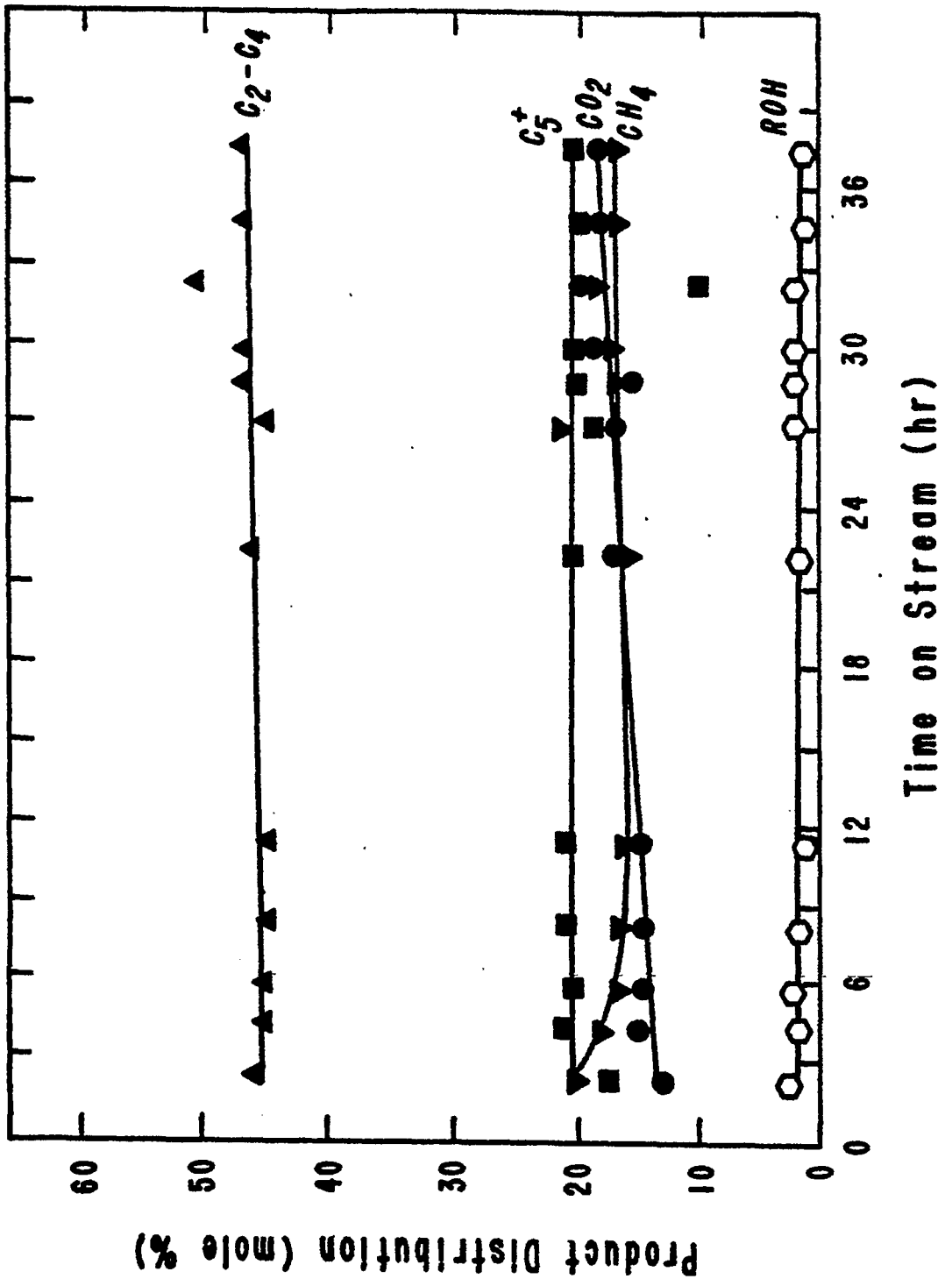
Product Distribution (mole %)
60
50
40
30
20
10
0
C_2-C_4
C_5^+
CO_2
CH_4
ROH
0
6
12
18
24
30
36
Time on Stream (hr)

TABLE 5

LOW MOLECULAR WEIGHT OLEFIN SELECTIVITY RATIO VERSUS TIME ON STREAM IN CATALYST STABILITY TEST[a]

Olefin/Paraffin Ratio	Time on Stream (hours)								
	2.0	4.0	5.5	9.0	12.0	21.5	27.0	30.0	36.0
$C_2^=/C_2$	0.6	1.1	1.3	1.5	1.5	1.4	1.4	1.3	1.3
$C_3^=/C_3$	3.1	4.1	4.3	4.4	4.3	4.3	4.2	4.2	4.2
$C_4^=/C_4$	2.2	2.6	3.2	3.0	2.9	3.0	3.0	2.9	2.8

[a]Dense Bed Catalyst Loading; Temperature = 483 K; Pressure = 1465 kPa; Space Velocity = 1.08 $cm^3g^{-1}s^{-1}$; H_2/CO = 2/1; YST-3.

the end of the run. The yields for C_2-C_4, C_5^+, and ROH, 45, 20, and 2 percent, respectively, were independent of the time on stream. The production of carbon dioxide increased at the expense of methane. During the initial 12 hour period both yields for methane and carbon dioxide stabilized up to the end of the experiment. The olefin/paraffin ratio of the C_2-C_4 hydrocarbon fraction increased gradually from 1.8 at 2 hours to 2.8 at 12 hours on stream. The olefin/paraffin ratio remained constant until the final 6 hours of the run during which time the olefin/paraffin ratio declined to about 2.5. The olefin selectivity ratios for C_2, C_3, and C_4 increased over the initial period of 9 - 12 hours and stabilized at 1.4, 4.3, and 3.0, respectively. During the final 6 hours of the run the olefin selectivity ratios for C_2, C_3, and C_4 declined slightly to 1.3, 4.2, and 2.8, respectively. A period of 12 - 15 hours was required to stabilize the activity, olefin selectivity, and product distribution for catalyst YST-3. No evidence of catalyst deactivation was observed during the experiment, but the trend of an initial decrease in the carbon monoxide conversion was considerably different from those for catalysts YST-1 and YST-2.

The stability test for catalyst YST-4 was conducted for 35 hours on stream. The carbon monoxide conversion, olefin selectivity, and product distribution are presented in Figures 13 and 14 and Table 6. The carbon monoxide conversion decreased gradually from approximately 5.4 percent at 27 hours and became constant up to the end of the experiment. The C_2-C_4 and C_5^+ yields increased, C_2-C_4 olefin selectivity increased, and the methane yield declined during the initial 12 hour period. The C_2-C_4 olefin/paraffin ratio

Figure 13

Catalyst Stability Test; Dense Bed Catalyst Loading; Carbon Monoxide Conversion and Olefin Selecivity Versus Time on Stream; Temperature = 483 K; Pressure = 1465 kPa; Space Velocity = 1.08 $cm^3 g^{-1} s^{-1}$; H_2/CO = 2/1; YST-4

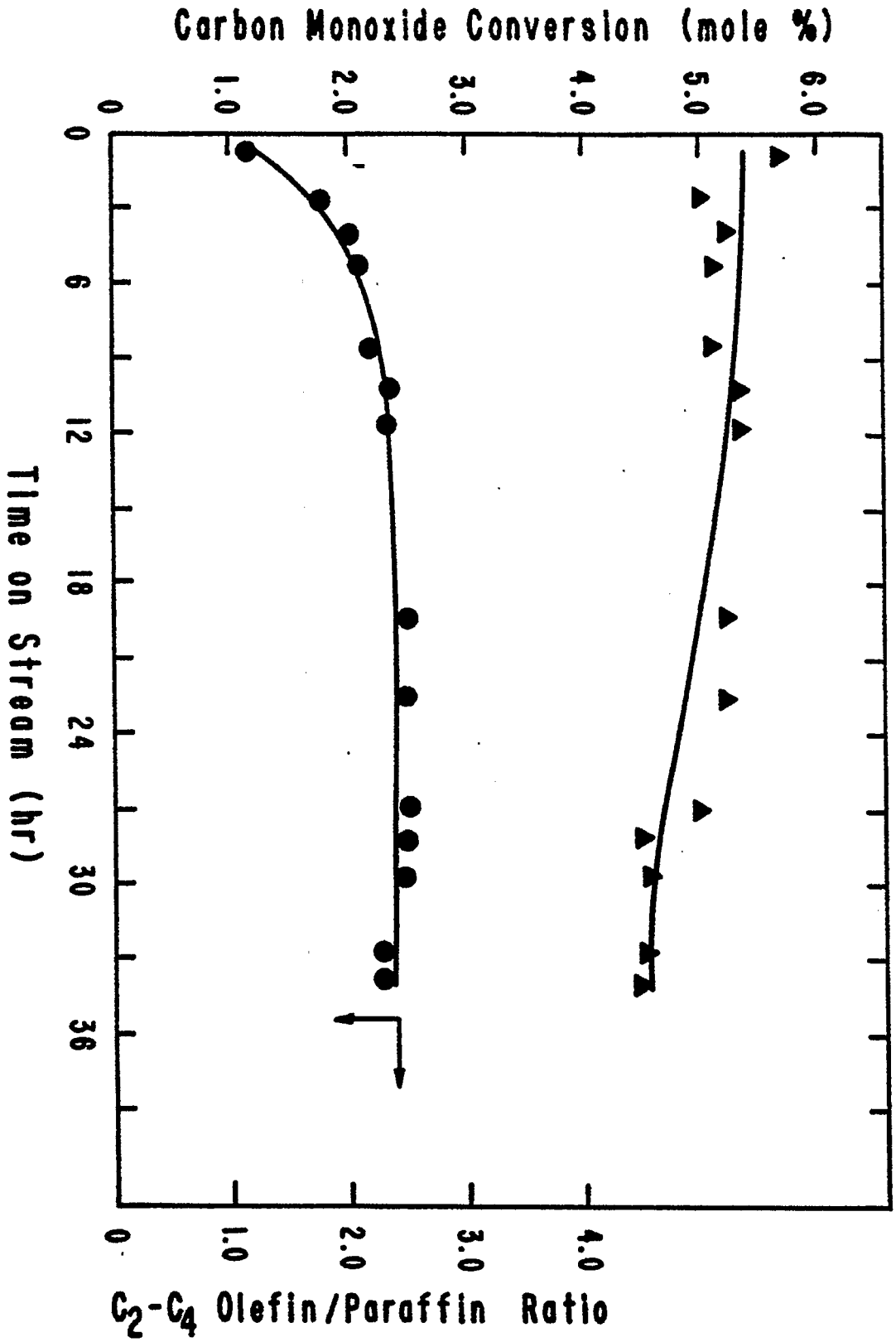
Carbon Monoxide Conversion (mole %)
0
1.0
2.0
3.0
4.0
5.0
6.0
Time on Stream (hr)
0
6
12
18
24
30
36
C2-C4 Olefin/Paraffin Ratio
0
1.0
2.0
3.0
4.0

Figure 14

Catalyst Stability Test; Dense Bed Catalyst Loading;
Product Distribution Versus Time on Stream;
Temperature = 483 K; Pressure = 1465 kPa;
Space Velocity = 1.08 $cm^3 g^{-1} s^{-1}$;
H_2/CO = 2/1; YST-4

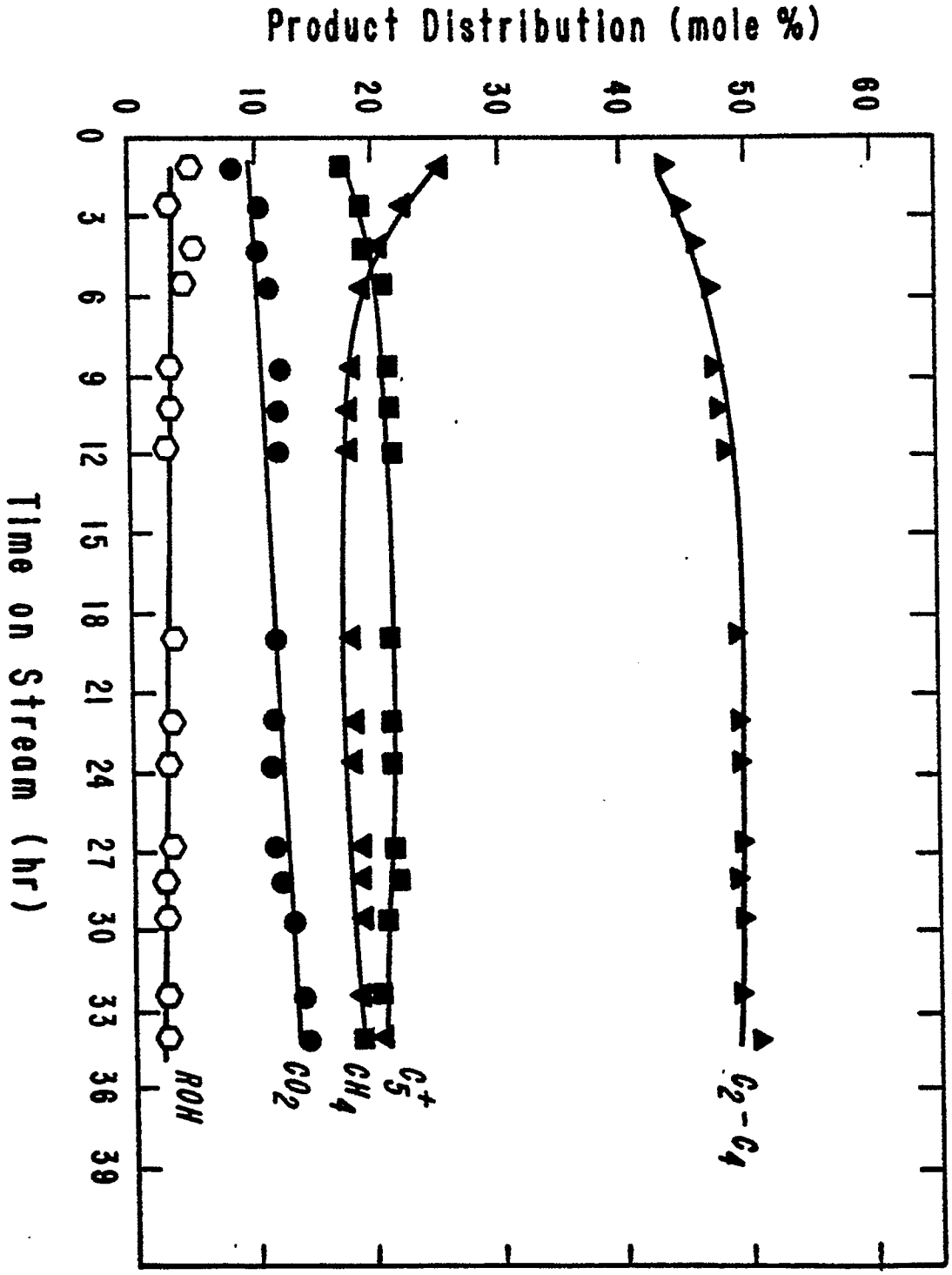
Product Distribution (mole %)
0
10
20
30
40
50
60
Time on Stream (hr)
0
3
6
9
12
15
18
21
24
27
30
33
36
39
ROH
CO2
CH4
C5+
C2-C4

TABLE 6

LOW MOLECULAR WEIGHT OLEFIN SELECTIVITY RATIO VERSUS TIME ON STREAM IN CATALYST STABILITY TEST[a]

Olefin/Paraffin Ratio	Time on Stream (hours)								
	1.0	4.0	8.5	10.0	11.5	19.5	22.0	27.0	34.0
$C_2^=/C_2$	0.4	0.8	1.1	1.2	1.2	1.4	1.4	1.4	1.3
$C_3^=/C_3$	2.2	3.3	3.7	3.8	3.8	4.0	4.1	4.1	3.9
$C_4^=/C_4$	1.4	2.4	2.5	2.7	2.7	2.9	3.0	2.9	2.8

[a]Dense Bed Catalyst Loading; Temperature = 483 K; Pressure = 1465 kPa; Space Velocity = 1.08 $cm^3g^{-1}s^{-1}$; Space Velocity = 1.08 $cm^3g^{-1}s^{-1}$; H_2/CO = 2/1; YST-4.

stabilized at 2.5 and the yields of C_2-C_4 hydrocarbons, methane, and C_5^+ hydrocarbons stabilized at 49, 18, and 20 percent, respectively, for the remainder of the experiment. The carbon dioxide showed a slight increase during the course of the experiment but it was generally in the range of 9 - 11 percent. The ROH yield was low and ranged from 2 to 4 percent during the test. The olefin selectivity ratios for C_2, C_3, and C_4 increased over the initial period of 10 - 12 hours and stabilized at 1.4, 4.0, and 2.9, respectively for the remainder of the test. Generally a period of 12 hours was needed to stabilize the activity, olefin selectivity, and product distribution for catalyst YST-4.

The data on the activity and the product distribution for the four YST series catalysts at 20 hours on stream were compiled to compare the catalyst performance for carbon monoxide hydrogenation and are reported in Table 7. The carbon monoxide conversions were generally in the range of 5 - 6 percent to minimize heat transfer influence. The C_2-C_4 hydrocarbon yields varied from 46 to 50 percent. The total yield of C_5^+ hydrocarbons and ROH ranged from 21 to 24 percent. The carbon dioxice yield ranged from 4.8 percent (YST-1) to 16.2 percent (YST-3). Catalysts YST-2, YST-3, and YST-4 generally gave methane yields of 16 - 18 percent whereas catalyst YST-1 gave a methane yield of 25.6 percent. Catalyst YST-1 was less selective for C_2-C_4 olefin formation (O/P ratio = 1.39) than the other iron-manganese catalysts (O/P ratio = 2.6 - 2.9). The data on the olefin selectivity ratios for C_2, C_3, and C_4 also indicated that catalyst YST-1 was less selective for C_2, C_3, and C_4 olefin formation ($C_2^=/C_2$ = 0.6, $C_3^=/C_3$ = 2.0, and $C_4^=/C_4$ = 1.7) than the other iron-manganese

TABLE 7

COMPARISON OF YIELD AND SELECTIVITY FOR Fe-Mn CATALYST STABILITY TEST[c]

Catalyst:	YST-1[a]	YST-2[b]	YST-3[b]	YST-4[b]
Mn/100 Fe:	0	3.6	3.5	3.5
CO Conversion (%):	4.9	5.6	5.6	5.2
	Product Distribution (mole %)			
CO_2	4.8	11.8	16.2	11.5
C_1	25.6	17.5	15.9	17.3
C_2	12.2	13.8	12.7	13.2
C_3	18.8	19.3	18.5	18.8
C_4	15.6	16.4	14.8	15.3
C_2-C_4	46.6	49.5	46.0	47.3
C_5^+	16.8	18.8	20.3	21.2
ROH	6.2	2.4	1.6	2.7
	Olefin Selectivity			
C_2-C_4 Olefin/ Paraffin Ratio	1.4	2.9	2.7	2.6
$C_2^=/C_2$	0.6	1.6	1.4	1.4
$C_3^=/C_3$	2.0	4.3	4.3	4.0
$C_4^=/C_4$	1.7	3.3	3.0	2.9

[a]Operating Conditions: T = 473 K; P = 1465 kPa; Space Velocity = 1.08 $cm^3 g^{-1} s^{-1}$; H_2/CO = 2/1.

[b]Operating Conditions: The same as (a) except for T = 483 K.

[c]Time on Stream: Approximately 20 hours.

catalysts ($C_2^=/C_2$ = 1.4 - 1.6; $C_3^=/C_3$ = 4.0 - 4.3, and $C_4^=/C_4$ = 2.9 - 3.3).

Catalyst Reduction Study

In the catalyst stability tests the catalysts were reduced in flowing hydrogen at 773 K and ambient pressure for 20 hours, however, it was recognized that these conditions may not have been the optimum for the catalyst activation. Therefore, a catalyst reduction study was undertaken in a thermogravimetric analysis (TGA) system to determine the optimum reduction temperature and the optimum reduction time for the iron-manganese catalysts.

Initially, an optimum heating rate was determined for the study. The TGA curves for the reduction of catalyst YST-2 at four different heating rates; 0.5 K min^{-1}, 2.0 K min^{-1}, 5.0 K min^{-1}, and 10.0 K min^{-1}, are presented in Figure 15. The initial temperature was 298 K in each experiment and the final temperature was 773 K. The four curves indicated that the catalyst weight loss was a function of the reduction temperature and the greatest weight loss occurred at the temperatures above 573 K. The total weight loss for this catalyst in each instance amounted to 39 - 40 percent of the initial catalyst weight. The temperatures for the complete weight loss at 0.5 K min^{-1}, 2.0 K min^{-1}, 5.0 K min^{-1}, and 10.0 K min^{-1} were 623 K, 648 K, 723 K, and 753, respectively. A heating rate of 2 K min^{-1} was chosen as the standard TGA heating rate because it resulted in a more complete weight loss than 5.0 K min^{-1} and 10.0 K min^{-1} and it was time-effective compared to the 0.5 K min^{-1} heating rate.

An oxidation test for the reduced catalyst was oxidized to

Figure 15

TGA Weight Loss Curves; Reducing Gas: Hydrogen; YST-2

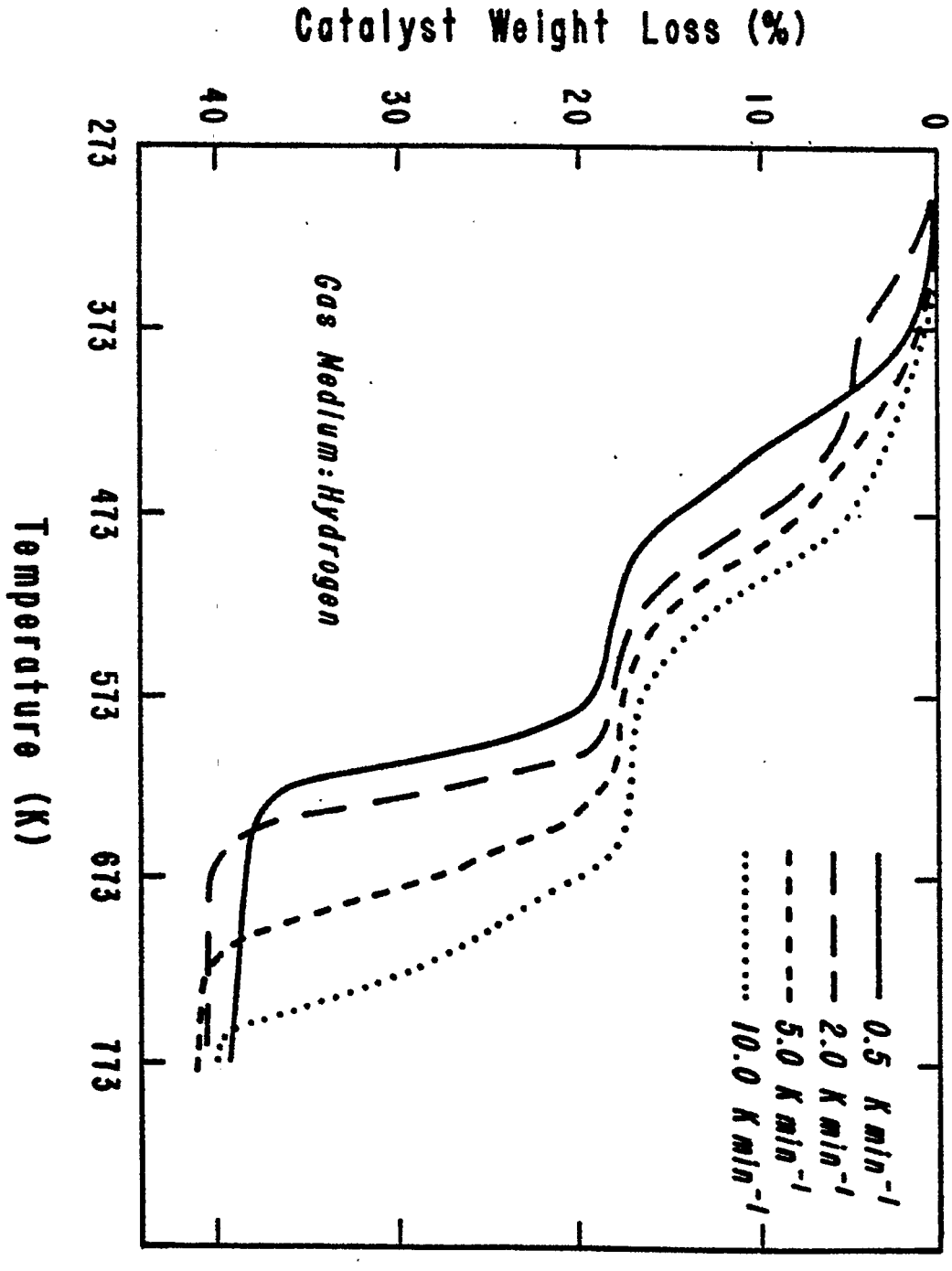
Catalyst Weight Loss (%)
0
10
20
30
40
273
373
473
573
673
773
Temperature (K)
Gas Medium: Hydrogen
0.5 K min-1
2.0 K min-1
5.0 K min-1
10.0 K min-1

determine the weight gain from the oxidation of the reduced catalyst. The reduced catalyst was cooled from 773 K to room temperature in flowing hydrogen. At 298 K hydrogen was shut off and air was passed through the system. After the air flowrate of 50 $cm^3 min^{-1}$ was established the temperature of the sample was raised from 298 K to 773 K at a heating rate of 2 K min^{-1}. The reduction and oxidation curves are presented in Figure 16. The catalyst weight loss in flowing hydrogen was 22 percent at 573 K. The curve then declined sharply at 623 K and became flat at 673 K. There was no additional weight loss up to 773 K. The total weight loss was 41 percent of the initial catalyst weight. In air the oxidation was initiated at 423 K and was completed at 653 K. The final position of the curve in the flowing air was equivalent to a weight loss of 22 percent of the initial catalyst weight. In other words, the catalyst gain in flowing air was 19 percent of the initial unreduced catalyst weight.

Similar experiments were carried out for the other three YST catalysts. The TGA curves for catalysts YST-1, YST-3, and YST-4 from 298 K to 773 K at the heating rate of 2 K min^{-1} are presented in Figure 17. These three curves were quite similar. All of the curves indicated that no weight loss occurred above 673 K. The final weight losses for catalysts YST-1, YST-3, and YST-4 were 43.0, 40.0, and 43.0 percent (of the initial catalyst weight), respectively. From these TGA curves it was evident that a temperature of 673 K was sufficient to obtain complete catalyst weight loss and to activate the catalyst for the hydrogenation of carbon monoxide. The time required to raise the temperature from 298 to 673 K at the heating rate of 2 K min^{-1} was 187.5 minutes. Therefore, it was determined

Figure 16

TGA Weight Loss Curves; Reducing Gas: Hydrogen; Oxidizing Gas: Air; Heating Rate: 2 K min^{-1}; YST-2

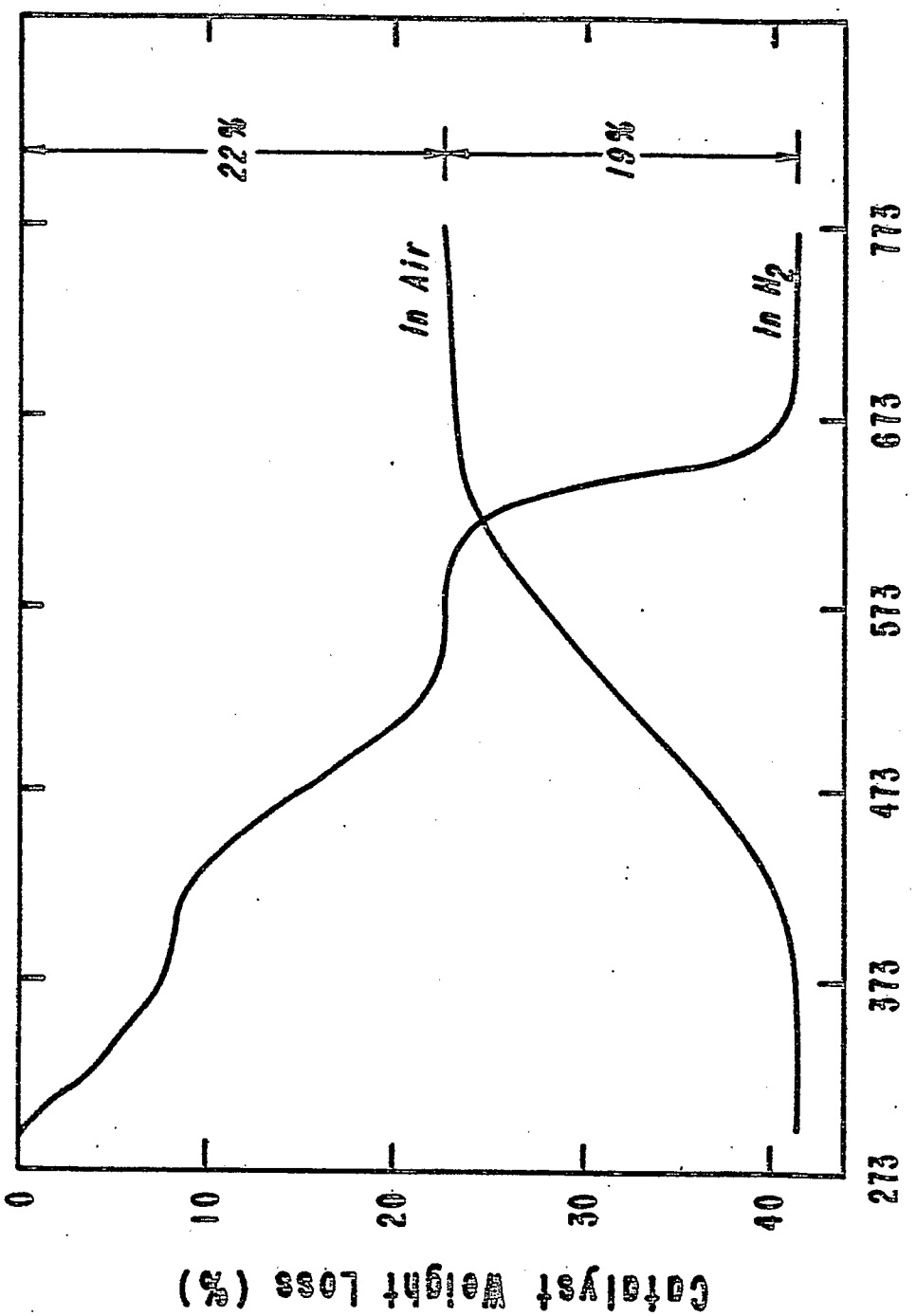
22 %
19 %
In Air
In N_2
0
10
20
30
40
273
373
473
573
673
773
Catalyst weight loss (%)
Temperature (K)

Figure 17

TGA Weight Loss Curves; Reducing Gas:

Hydrogen; Heating Rate: 2 K min^{-1}

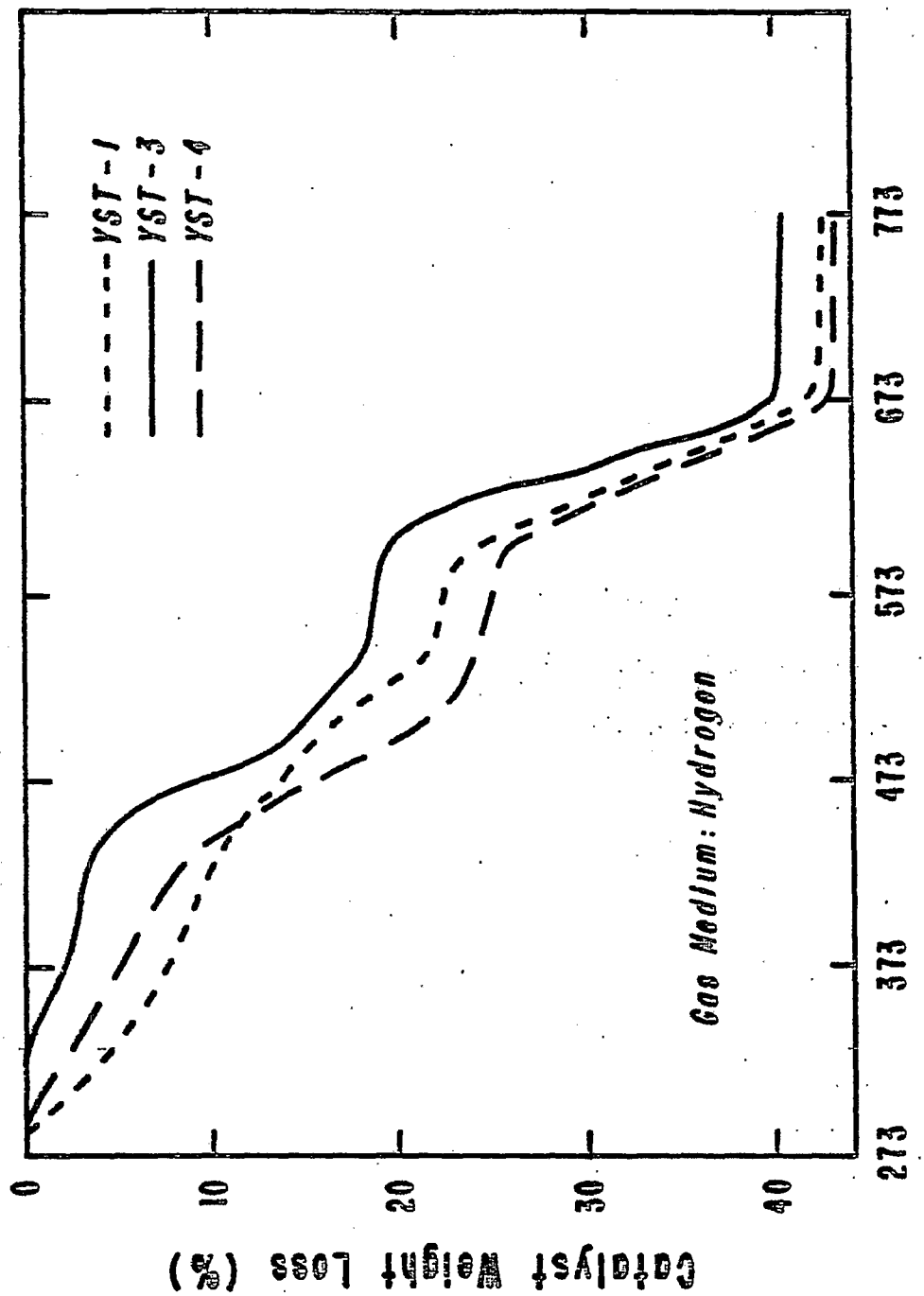
YST-1
YST-3
YST-4
Gas Medium: Hydrogen
Catalyst Weight Loss (%)
0
10
20
30
40
273
373
473
573
673
773
Temperature (K)

that the catalyst reduction conditions should be a temperature of 673 K for a period of 8 hours in flowing hydrogen at ambient pressure. These reduction conditions were used throughout the course of this investigation.

The YST series of catalysts were also tested in the TGA system in flowing helium from 298 K to 773 K. The TGA curves for catalysts YST-1 through YST-4 in helium are presented in Figure 18. The catalyst weight loss was also a function of temperature; however, all the curves became flat at approximately 623 K. The final catalyst weight losses for catalysts YST-1, YST-2, YST-3, and YST-4 were 20, 13, 15, and 21 percent (of the initial catalyst weight), respectively. The final catalyst weight loss in helium was attributed to the evaporation of adsorbed moisture from the catalyst sample since there could be no reaction between the catalyst and the inert helium gas.

A pure manganese catalyst was tested in both flowing hydrogen and flowing helium from 298 K to 773 K. The helium and hydrogen TGA curves are presented in Figure 19. The final catalyst weight loss in helium was only 2.5 percent of the initial weight, but that in hydrogen was 10 percent of the initial weight. The curve in flowing hydrogen also showed that the sharpest decline of the curve began at 623 K and leveled off at 653 K. There was no more weight loss between 673 K and 773 K. It was clear again that the reduction of the iron-manganese catalysts in hydrogen at 673 K for 8 hours was sufficient for the catalyst activation.

Figure 18

TGA Weight Loss Curves; Gas Medium: Helium;
Heating Rate: 2-K min^{-1}; YST-1; YST-2;
YST-3; YST-4

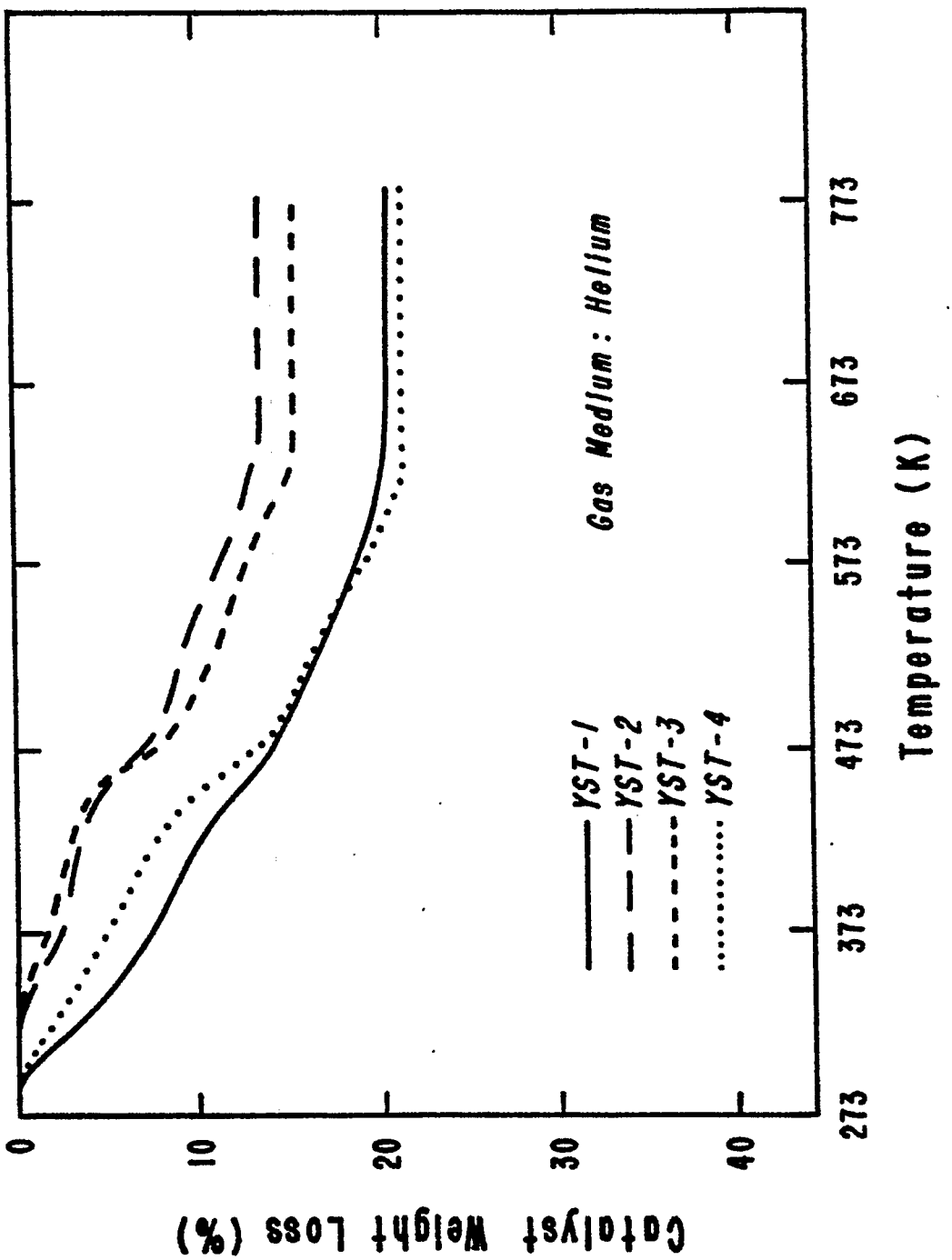
Catalyst Weight Loss (%)
0
10
20
30
40
273
373
473
573
673
773
Temperature (K)
Gas Medium : Hellum
YST-1
YST-2
YST-3
YST-4

Figure 19

TGA Weight Loss Curves; Hydrogen Gas;
Helium Gas; Heating Rate: 2 K min^{-1};
Pure Manganese

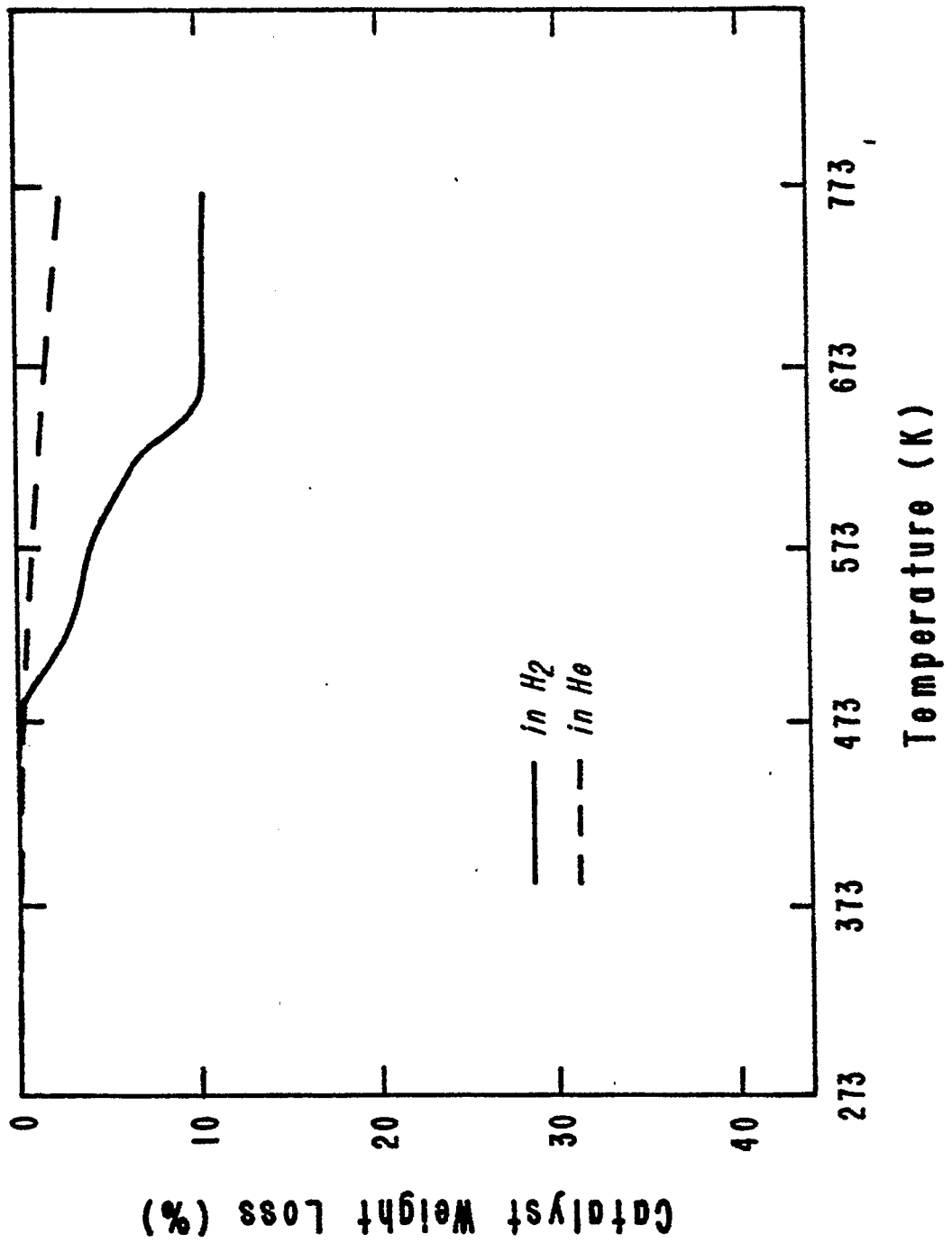
Catalyst Weight Loss (%)
0
10
20
30
40
273
373
473
573
673
773
Temperature (K)
in H_2
in He

The Effect of Catalyst Bed Dilution on Activity and Selectivity

In the previous experiments the catalyst zone in the fixed-bed reactor was dense-packed without any dilution. The effects of the catalyst bed dilution on the carbon monoxide conversion, olefin selectivity, and product distribution were studied by diluting the catalyst bed with inert Denstone 57 ceramic spacers. The dilution ratio was based on volume. The catalyst and the Denstone 57 (both 24 - 32 mesh) were mixed together in a 150 cm^3 bottle. The bottle was rotated continuously for 2 minutes to insure a homogeneous mixture of the catalyst and the inert Denstone 57 before loading into the reactor. The operating conditions for the experiments were as follows: a H_2/CO ratio of 2/1, a pressure of 1378 kPa, and a space velocity of 1.0 $cm^3 g^{-1} s^{-1}$. Catalyst YST-4 (3.5 Mn/100 FE) was evaluated at 473 K for 20 hours to attain a stationary state prior to determining the conversion, olefin selectivity, product distribution, and catalyst bed temperature profile.

The temperature profiles for the dense-packed catalyst bed are presented in Figure 20 at two carbon monoxide conversion levels. There was no temperature rise in the catalyst bed at 1.5 percent conversion; however, the profile at 6.7 percent conversion indicated a 7 K temperature rise due to the heat of reaction. The temperature profiles for the diluted catalyst bed at a 1/1 dilution ratio are presented in Figure 21. The average temperature rise in the catalyst bed at 5.7 percent conversion was 7 K and that for 7.3 percent conversion as 8 K. Thus the 1/1 dilution was ineffective in disipating the heat of reaction.

Figure 20

Catalyst Bed Temperature Profiles; Carbon Monoxide Hydrogenation; Dense Bed Reactor Loading; Pressure = 1465 kPa; Space Velocity = 1.0 $cm^3g^{-1}s^{-1}$; H_2/CO = 2/1; Catalyst Mass: 8 g; (a) 1.5% CO Conversion; (b) 6.7 % CO Conversion

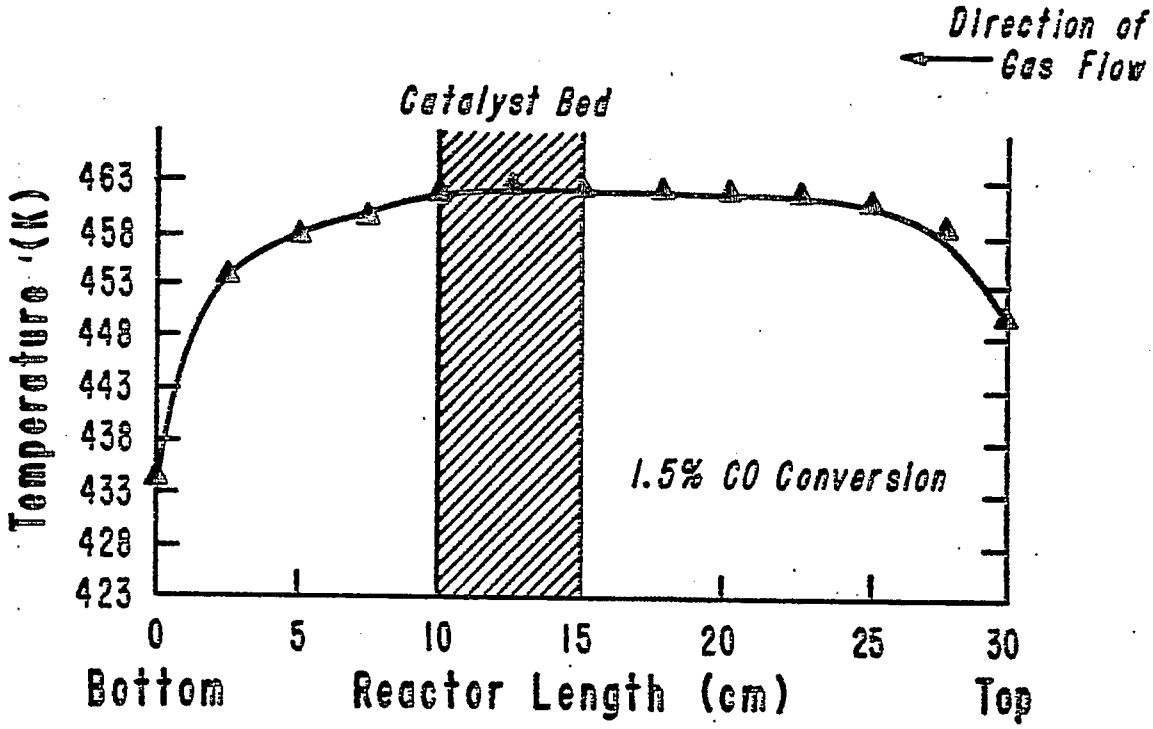
Direction of
Gas Flow
Catalyst Bed
Temperature (K)
463
458
453
448
443
438
433
428
423
1.5% CO Conversion
0
5
10
15
20
25
30
Bottom
Reactor Length (cm)
Top

(a)

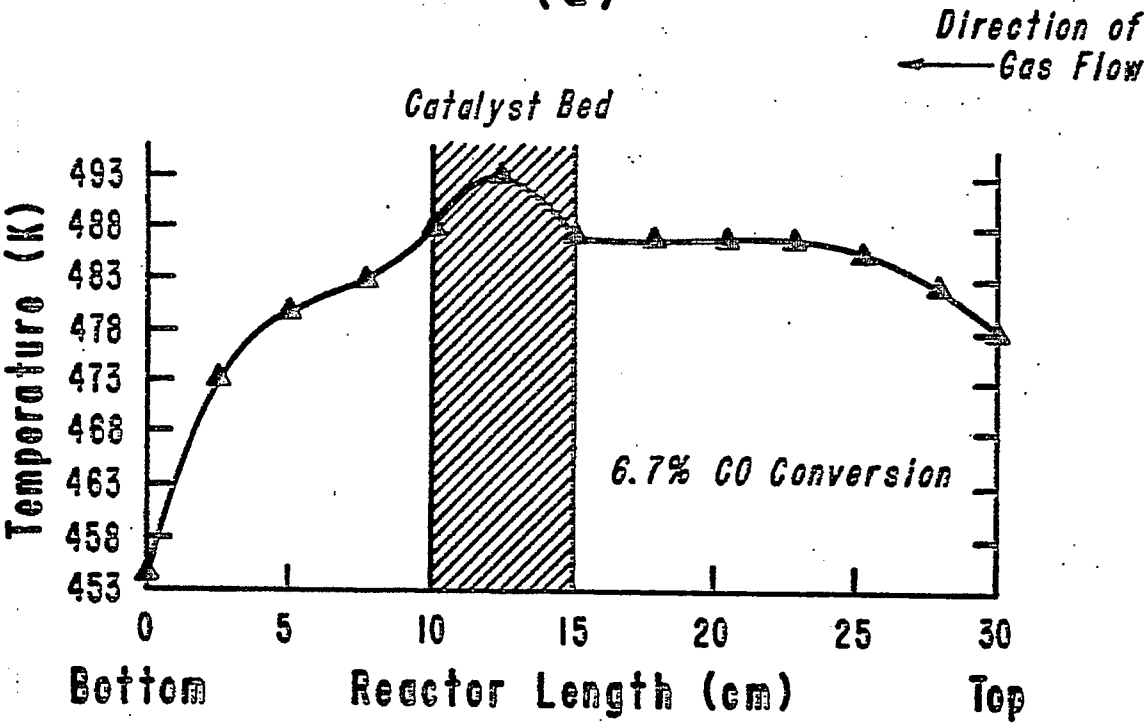
Direction of
Gas Flow
Catalyst Bed
Temperature (K)
493
488
483
478
473
468
463
458
453
6.7% CO Conversion
0
5
10
15
20
25
30
Bottom
Reactor Length (cm)
Top

(b)

Figure 21

Catalyst Bed Temperature Profiles; Carbon Monoxide Hydrogenation; Diluted Bed Reactor Loading; Denstone 57/Catalyst = 1/1; Pressure = 1465 kPa; Space Velocity = 1.0 $cm^3 g^{-1} s^{-1}$; H_2/CO = 2/1; Catalyst Mass: 8 g; (a) 5.7% CO Conversion; (b) 7.3% CO Conversion

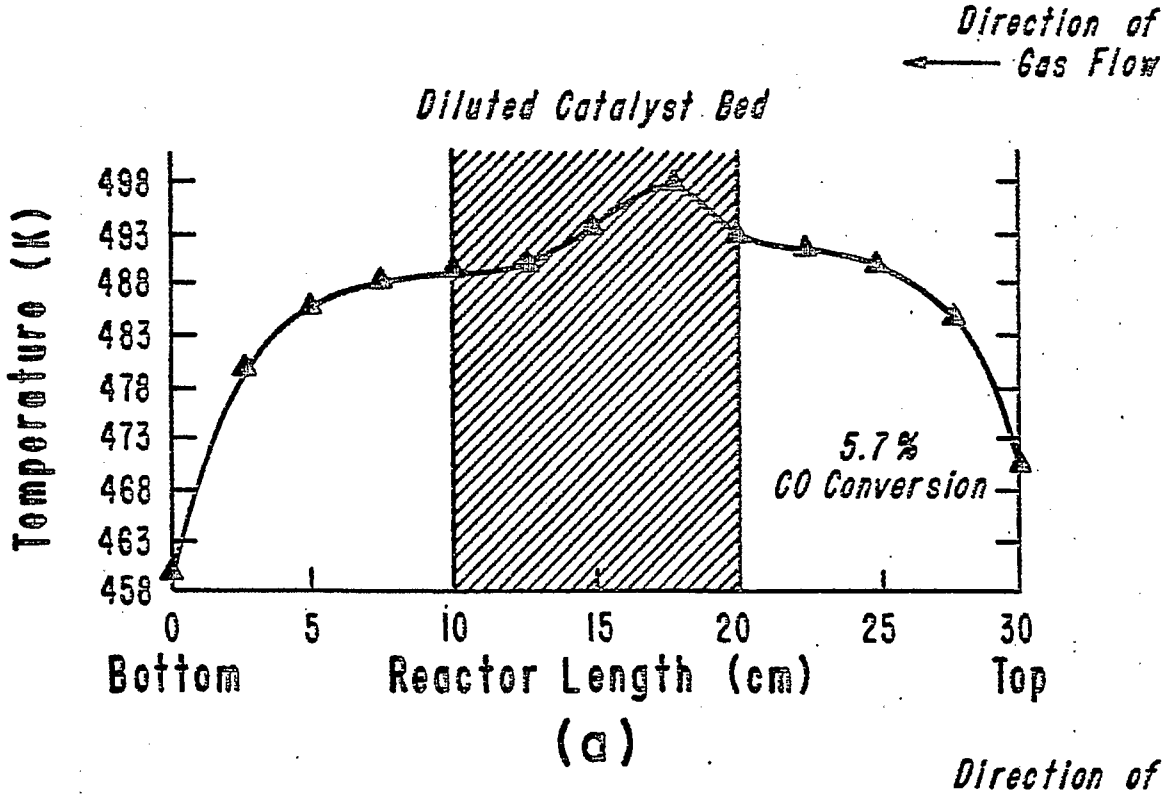
Direction of
Gas Flow
Diluted Catalyst Bed
Temperature (K)
498
493
488
483
478
473
468
463
458
5.7%
CO Conversion
0
5
10
15
20
25
30
Bottom
Reactor Length (cm)
Top

(a)

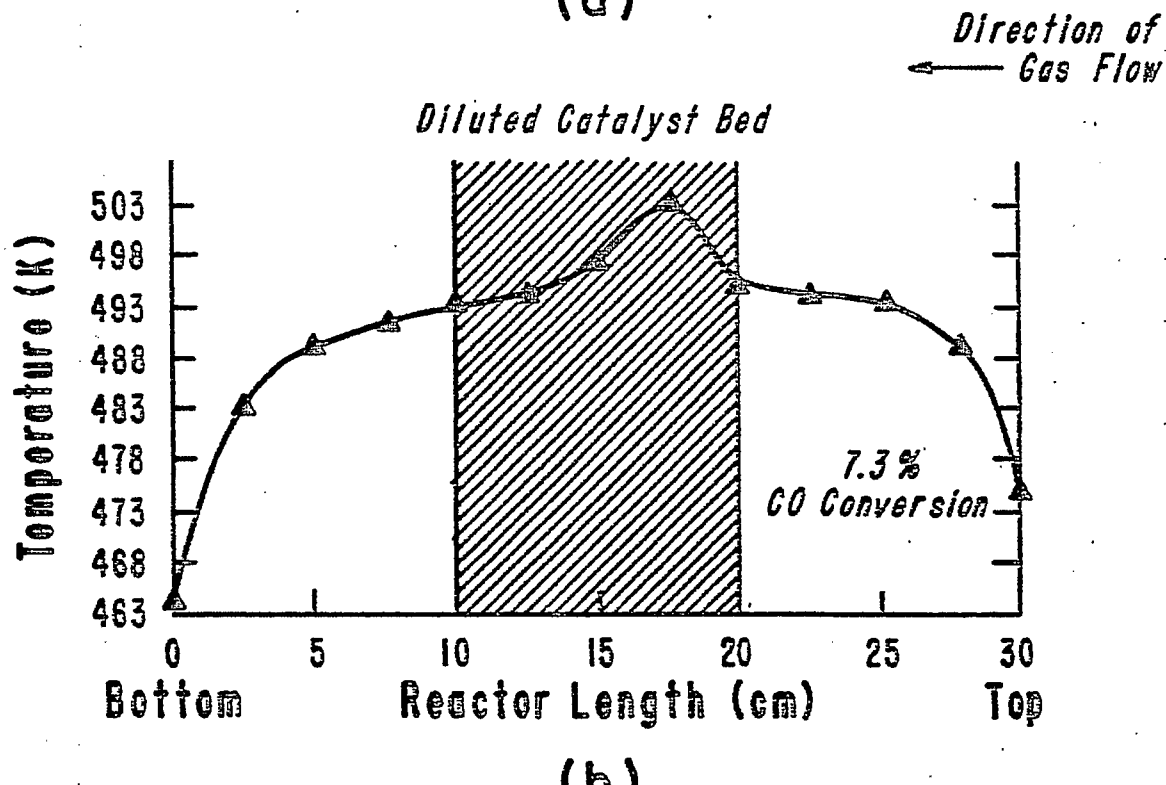
Direction of
Gas Flow
Diluted Catalyst Bed
Temperature (K)
503
498
493
488
483
478
473
468
463
7.3%
CO Conversion
0
5
10
15
20
25
30
Bottom
Reactor Length (cm)
Top

(b)

The catalyst bed was further diluted with Denstone 57 to decrease the temperature rise in the catalyst zone. The temperature profiles for the volumetric dilution ratios (Denstone 57/catalyst) of 2/1, 3/1, and 4/1 at different carbon monoxide conversions are presented in Figures 22, 23, and 24 at a dilution ratio of 2/1 and a carbon monoxide conversion of 6 - 7 percent. The temperature rise in the catalyst bed was still 6 K. The temperature rise in the catalyst bed was 5 K at a dilution ratio of 3/1 and a carbon monoxide conversion of 6.5 - 8.5 percent. The influence of the catalyst bed dilution was significant for a dilution ratio of 4/1 because the temperature rise was only 3 K. Even for a carbon monoxide conversion of 7.2 percent, a temperature rise of 3 K was observed. Thus, the dilution ratio of 4/1 was sufficient to reduce the heat effect in the catalyst bed.

The catalyst weight used for the dilution experiment ratio 4/1 was 8.0 g. The diluted catalyst bed was almost 25.4 cm long, thus it was not appropriate to load the Denstone catalyst mixture into the reactor which had an overall length of 30.48 cm. Therefore, a dilution experiment with a catalyst weight of 4.8 g and a dilution ratio of Denstone 57/catalyst of 4/1 was run at the same operating conditions. The temperature profiles in the diluted catalyst bed for carbon monoxide conversions of 7.3 and 8.9 percent are presented in Figure 25. In both cases the temperature profiles were uniform across the entire bed. The temperature rise for 7.3 percent conversion was only 2 K and that for 8.9 percent conversion was 3 K. It was obvious that this 4/1 ratio reduced the heat effect in the catalyst bed very significantly. This dilution ratio was used in the subsequent

Figure 22

Catalyst Bed Temperature Profiles; Carbon Monoxide Hydrogenation; Diluted Bed Reactor Loading; Denstone 57/Catalyst = 2/1; Pressure = 1465 kPa; Space Velocity = 1.0 $cm^3 g^{-1} s^{-1}$; H_2/CO = 2/1; Catalyst Mass: 8 g; (a) 5.9% CO Conversion; (b) 7.0% CO Conversion

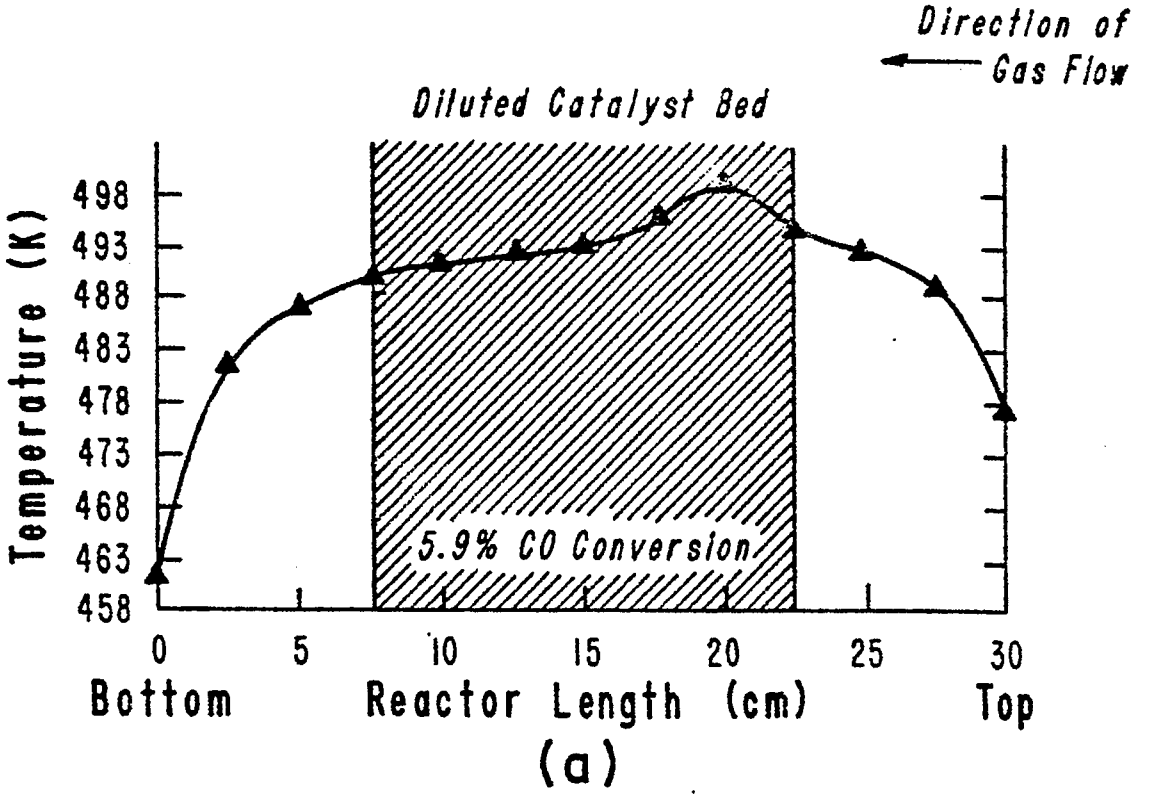
Direction of
Gas Flow
Diluted Catalyst Bed
Temperature (K)
498
493
488
483
478
473
468
463
458
5.9% CO Conversion
0
5
10
15
20
25
30
Bottom
Reactor Length (cm)
Top

(a)

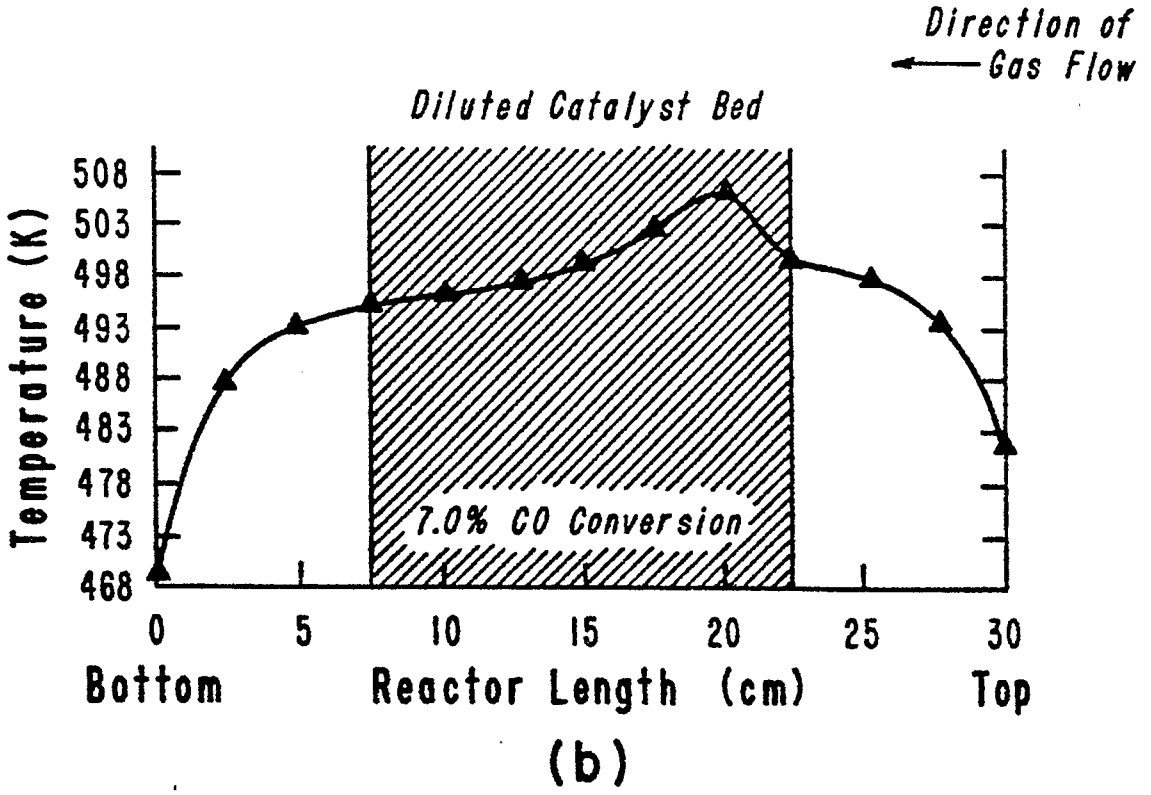
Direction of
Gas Flow
Diluted Catalyst Bed
Temperature (K)
508
503
498
493
488
483
478
473
468
7.0% CO Conversion
0
5
10
15
20
25
30
Bottom
Reactor Length (cm)
Top

(b)

Figure 23

Catalyst Bed Temperature Profiles; Carbon Monoxide Hydrogenation; Diluted Bed Reactor Loading; Denstone 57/Catalyst = 3/1; Pressure = 1465 kPa; Space Velocity = 1.0 $cm^3g^{-1}s^{-1}$; H_2/CO = 2/1; Catalyst Mass: 8 g; (a) 6.5% CO Conversion; (b) 8.2% CO Conversion

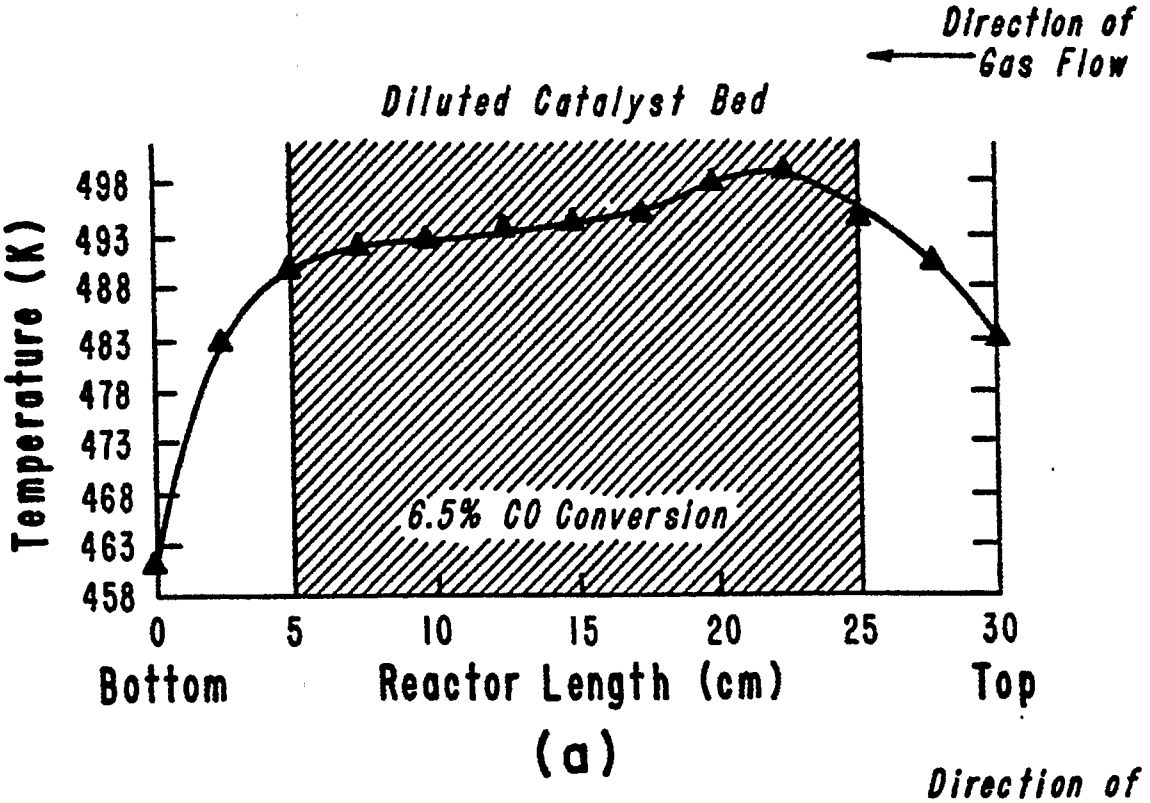
Direction of
Gas Flow
Diluted Catalyst Bed
Temperature (K)
498
493
488
483
478
473
468
463
458
6.5% CO Conversion
0
5
10
15
20
25
30
Bottom
Reactor Length (cm)
Top

(a)

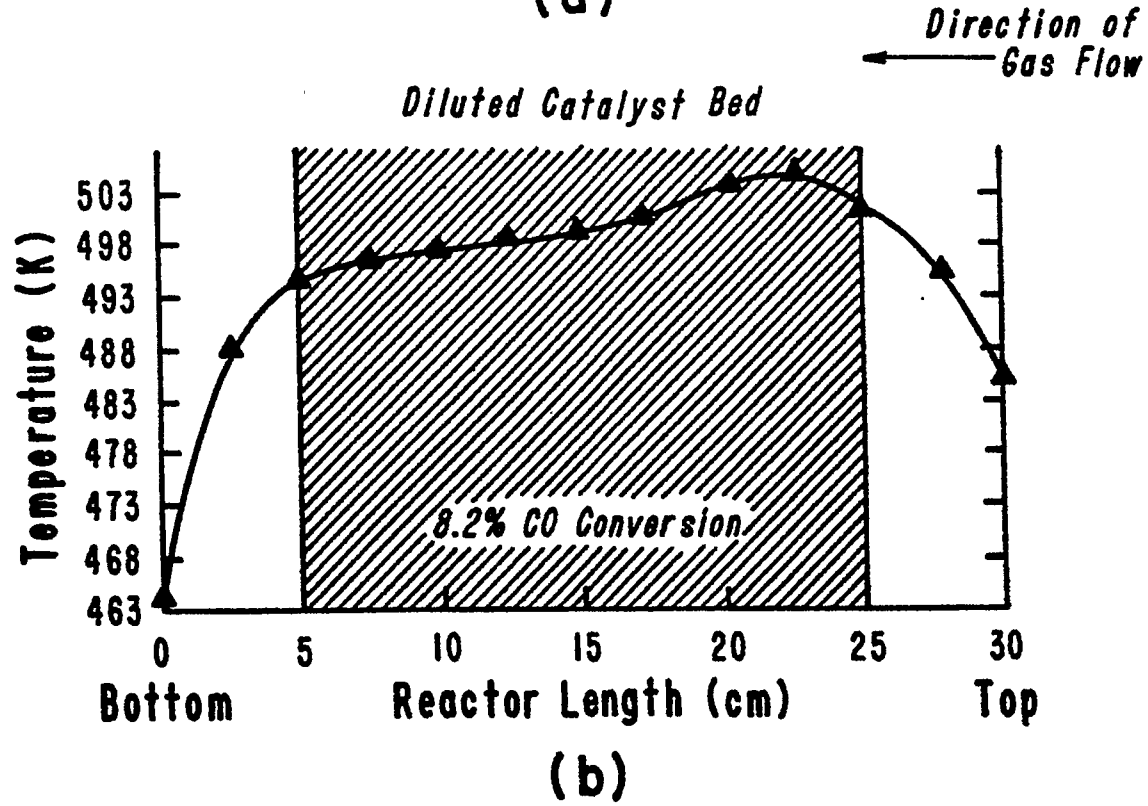
Direction of
Gas Flow
Diluted Catalyst Bed
Temperature (K)
503
498
493
488
483
478
473
468
463
8.2% CO Conversion
0
5
10
15
20
25
30
Bottom
Reactor Length (cm)
Top

(b)

Figure 24

Catalyst Bed Temperature Profiles; Carbon Monoxide Hydrogenation; Diluted Bed Reactor Loading; Denstone 57/Catalyst = 4/1; Pressure = 1465 kPa; Space Velocity = 1.0 $cm^3g^{-1}s^{-1}$; H_2/CO = 2/1; Catalyst Mass: 8 g; (a) 5.8% CO Conversion; (b) 7.2% CO Conversion

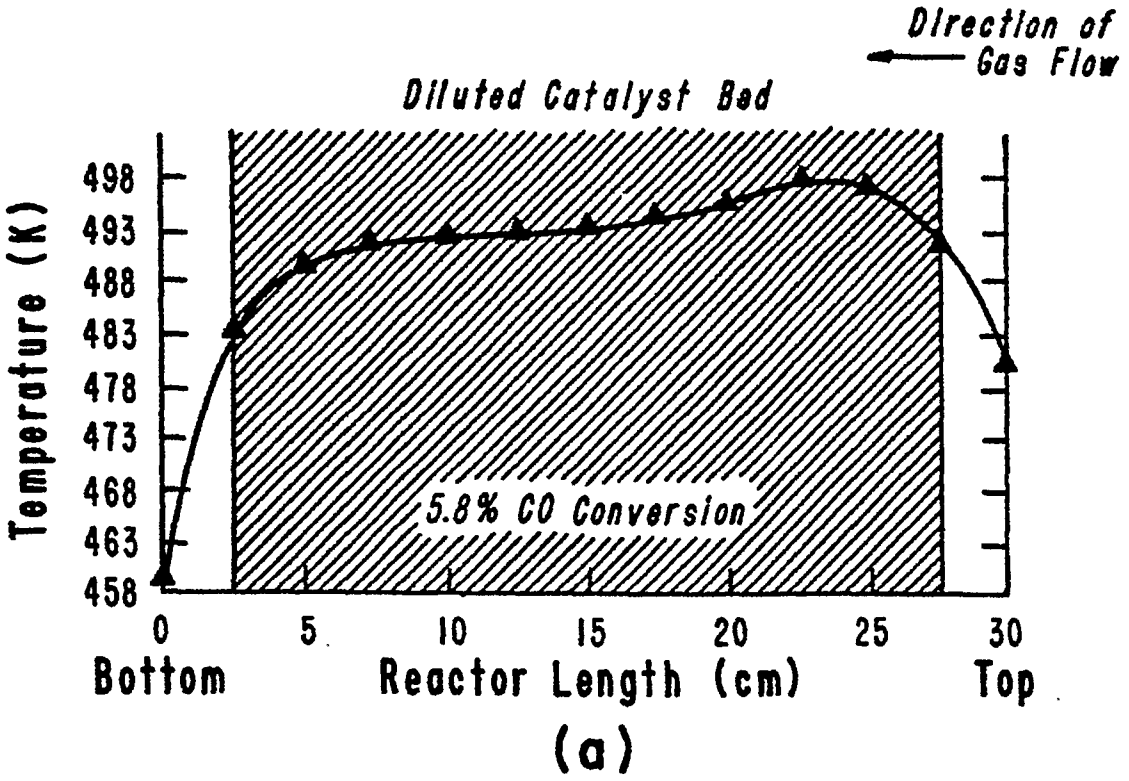
Direction of
Gas Flow
Diluted Catalyst Bed
Temperature (K)
498
493
488
483
478
473
468
463
458
5.8% CO Conversion
0
5
10
15
20
25
30
Bottom
Reactor Length (cm)
Top

(a)

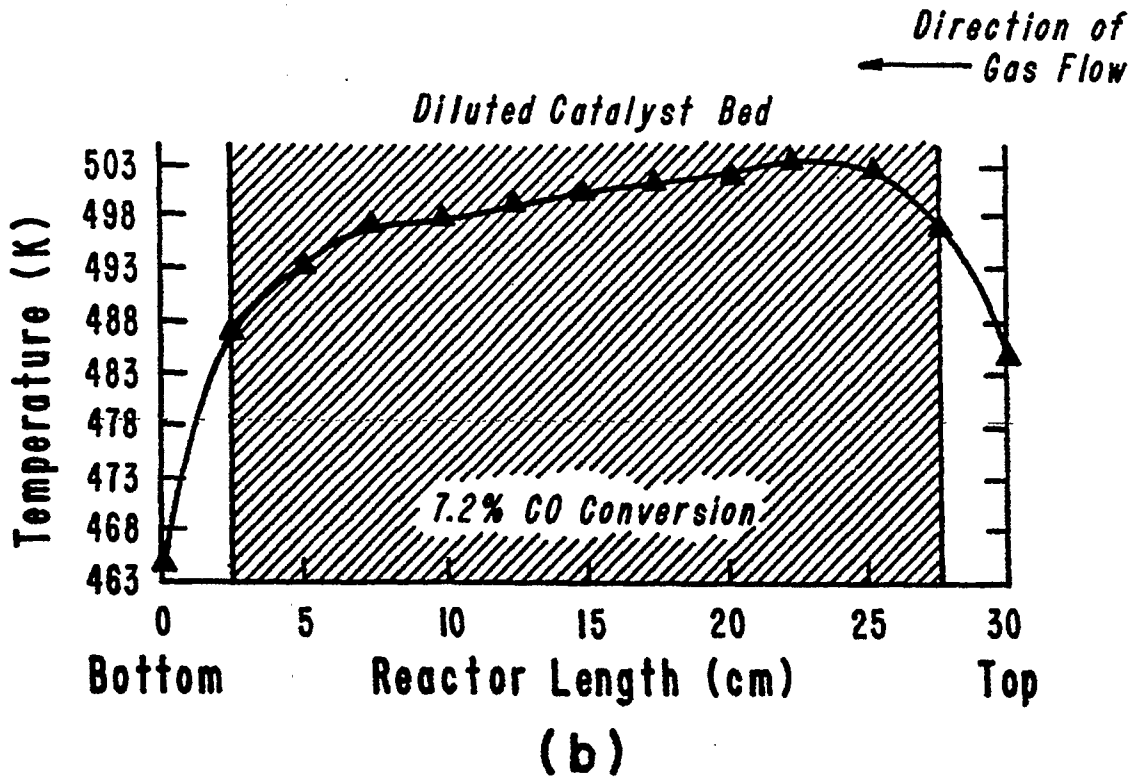
Direction of
Gas Flow
Diluted Catalyst Bed
Temperature (K)
503
498
493
488
483
478
473
468
463
7.2% CO Conversion
0
5
10
15
20
25
30
Bottom
Reactor Length (cm)
Top

(b)

Figure 25

Catalyst Bed Temperature Profiles; Carbon Monoxide Hydrogenation; Diluted Bed Reactor Loading; Denstone 57/Catalyst = 4/1; Pressure = 1465 kPa; Space Velocity = 1.0 $cm^3g^{-1}s^{-1}$; H_2/CO = 2/1; Catalyst Mass: 4.8 g; (a) 7.3% CO Conversion; (b) 8.9% CO Conversion

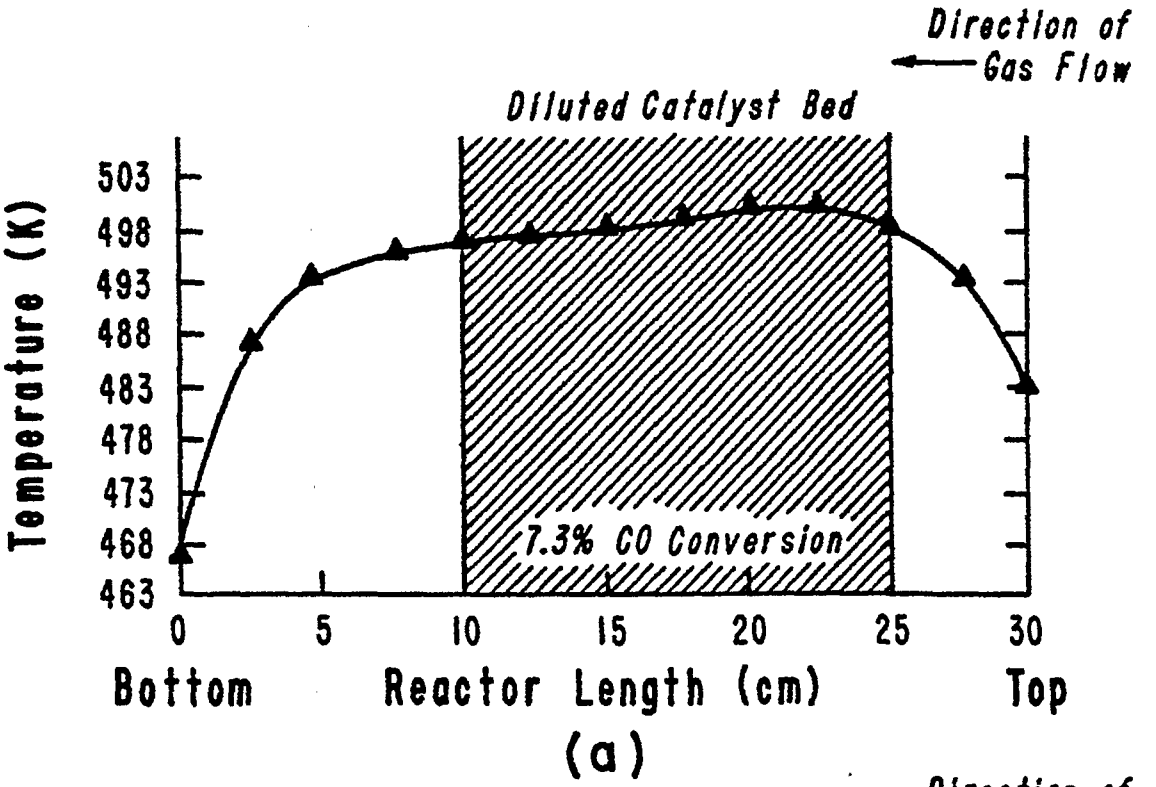
Direction of
Gas Flow
Diluted Catalyst Bed
Temperature (K)
503
498
493
488
483
478
473
468
463
7.3% CO Conversion
0
5
10
15
20
25
30
Bottom
Reactor Length (cm)
Top

(a)

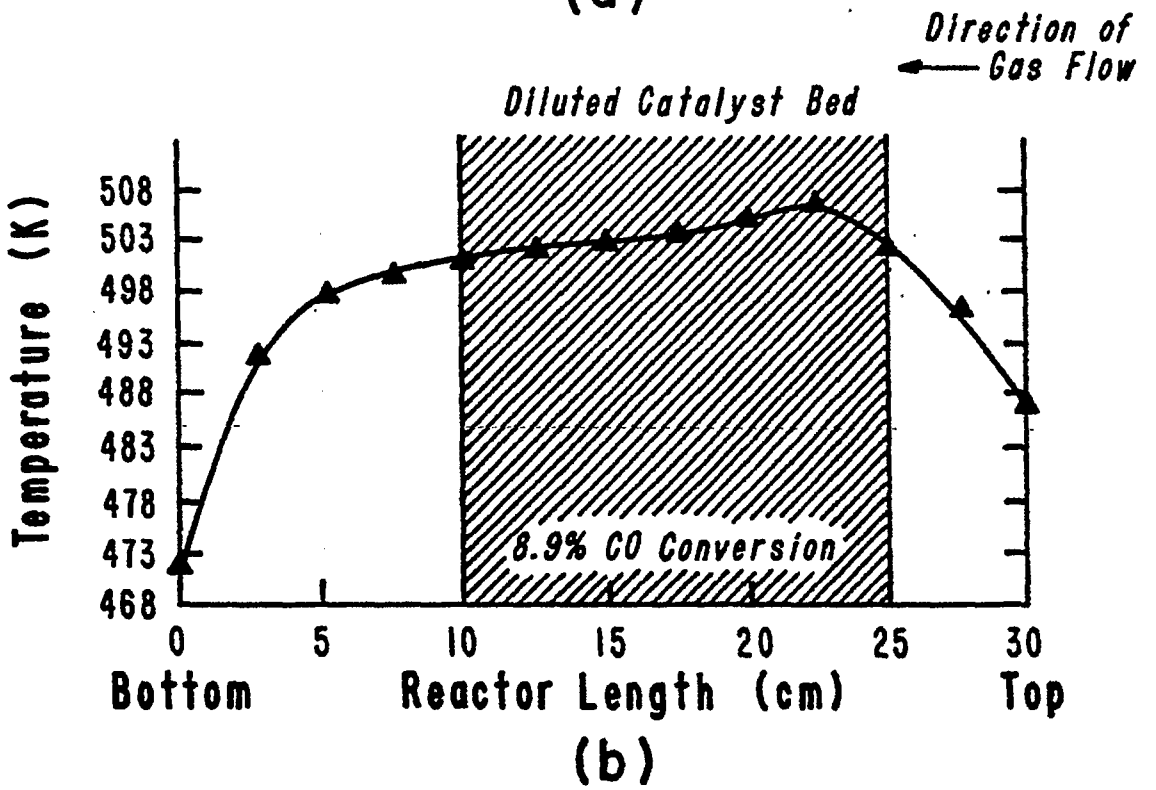
Direction of
Gas Flow
Diluted Catalyst Bed
Temperature (K)
508
503
498
493
488
483
478
473
468
8.9% CO Conversion
0
5
10
15
20
25
30
Bottom
Reactor Length (cm)
Top

(b)

experiments.

The data on the catalyst activity, olefin selectivity, and product distribution for catalyst YST-4 with the dilution ratios ranging from 0 to 4/1 at 20 hours on stream is presented in Table 8. The carbon monoxide conversion was maintained in the range of 6.5 - 7.5 percent. The yields of carbon dioxide and methane for the dense-packed bed, that is, 15.9 and 22.5 percent, respectively, were relatively higher than the yields obtained with the diluted bed (i.e., yields of carbon dioxide and methane of 10 - 14 and 18.5 - 19.5 percent, respectively). The C_2-C_4 yield and the olefin selectivity, that is, olefin/paraffin ratio, for the dense-packed bed, 42.3 percent and 1.81, respectively, were lower than those for the diluted bed, 45.5 - 46.5 percent for C_2-C_4 yield and 2.6 - 2.8 for the olefin/paraffin ratio . The catalyst dilution obviously increased the C_2-C_4 hydrocarbon yield and the olefin selectivity. The data for the 4.8 gram and 8.0 gram catalyst loadings were in excellent agreement. The data on the olefin selectivity ratios for C_2, C_3, and C_4 also indicated that the olefin ratios for the dense-packed bed ($C_2^=/C_2$ = 1.0, $C_3^=/C_3$ = 2.8, and $C_4^=/C_4$ = 2.1) were generally lower than those for the diluted bed ($C_2^=/C_2$ = 1.4 - 1.9, $C_3^=/C_3$ = 3.4 - 3.8, and $C_4^=/C_4$ = 2.9 - 3.2).

Effects of Catalyst Pretreatment

The 8 hour hydrogen reduction at 673 K was the standard catalyst pretreatment in this investigation; however, the effects of the pretreating gas composition on activity, olefin selectivity, and product distribution were also investigated. Catalyst YST-2

TABLE 8

EFFECTS OF CATALYST BED DILUTION ON CATALYST ACTIVITY AND PRODUCT DISTRIBUTION OVER CATALYST YST-4 (3.5 Mn/100 Fe)[a]

Dilution Ratio:	0	1/1	2/1	3/1	4/1	4/1[b]
CO Conversion (mole %):	6.7	7.3	7.0	6.5	7.2	7.3
	Product Distribution (mole %)					
CO_2	15.9	11.1	13.7	9.6	11.1	10.6
C_1	22.5	19.4	18.4	19.7	19.2	19.3
C_2	12.5	12.5	13.3	12.7	12.9	13.0
C_3	17.0	17.5	18.1	17.6	18.1	18.2
C_4	12.8	15.8	15.1	16.3	15.2	15.4
C_2-C_4	42.3	45.8	46.5	46.6	46.2	46.6
C_5^+	13.8	18.6	18.3	18.2	19.3	19.1
ROH	5.5	5.1	3.1	5.9	4.2	4.4
	Olefin Selectivity					
C_2-C_4 Olefin/ Paraffin Ratio	1.8	2.5	2.8	2.6	2.6	2.6
$C_2^=/C_2$	1.0	1.4	1.9	1.6	1.5	1.5
$C_3^=/C_3$	2.8	3.4	3.8	3.5	3.7	3.6
$C_4^=/C_4$	2.1	3.0	3.0	3.2	2.9	2.9

[a]Operating Conditions: P = 1465 kPa; Space Velocity = 1.0 $cm^3g^{-1}s^{-1}$; H_2/CO = 2/1; 20 hours on stream.

[b]Catalyst mass: 4.8 g; for other cases: 8.0 g.

(3.6 Mn/100 Fe) was chosen for the pretreating study. The pretreatment conditions were as follows: a temperature of 673 K, ambient pressure, a space velocity of 0.3 $cm^3g^{-1}s^{-1}$, and a period of 8 hours. The following standard operating conditions were used to evaluate the effect of the pretreating gas composition on activity, olefin selectivity, and product distribution: a H_2/CO of 2/1, a pressure of 1465 kPa, a space velocity of 1.0 $cm^3g^{-1}s^{-1}$, and a temperature of 483 K. For the case of hydrogen reduction, a temperature of 499 K was also used to increase the carbon monoxide conversion to a level of 6.5 - 7.5 percent. The catalyst was usually evaluated over 12 - 14 hours on stream to insure that the catalyst had attained a stationary state activity and selectivity.

The data on the activity, olefin selectivity, and the product distribution for the hydrogen reduction are listed in Table 9. At 483 K the carbon monoxide conversion, the yield of C_2-C_4, and C_5^+ hydrocarbons and the olefin-to-paraffin ratio of the C_2-C_4 fraction increased with the time on stream. However, the yields of carbon dioxide and methane declined with time. The olefin selectivity ratios of C_2, C_3, and C_4 increased with time on stream at 483 K. At 11.5 hours on stream these ratios for C_2, C_3, and C_4 were 1.5, 3.1, and 2.7, respectively. The reaction temperature was raised to 499 K at 11.5 hours on stream. The data at 13.5 hours on stream indicated that the carbon monoxide conversion increased from 3.5 to 7.2 percent. In addition, the carbon dioxide yield increased and the yields of methane and the C_2-C_4 hydrocarbons declined. The olefin-to-paraffin ratio of the C_2-C_4 fraction increased from 2.4 to 2.70 when the temperature was increased from 483 to 499 K. The data for

TABLE 9

PRODUCT DISTRIBUTION AND SELECTIVITY AS A FUNCTION OF TIME ON STREAM;[a] HYDROGEN REDUCTION FOR 8 HOURS; CATALYST YST-2

Time on Stream (hours):	0.5	3.0	7.2	11.5	13.5	12.6[b]
Temperature (K):	483	483	483	483	499	499
CO Conversion (mole %):	2.9	3.1	3.4	3.5	7.2	6.7
	Product Distribution (mole %)					
CO_2	9.2	5.5	6.8	7.1	12.1	11.6
C_1	31.3	24.7	21.5	21.0	18.3	18.2
C_2	12.6	13.3	13.8	14.1	13.0	13.5
C_3	17.3	18.2	18.8	19.0	17.9	18.5
C_4	12.3	16.0	16.4	16.7	16.8	15.4
C_2-C_4	42.2	47.5	49.0	49.8	46.7	47.4
C_5^+	11.3	16.5	18.2	18.0	18.1	19.1
ROH	6.0	5.8	4.5	4.1	4.1	3.7
	Olefin Selectivity					
C_2-C_4 Olefin/ Paraffin Ratio	0.9	1.7	2.2	2.4	2.7	2.8
$C_2^=/C_2$	0.3	0.8	1.3	1.5	1.7	1.9
$C_3^=/C_3$	1.8	2.5	3.0	3.1	3.6	3.8
$C_4^=/C_4$	1.0	2.2	2.6	2.7	3.1	3.0

[a]Operating Conditions: H_2/CO = 2/1; P = 1465 kPa; Space Velocity = 1.0 $cm^3 g^{-1} s^{-1}$.

[b]Reduction time: 20 hours.

catalyst YST-2 after a hydrogen reduction at 673 K for 20 hours are also presented in Table 9. The data on the activity, the olefin selectivity, and the product distribution for both reductions were very close with some minor differences (less than 10 percent). This similarity in the catalyst performances indicated that the shorter catalyst reduction time was sufficient to activate the catalyst for the hydrogenation of carbon monoxide.

The data for the catalyst activity, the olefin selectivity, and the product distribution as a function of time on stream for the carbon monoxide pretreatment are presented in Table 10. The carbon monoxide conversion, initially 21.9 percent at 0.5 hour on stream, declined to 8.4 percent at 12.5 hours on stream. The yields of methane and C_2-C_4 hydrocarbons decreased with time and the carbon dioxide and C_5^+ hydrocarbon yields increased. The C_2-C_4 fraction olefin-to-parrafin ratio increased to 1.7 over a period of 12.5 hours on stream. The olefin selectivity ratios for C_2, C_3, and C_4 also increased with time on stream. The ratios for C_2, C_3, and C_4 at 12.5 hours were 1.1, 2.5, and 1.5, respectively. The data for the catalyst activity, olefin selectivity, and product distribution for the carbon monoxide pretreatment after 20 hours are also shown in Table 10. The similarity in the catalyst performance (differences generally less than 10 percent) again indicated that the shorter pretreatment time was satisfactory for the activation of the catalyst.

The data for the activity, olefin selectivity, and product distribution for the synthesis gas (1 H_2/1 CO) pretreatment as a function of time on stream are presented in Table 11. The carbon monoxide conversion gradually decreased from 12.1 percent at 0.2

TABLE 10

PRODUCT DISTRIBUTION AND SELECTIVITY AS A FUNCTION OF TIME ON STREAM;[a] CARBON MONOXIDE PRETREATMENT FOR 8 HOURS; CATALYST YST-2

Time on Stream (hours):	0.5	4.5	6.5	9.0	12.5	12.3[b]
Temperature (K):	483	483	483	483	483	483
CO Conversion (mole %):	21.9	9.4	9.2	9.1	8.4	8.7
	Product Distribution (mole %)					
CO_2	2.2	5.6	8.3	9.7	9.3	6.8
C_1	28.3	26.5	25.0	24.0	23.8	24.1
C_2	24.3	11.1	10.9	10.8	10.9	11.7
C_3	15.5	19.0	17.6	17.2	17.2	13.6
C_4	12.3	13.8	14.6	14.2	14.0	19.8
C_2-C_4	52.1	43.9	43.1	42.2	42.1	45.1
C_5^+	15.0	21.5	20.4	21.1	22.3	21.5
ROH	2.4	2.5	3.2	3.0	2.5	2.5
C_2-C_4 Olefin/ Paraffin Ratio	Olefin Selectivity 1.1	1.4	1.5	1.6	1.7	1.4
$C_2^=/C_2$	2.2	0.8	0.9	1.0	1.1	0.8
$C_3^=/C_3$	0.8	2.1	2.3	2.4	2.5	2.2
$C_4^=/C_4$	0.4	1.3	1.4	1.5	1.5	1.3

[a]Operating Conditions: $H_2/CO = 2/1$; P = 1465 kPa; Space Velocity = 1.0 $cm^3 g^{-1} s^{-1}$.

[b]Pretreatment time: 20 hours.

TABLE 11

PRODUCT DISTRIBUTION AND SELECTIVITY AS A FUNCTION OF TIME ON STREAM;[a] 1 H_2/1 CO PRETREATMENT FOR 8 HOURS; CATALYST YST-2

Time on Stream (hours):	0.2	3.6	7.5	10.5	12.8
Temperature (K):	483	483	483	483	483
CO Conversion (mole %):	12.1	11.6	9.9	9.3	9.2
	Product Distribution (mole %)				
CO_2	13.8	13.7	12.6	12.6	12.8
C_1	46.6	26.4	25.9	26.4	27.1
C_2	8.1	14.2	14.9	15.3	15.9
C_3	12.4	15.8	15.1	15.7	15.9
C_4	9.7	12.3	12.1	11.8	11.1
C_2-C_4	30.2	42.3	42.1	42.8	42.9
C_5^+	7.7	14.9	16.8	15.9	14.9
ROH	1.7	2.7	2.6	2.3	2.3
	Olefin Selectivity				
C_2-C_4 Olefin/ Paraffin Ratio	2.4	2.8	3.8	3.7	3.8
$C_2^=/C_2$	0.2	0.9	1.3	1.3	1.4
$C_3^=/C_3$	13.5	6.6	14.6	10.6	11.6
$C_4^=/C_4$	9.3	7.3	9.2	9.4	10.5

[a]Operating Conditions: H_2/CO = 2/1; P = 1465 kPa; Space Velocity = 1.0 $cm^3 g^{-1} s^{-1}$.

hours to 9.2 percent at 12.8 hours on stream. The carbon dioxide yield was relatively constant during the course of the experiment. The yields for the C_2-C_4 and C_5^+ hydrocarbon increased and the methane production decreased with time on stream. The olefin-to-paraffin ratio of the C_2-C_4 hydrocarbon fraction also showed an increase with time on stream, from 2.4 at 0.2 hours to 3.8 at 12.8 hours. The olefin selectivity ratios for C_3 and C_4 fluctuated with time on stream; however, that for C_2 showed an increase, from 0.2 at 0.2 hours to 1.4 at 12.8 hours on stream. At 12.8 hours these ratios for C_2, C_3, and C_4 were 1.4, 11.6, and 10.5, respectively. The data for the activity, the olefin selectivity, and the product distribution for the synthesis gas (2 H_2/1 CO) pretreatment as a function of time on stream are presented in Table 12. The carbon monoxide conversion and the methane yield declined and the yields of carbon dioxide and C_2-C_4 hydrocarbons increased with the time on stream. The C_5^+ hydrocarbon yield was relatively constant at 15 - 16.5 percent during the test. The olefin-to-paraffin ratio in C_2-C_4 hydrocarbons increased slightly, that is, from 3.7 at 0.4 hours to 4.1 at 12.5 hours on stream. The olefin selectivity ratio for C_2 increased with the time on stream as that for C_3 decreased. The ratio for C_4 fluctuated with the time on stream. At 12.5 hours these ratios for C_2, C_3, and C_4 were 1.4, 10.5, and 13.0, respectively. The data for the activity, the olefin selectivity, and the product distribution for the synthesis gas (3 H_2/ 1 CO) pretreatment as a function of time on steam are presented in Table 13. The carbon monoxide conversion initially fluctuated but decreased to 6.6 percent at 12.5 hours on stream. The carbon dioxide yield was relatively independent of the time on stream. The yields

TABLE 12

PRODUCT DISTRIBUTION AND SELECTIVITY VERSUS TIME ON STREAM;[a] 2 H_2/1 CO PRETREATMENT FOR 8 HOURS; CATALYST YST-2

Time on Stream (hours):	0.4	4.5	7.2	10.2	12.5
Temperature (K):	483	483	483	483	483
CO Conversion (mole %):	10.5	9.2	7.6	7.3	7.1
	Product Distribution (mole %)				
CO_2	5.0	2.8	3.7	9.4	9.7
C_1	41.8	31.1	31.5	28.2	27.8
C_2	8.6	16.8	16.9	15.7	15.8
C_3	16.2	16.6	17.0	16.1	15.9
C_4	13.5	13.7	12.5	11.7	12.9
C_2-C_4	38.3	47.1	46.4	43.5	44.6
C_5^+	14.9	16.5	16.0	16.6	15.8
ROH	0	2.5	2.4	2.3	2.2
	Olefin Selectivity				
C_2-C_4 Olefin/ Paraffin Ratio	3.7	3.1	3.5	3.8	4.1
$C_2^=/C_2$	0.2	1.1	1.2	1.4	1.4
$C_3^=/C_3$	16.2	11.7	11.5	10.3	10.5
$C_4^=/C_4$	9.8	6.0	10.0	10.7	13.0

[a]Operating Conditions: H_2/CO = 2/1; P = 1465 kPa; Space Velocity = 1.0 $cm^3 g^{-1} s^{-1}$.

TABLE 13

PRODUCT DISTRIBUTION AND SELECTIVITY AS A FUNCTION OF TIME ON STREAM;[a] 3 H_2/1 CO PRETREATMENT FOR 8 HOURS; CATALYST YST-2

Time on Stream (hours):	0.5	3.6	5.0	7.5	12.5
Temperature (K):	483	483	483	483	483
CO Conversion (mole %):	8.7	12.4	9.5	8.2	6.6
	Product Distribution (mole %)				
CO_2	8.2	8.8	9.4	9.6	9.8
C_1	43.2	31.6	30.3	29.3	28.6
C_2	11.9	14.1	14.4	14.8	15.1
C_3	14.6	15.8	16.3	15.8	16.4
C_4	11.0	12.3	13.1	13.0	12.8
C_2-C_4	37.5	42.2	43.8	43.6	44.3
C_5^+	8.1	15.3	14.7	15.5	15.4
ROH	3.0	2.1	1.8	2.0	1.9
	Olefin Selectivity				
C_2-C_4 Olefin/ Paraffin Ratio	2.0	2.8	3.1	3.5	3.8
$C_2^=/C_2$	0.2	0.7	0.8	1.0	1.3
$C_3^=/C_3$	11.9	11.9	12.0	15.9	12.6
$C_4^=/C_4$	5.5	8.1	6.8	8.1	8.6

[a]Operating Conditions: H_2/CO = 2/1; P = 1465 kPa; Space Velocity = 1.0 $cm^3 g^{-1} s^{-1}$.

for C_2-C_4 and C_5^+ hydrocarbons increased as the methane production declined with the reaction time. The olefin-to-paraffin ratio of the C_2-C_4 hydrocarbon fraction also increased from 2.0 at 0.5 hours to 3.8 at 12.5 hours. The alcohol yield was very little, usually less than 2 percent of the total carbon products. The olefin selectivity ratios for C_2, C_3, and C_4 generally increased with the time on stream. At 12.5 hours on steam these ratios for C_2, C_3, and C_4 were 1.3, 12.6, and 8.6, respectively.

The data for the activity, the olefin selectivity, and the product distribution at 12 hours on stream for the five different pretreating gas compositions are presented in Table 14. The catalyst activity in terms of the carbon monoxide conversion for the hydrogen reduction was lower than the conversion observed for the other pretreatment. The total yield of carbon dioxide and methane following the hydrogen reduction was less than 29 percent whereas for the other pretreating gas compositions it was greater than 33 percent. The C_2-C_4 hydrocarbon yield for the hydrogen reduction was 49.8 percent whereas for the other pretreating gas compositions the yield was generally less than 45 percent. The olefin-to-paraffin ratio of C_2-C_4 hydrocarbon fraction for the hydrogen reduction, 2.4, was less than that obtained for the synthesis gas pretreatment, 3.8 - 4.1; however, it was higher than that obtained for the carbon monoxide pretreatment, 1.7. The C_2 olefin selectivity ratios for these five different pretreating gas compositions were in the range of 1.1 - 1.5. The olefin selectivity ratios for C_3 and C_4 for synthesis gas pretreatment, 10.5 - 12.6 and 8.6 - 13.0, respectively, were much greater than those obtained for the hydrogen reduction and the carbon monoxide

TABLE 14

INFLUENCE OF CATALYST PRETREATMENT ON PRODUCT DISTRIBUTION AND OLEFIN SELECTIVITY[a]

			H_2/CO Ratio		
Pretreatment:	H_2	CO	1/1	2/1	3/1
Temperature (K):	483	483	483	483	483
CO Conversion (mole %):	3.5	8.4	9.2	7.1	6.6
	Product Distribution (mole %)				
CO_2	7.1	9.3	12.8	9.7	9.8
C_1	21.0	23.8	27.1	27.8	28.6
C_2	14.1	10.9	15.9	15.8	15.1
C_3	19.0	17.2	15.9	15.9	16.4
C_4	16.7	14.0	11.1	15.9	12.8
C_2-C_4	49.8	42.1	42.9	44.6	44.3
C_5^+	18.0	22.3	14.9	15.8	15.4
ROH	4.1	2.5	2.3	2.2	1.9
	Olefin Selectivity				
C_2-C_4 Olefin/ Paraffin Ratio	2.4	1.7	3.8	4.1	3.8
$C_2^=/C_2$	1.5	1.1	1.4	1.4	1.3
$C_3^=/C_3$	3.1	2.5	11.6	10.5	12.6
$C_4^=/C_4$	2.7	1.5	10.5	13.0	8.6

[a]Operating Conditions: H_2/CO = 2/1; P = 1465 kPa; Space Velocity = 1.0 $cm^3 g^{-1} s^{-1}$; Catalyst YST-2 (3.6 Mn/100 Fe); Time on Stream: 12 hours.

pretreatment, 2.5 - 3.1 and 1.5 - 2.7, respectively.

Effects of Manganese on Activity and Selectivity

Five FT series iron-manganese catalysts were prepared to determine the influence of the manganese concentration on the product yield and the selectivity for the carbon monoxide hydrogenation. The operating conditions for the catalyst pretreatment were as follows: hydrogen reduction at the ambient pressure, a temperature of 673 K, a space velocity of 0.3 $cm^3g^{-1}s^{-1}$, and a period of 8 hours. The carbon monoxide hydrogenation reaction was carried out at the following conditions: a H_2/CO ratio of 2/1, a pressure of 1465 kPa, and a space velocity of 1.0 $cm^3g^{-1}s^{-1}$. The reaction temperature was adjusted to maintain the carbon monoxide conversion in the range of 6 - 8 mole percent.

The data on the activity, the olefin selectivity, and the product distribution as a function of the time on stream for catalyst FT-1 (pure iron) at 483 K is presented in Table 15. The experiment was conducted for a period of 14 hours. The carbon monoxide conversion was generally constant at 8.5 percent during the experiment. The carbon dioxide yield increased slightly from 9.3 percent at 3.0 hours to 11.8 percent at 13.5 hours on stream and the yields of methane and C_5^+ hydrocarbons declined with time. The C_2-C_4 hydrocarbon yield increased from 38.9 percent at 3.0 hours to 42.0 percent at 13.5 hours and the olefin-to-paraffin ratio in the C_2-C_4 fraction increased with the time on stream. The olefin selectivity ratios for C_2, C_3, and C_4 also increased with the time on stream. These ratios for C_2, C_3, and C_4 were 0.3, 3.3, and 9.0, respectively,

TABLE 15

PRODUCT DISTRIBUTION AND OLEFIN SELECTIVITY FOR CATALYST FT-1[a]

Time on Stream (hours):	3.0	6.5	7.7	13.5
Temperature (K):	483	483	483	483
CO Conversion (mole %):	9.7	8.6	8.4	8.5
	Product Distribution (mole %)			
CO_2	9.3	10.9	11.5	11.3
C_1	39.3	33.6	32.9	31.3
C_2	15.0	14.5	14.5	14.1
C_3	13.7	15.0	14.7	15.0
C_4	10.2	12.0	11.6	12.9
C_2-C_4	38.9	41.5	40.8	42.0
C_5^+	10.0	12.5	12.4	13.3
ROH	2.5	1.5	2.4	2.1
	Olefin Selectivity			
C_2-C_4 Olefin/ Paraffin Ratio	1.2	1.4	1.5	1.6
$C_2^=/C_2$	0.2	0.2	0.3	0.3
$C_3^=/C_3$	2.7	2.8	3.5	3.3
$C_4^=/C_4$	6.7	7.6	7.8	9.0

[a]Operating Conditions: H_2/CO = 2/1; P = 1465 kPa; Space Velocity = 1.0 $cm^3 g^{-1} s^{-1}$; 0 Mn/100 Fe atomic ratio.

at 13.5 hours on stream.

The data on the activity, olefin selectivity, and product distribution as a function of time on stream for catalyst FT-2 (2.5 Mn/100 Fe) at 493 K are presented in Table 16. The yields of C_2-C_4 hydrocarbon and alcohols were independent of the time on stream. The methane yield decreased and the yields of carbon dioxide and C_5^+ hydrocarbon increased with the time on stream. The C_2-C_4 olefin selectivity also increased with time on stream. The olefin selectivity ratio for C_2 increased with the time on stream as those for C_3 and C_4 fluctuated with time. The ratios for C_2, C_3, and C_4 at 12.5 hours on stream were 1.6, 12.2, and 14.2, respectively. The similarity between the data at 12.5 hours and 17.5 hours indicated that the catalyst reached a stationary state level of activity and selectivity after 12 hours on stream.

The data on the activity, the olefin selectivity, and the product distribution as a function of the time on stream for catalyst FT-3 (5.1 Mn/100 Fe) at 504 K are presented in Table 17. The carbon monoxide conversion, the olefin/paraffin ratio in the C_2-C_4 hydrocarbon fraction, and the carbon dioxide and C_5^+ hydrocarbon increased with time on stream. The methane yield declined with time on stream. The yields of C_2-C_4 and alcohol were insensitive to the time on stream. The olefin selectivity ratio for C_2 increased with time on stream; however, those for C_3 and C_4 fluctuated with time on stream. The ratios for C_2, C_3, and C_4 at 12.5 hours on stream were 1.9, 10.9, and 12.7, respectively.

The data on the activity, the olefin selectivity, and the product distribution for catalyst FT-4 (8.2 Mn/100 Fe) as a function

TABLE 16

PRODUCT DISTRIBUTION AND OLEFIN SELECTIVITY FOR CATALYST FT-2[a]

Time on Stream (hours):	3.0	8.5	12.5	17.5
Temperature (K):	493	493	493	493
CO Conversion (mole %):	4.1	4.7	6.2	6.2
	Product Distribution (mole %)			
CO_2	8.4	8.7	14.5	13.5
C_1	31.3	27.0	22.2	22.4
C_2	15.8	15.4	15.1	15.3
C_3	17.0	17.1	16.5	16.3
C_4	14.2	14.3	14.5	14.3
C_2-C_4	47.0	46.8	46.1	45.9
C_5^+	10.8	14.8	14.9	16.1
ROH	2.5	2.7	2.3	2.1
	Olefin Selectivity			
C_2-C_4 Olefin/ Paraffin Ratio	2.7	3.4	4.7	4.6
$C_2^=/C_2$	0.6	1.4	1.6	1.6
$C_3^=/C_3$	6.5	3.6	12.2	12.5
$C_4^=/C_4$	24.0	12.5	14.2	14.0

[a]Operating Conditions: H_2/CO = 2/1; P = 1465 kPa; Space Velocity = 1.0 $cm^3 g^{-1} s^{-1}$; 2.5 Mn/100 Fe atomic ratio.

TABLE 17

PRODUCT DISTRIBUTION AND OLEFIN SELECTIVITY FOR CATALYST FT-3[a]

Time on Stream (hours):	2.0	4.0	7.7	10.0	12.5
Temperature (K):	504	504	504	504	504
CO Conversion (mole %):	4.4	4.6	5.4	6.2	6.9
	Product Distribution (mole %)				
CO_2	7.8	13.8	14.5	15.0	19.0
C_1	33.7	25.8	21.8	20.9	19.8
C_2	14.0	13.8	13.7	14.4	13.9
C_3	16.2	15.3	15.9	16.0	15.6
C_4	14.2	14.1	15.2	14.9	13.5
C_2-C_4	44.4	43.2	44.8	45.3	43.0
C_5^+	12.0	14.7	16.9	16.7	16.0
ROH	2.1	2.5	2.1	2.1	1.9
	Olefin Selectivity				
C_2-C_4 Olefin/ Paraffin Ratio	2.6	3.6	4.4	4.6	5.0
$C_2^=/C_2$	0.4	1.0	1.6	1.8	1.9
$C_3^=/C_3$	6.4	11.2	12.8	14.4	10.9
$C_4^=/C_4$	42.9	10.5	7.8	6.8	12.7

[a]Operating Conditions: H_2/CO = 2/1; P = 1465 kPa; Space Velocity = 1.0 $cm^3 g^{-1} s^{-1}$; 5.1 Mn/100 Fe atomic ratio.

of time on stream at 503 K are presented in Talbe 18. The carbon monoxide conversion, the olefin-to-paraffin ratio of the C_2-C_4 hydrocarbon fraction, and the yields fo carbon dioxide and C_5^+ hydrocarbon increased with time on stream whereas the methane yield decreased. The yield of C_2-C_4 hydrocarbons and alcohols remained relatively constant at 42 - 45 percent and 2.5 percent, respectively, with time on stream. The olefin selectivity ratio for C_2 increased with time on stream but those for C_3 and C_4 generally fluctuated with the time on stream. The ratios for C_2, C_3, and C_4 at 12.5 hours on stream were 2.1, 12.3, and 15.5, respectively.

The data on the activity, the olefin selectivity, and the product distribution for the catalyst FT-5 (11.8 Mn/100 Fe) as a function of time on stream at 504 K is presented in Table 19. During this test the carbon monoxide conversion and the yields of the C_2-C_4 smf C_5^+ hydrocarbon and the alcohols were relatively constant at 7.0, 43.0, 15.5, and 2.5 percent, respectively. However, the carbon dioxide yield and the olefin-to-paraffin ratio in the C_2-C_4 hydrocarbon fraction increased and the methane yield decreased with time on stream. The olefin selectivity ratio for C_2 increased with time on stream but those for C_3 and C_4 fluctuated with time on stream. The ratios for C_2, C_3, and C_4 at 12.8 hours on stream were 2.0, 11.1, and 17.6, respectively.

The activity, olefin selectivity, and the product selectivity for these five iron-manganese catalysts at 12 hours on stream are compared in Table 20. Catalyst FT-1 was relatively more active then the iron-manganese catalysts since the carbon monoxide conversion was 8.5 percent at 483 K while for the other catalysts it was 6 - 8 percent at temperatures ranging from 493 to 504 K. The iron-manganese

TABLE 18

PRODUCT DISTRIBUTION AND OLEFIN SELECTIVITY FOR CATALYST FT-4[a]

Time on Stream (hours):	3.0	4.5	7.5	10.5	12.5
Temperature (K):	503	503	503	503	503
CO Conversion (mole %):	6.5	5.6	7.0	7.2	7.7
	Product Distribution (mole %)				
CO_2	13.2	13.3	19.7	21.1	21.4
C_1	28.3	22.5	20.7	19.1	19.1
C_2	15.0	14.8	14.8	14.7	14.7
C_3	15.9	16.5	15.9	15.2	15.7
C_4	13.4	13.0	12.1	12.3	11.9
C_2-C_4	44.3	46.2	42.8	42.2	42.3
C_5^+	11.8	15.6	14.2	15.4	14.8
ROH	2.4	2.4	2.6	2.2	2.4
	Olefin Selectivity				
C_2-C_4 Olefin/ Paraffin Ratio	2.7	4.0	4.9	5.1	5.0
$C_2^=/C_2$	0.7	1.4	1.8	2.1	2.1
$C_3^=/C_3$	8.1	7.1	13.8	15.8	12.3
$C_4^=/C_4$	9.5	17.0	13.2	17.3	15.5

[a]Operating Conditions: H_2/CO = 2/1; P = 1465 kPa; Space Velocity = 1.0 $cm^3g^{-1}s^{-1}$; 8.2 Mn/100 Fe atomic ratio.

TABLE 19

PRODUCT DISTRIBUTION AND OLEFIN SELECTIVITY FOR CATALYST FT-5[a]

Time on Stream (hours):	3.3	5.8	7.0	10.0	12.8
Temperature (K):	504	504	504	504	504
CO Conversion (mole %):	7.1	7.3	7.0	6.9	6.8
	Product Distribution (mole %)				
CO_2	13.4	17.5	18.2	19.1	19.7
C_1	25.2	21.8	20.4	19.8	19.1
C_2	14.1	13.2	13.9	14.1	14.3
C_3	15.7	15.1	16.1	15.6	15.8
C_4	13.4	14.6	13.2	13.0	13.1
C_2-C_4	43.2	42.9	43.2	42.7	43.1
C_5^+	15.6	15.2	15.8	15.9	15.8
ROH	2.6	2.6	2.4	2.5	2.3
	Olefin Selectivity				
C_2-C_4 Olfefin/ Paraffin Ratio	3.0	4.1	4.6	5.2	5.3
$C_2^=/C_2$	0.9	1.3	1.6	1.8	2.0
$C_3^=/C_3$	7.7	10.8	9.8	15.1	11.1
$C_4^=/C_4$	8.7	9.8	12.9	12.9	17.6

[a]Operating Conditions: H_2/CO = 2/1; P = 1465 kPa; Space Velocity = 1.0 $cm^3 g^{-1} s^{-1}$; 11.8 Mn/100 Fe atomic ratio.

TABLE 20

COMPARISON OF PRODUCT DISTRIBUTION AND OLEFIN SELECTIVITY FOR FT SERIES Fe-Mn PRECIPITATED CATALYSTS[a]

Catalyst:	FT-1	FT-2	FT-3	FT-4	FT-5
Mn/100 Fe	0	2.5	5.1	8.2	11.8
Temperature (K):	483	493	504	503	504
CO Conversion (mole %):	8.5	6.2	6.9	7.7	6.8
	Product Distribution (mole %)				
CO_2	11.3	14.5	19.3	21.4	19.7
C_1	31.3	22.2	19.8	19.1	19.1
C_2	14.1	15.1	13.9	14.7	14.3
C_3	15.0	16.5	15.6	15.7	15.8
C_4	12.9	14.5	13.5	11.9	13.1
C_2-C_4	42.0	46.1	43.0	42.3	43.1
C_5^+	13.3	14.9	16.0	14.8	15.8
ROH	2.1	2.3	1.9	2.4	2.3
	Olefin Selectivity				
C_2-C_4 Olefin/ Paraffin Ratio	1.6	4.7	5.0	5.0	5.3
$C_2^=/C_2$	0.3	1.6	1.9	2.1	2.0
$C_3^=/C_3$	3.3	12.2	10.9	12.3	11.1
$C_4^=/C_4$	9.0	14.2	12.7	15.5	17.6

[a]Operating Conditions: H_2/CO = 2/1; P = 1465 kPa; Space Velocity = 1.0 $cm^3 g^{-1} s^{-1}$; Time on Stream: 12 hours.

at temperatures ranging from 493 to 504 K. The iron-manganese catalysts were more selective for the production of C_2-C_4 olefins than the pure iron catalyst since catalyst FT-1 (pure iron) had an olefin-to-paraffin ratio in the C_2-C_4 hydrocarbon fraction of only 1.6 and the iron-manganese catalysts generally gave olefin-to-paraffin ratios ranging from 4.7 to 5.3. The C_2-C_4 hydrocarbon yields for these five catalysts were generally in the range of 42 - 46 percent. The methane yield for catalyst FT-1, 31.3 percent, was greater than that for the iron-manganese catalysts, 19 - 22 percent. However, the carbon dioxide and C_5^+ hydrocarbon yields for catalyst FT-1, 11.3 and 13.3 respectively, were lower than those for the iron-manganese catalysts, 14 - 22 and 14 - 16 percent, respectively. The alcohol yield, 1.9 - 2.4 percent, was relatively small for these five catalysts. The olefin selectivity ratios for C_2, C_3, and C_4 for catalyst FT-1, 0.3, 3.3, and 9.0, respectively, were also lower than those for the iron-manganese catalysts, 1.6 - 2.1, 10.9 - 12.3, and 12.7 - 17.6, respectively. It was obvious that the iron-manganese catalysts were more selective for the production of low molecular weight olefins than the pure iron catalyst.

Effects of Manganese on Selective Chemisorption

The adsorption properties of the FT series of iron-manganese catalysts were determined in a constant gas adsorption apparatus. Hydrogen and carbon monoxide were used as the adsorptives for the determination of the adsorption isotherms at an ambient temperature of 292 K. The details for the calculations of the adsorption isotherm are listed in Appendix C. The total amount of the gas adsorbed

by the catalyst at each equilibrium pressure was plotted versus the equilibrium pressure. The best straight line through the n isotherm point was extrapolated to zero pressure and the intercept was the monolayer amount of gas adsorbed by the catalyst.

The hydrogen chemisorption isotherm for catalyst FT-1 at 292 K is presented in Figure 26. The range of the equilibrium pressures was 60 - 230 Torr. The intercept at zero pressure indicated that the amount of the hydrogen chemisorption was 1.5 μ mole $(g\ catalyst)^{-1}$. The hydrogen isotherms for catalyst FT-2 were determined at 292 K. The amount of hydrogen chemisorbed at 292 K was 7.6 μ mole g^{-1}. The hydrogen adsorption isotherms at 292 K for catalysts FT-3, FT-4, and FT-5 are presented in Figures 28, 29, and 30, respectively. The adsorption isotherm was generally linear in the pressure range 100 - 350 Torr. The amount of the hydrogen gas adsorbed by catalysts FT-3, FT-4, and FT-5 were 0.5 μ mole g^{-1}, 0.35 μ mole g^{-1}, and 0.30 μ mole g^{-1}, respectively. Generally speaking the amount of the hydrogen chemisorption at 292 K for the FT series of catalysts was very small except for catalyst FT-2.

The carbon monoxide chemisorption isotherms were also determined at 292 K for the FT series catalysts. The linear region is 100 - 400 Torr. The carbon monoxide isotherms for catalysts FT-1 through FT-5 are presented in Figures 31 through 35. The intercepts at zero pressure for these adsorption isotherms indicated the amounts of the carbon monoxide gas chemisorbed by these catalysts. The intercepts at zero pressure for the second adsorption isothersm were zero for these catalysts. These results indicated that the amount of the physically adsorbed carbon monoxide gas at zero pressure for the

Figure 26

Hydrogen Chemisorption Isotherm;

Temperature = 292 K;

Catalyst FT-1

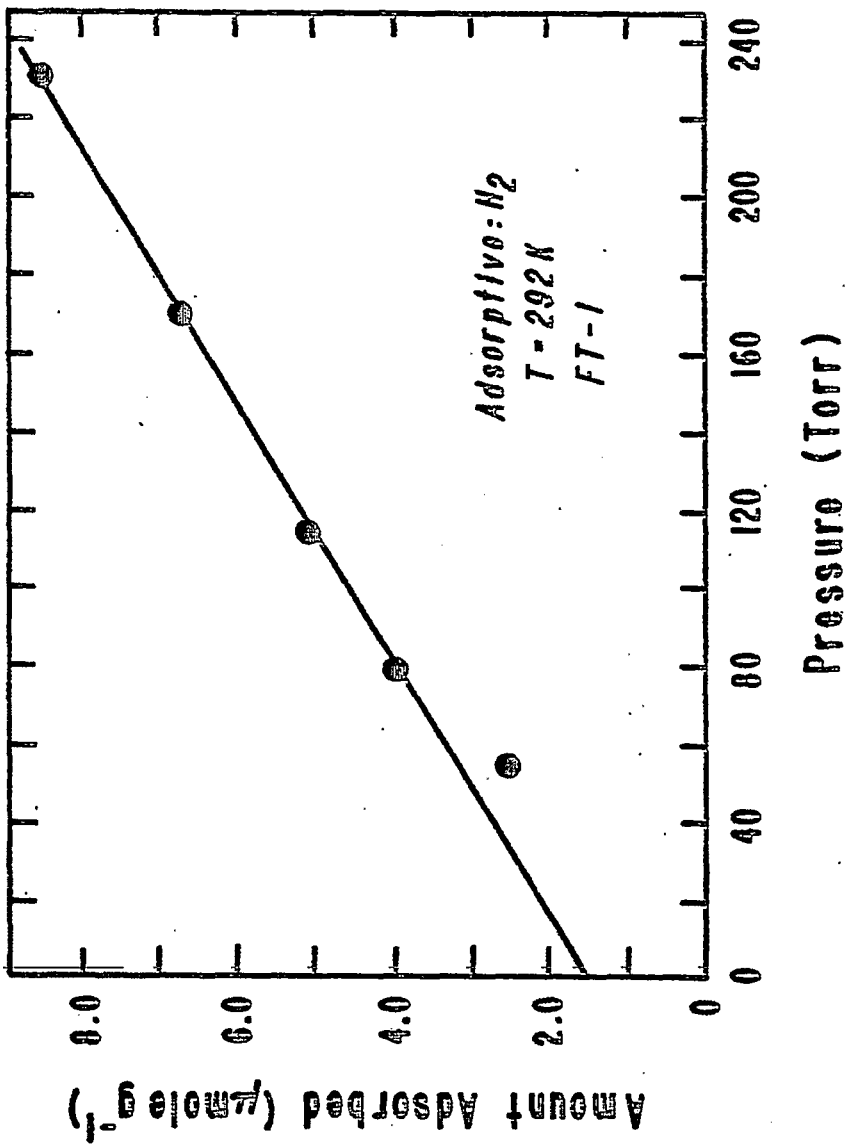
Amount Adsorbed (μmole g⁻¹)
8.0
6.0
4.0
2.0
0
0
40
80
120
160
200
240
Pressure (Torr)
Adsorptive: H2
T - 292 K
FT-1

Figure 27

Hydrogen Chemisorption Isotherm;

Temperature = 292 K;

Catalyst FT-2

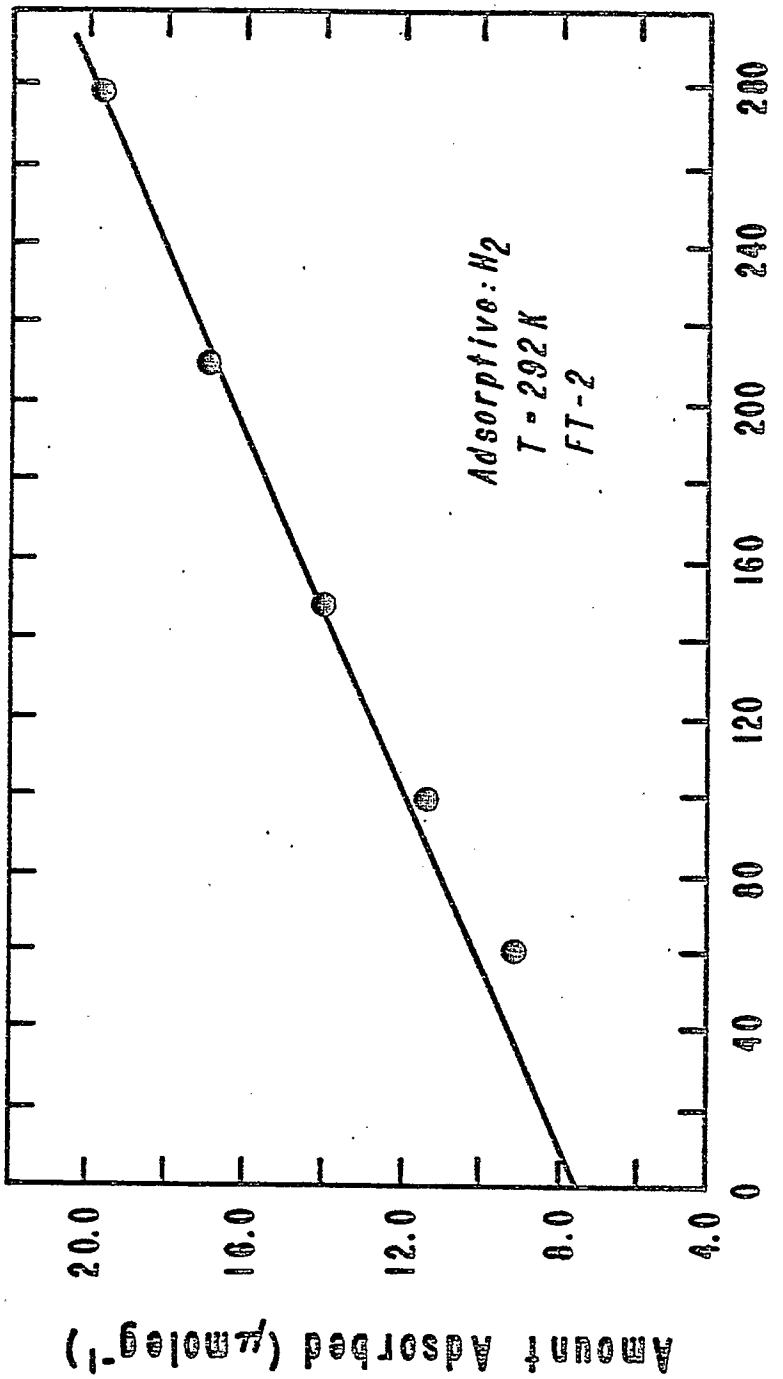
Amount Adsorbed (μmole g⁻¹)
20.0
16.0
12.0
8.0
4.0
0
40
80
120
160
200
240
280
Pressure (Torr)
Adsorptive: H2
T = 292 K
FT-2

Figure 28

Hydrogen Chemisorption Isotherm;

Temperature = 292 K;

Catalyst FT-3

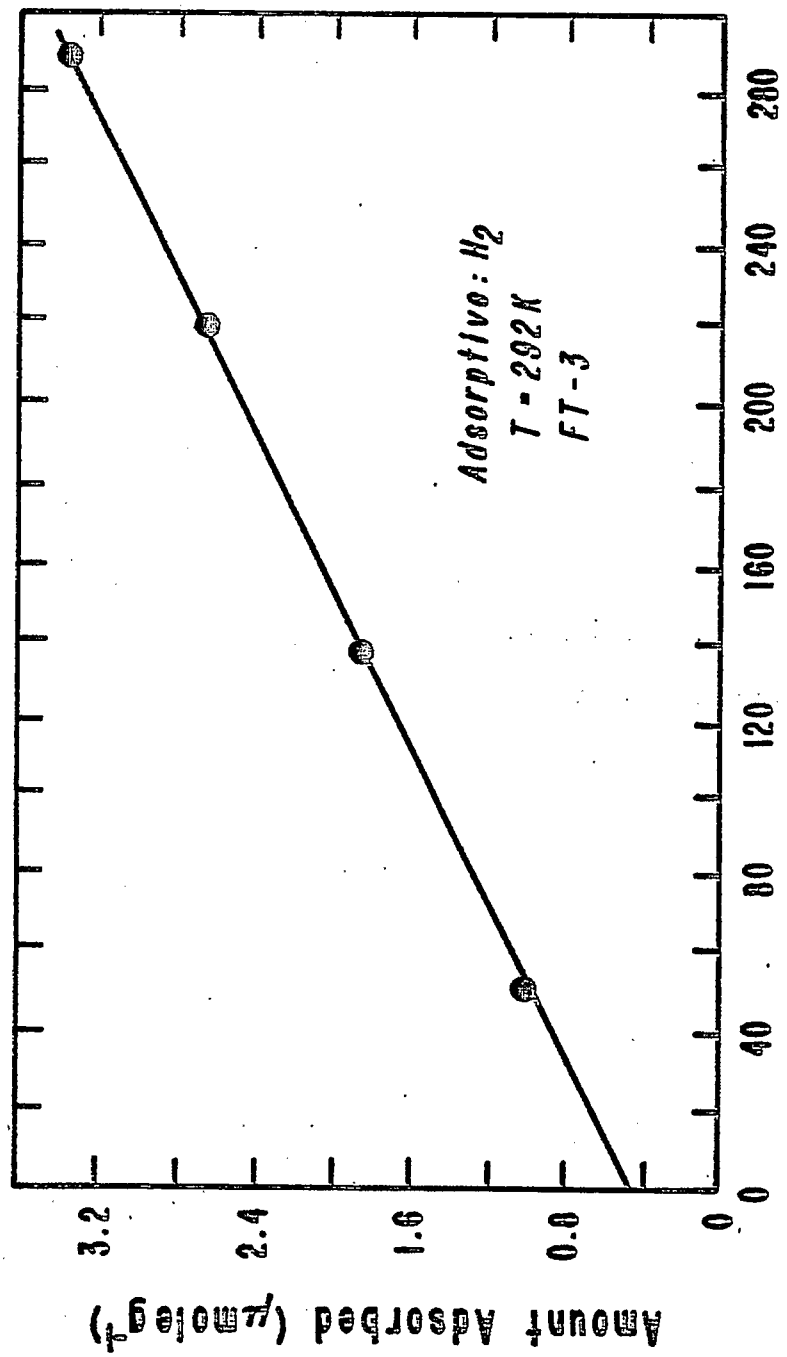
Adsorptive: H_2
T - 292 K
FT-3
Amount Adsorbed (μmole g^{-1})
Pressure (Torr)
0.0
1.6
2.4
3.2
0
40
80
120
160
200
240
280

Figure 29

Hydrogen Chemisorption Isotherm;

Temperature = 292 K;

Catalyst FT-4

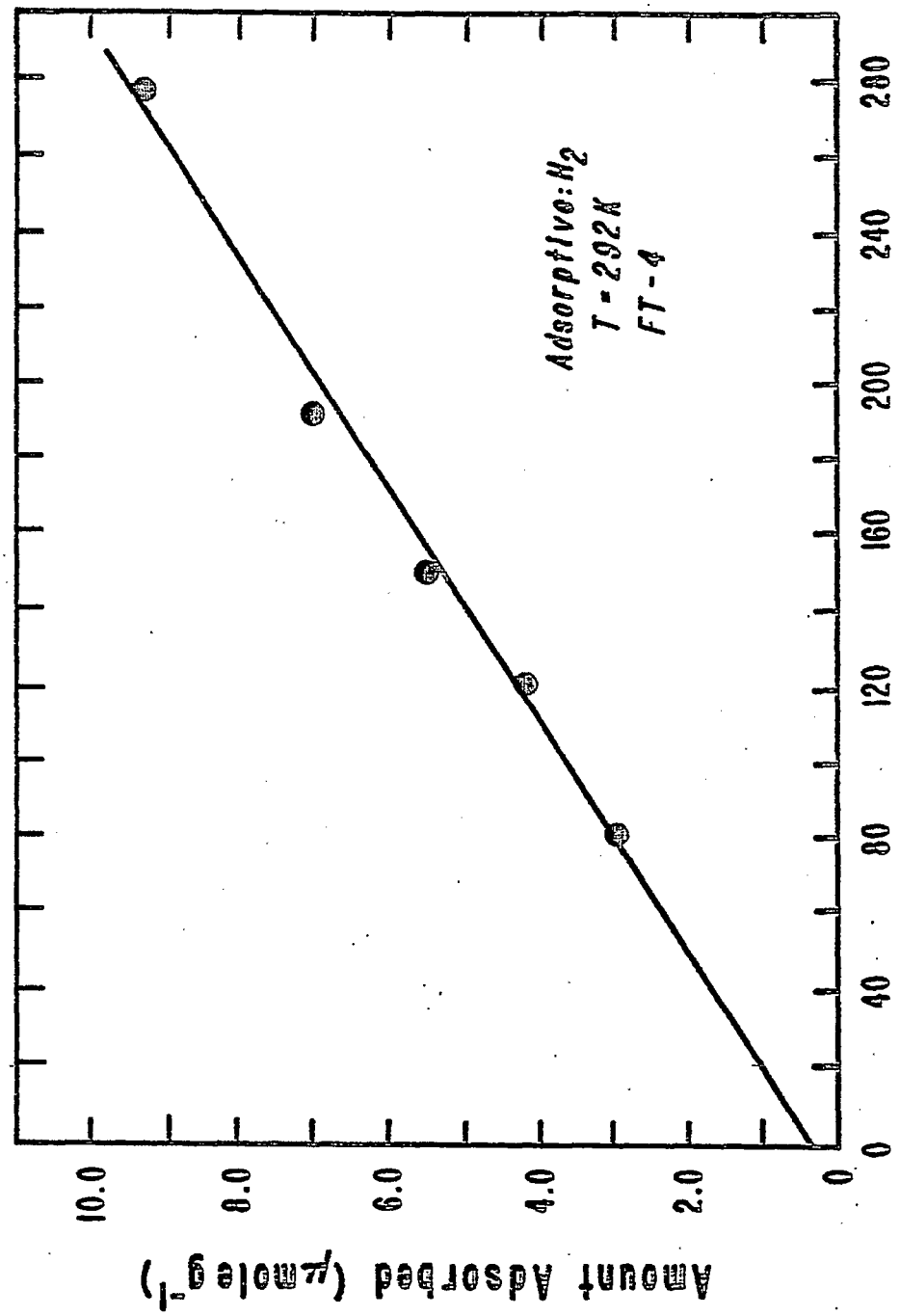
Adsorptive: H_2
T - 292K
FT - 4
Amount Adsorbed (μmole g^{-1})
Pressure (Torr)
0
2.0
4.0
6.0
8.0
10.0
40
80
120
160
200
240
280

Figure 30

Hydrogen Chemisorption Isotherm;

Temperature = 292 K;

Catalyst FT-5

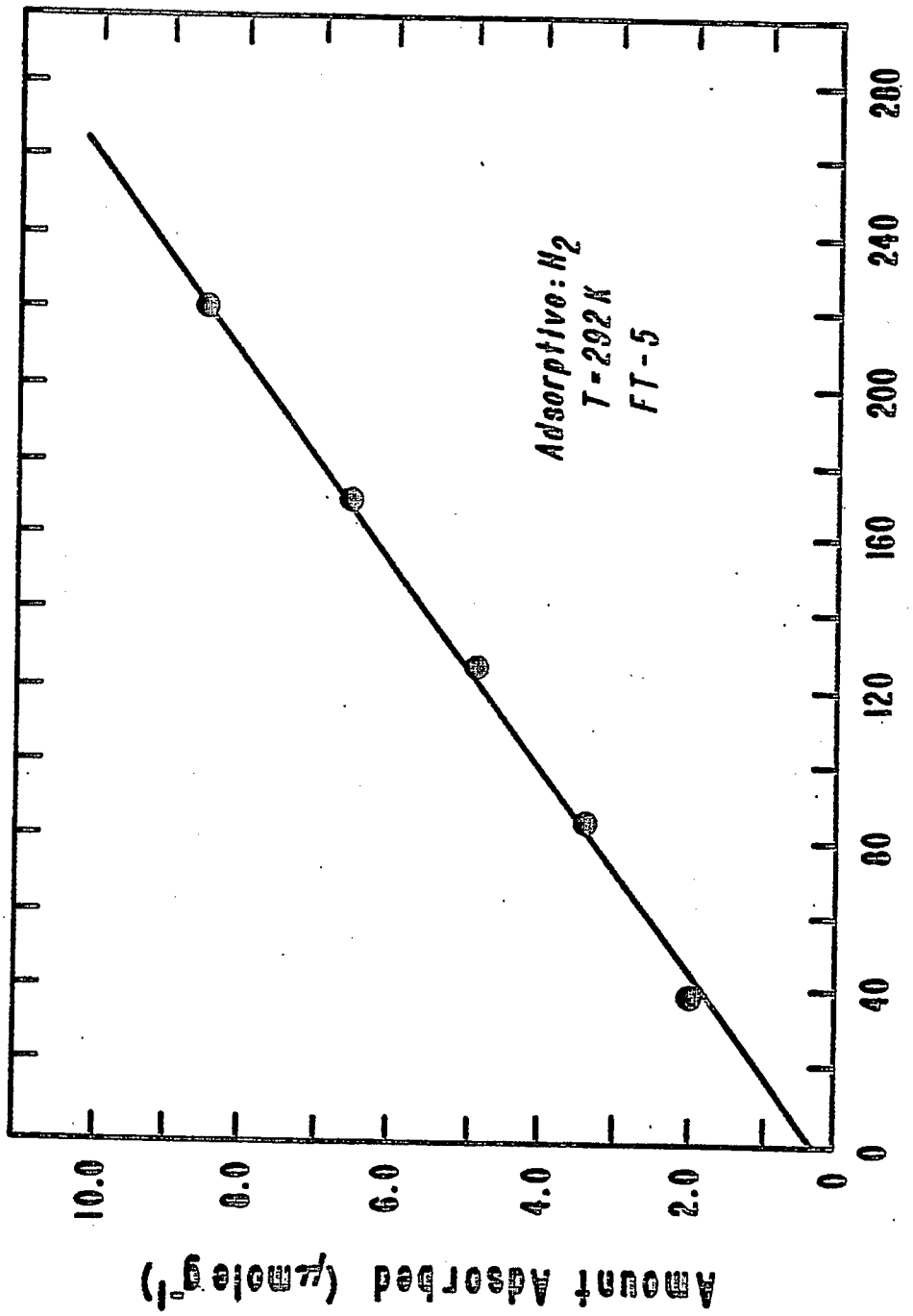
Amount Adsorbed (μmole g⁻¹)
10.0
8.0
6.0
4.0
2.0
0
0
40
80
120
160
200
240
280
Pressure (Torr)
Adsorptive: H2
T-292 K
FT-5

Figure 31

Carbon Monoxide Chemisorption Isotherm;

Temperature = 292 K;

Catalyst FT-1

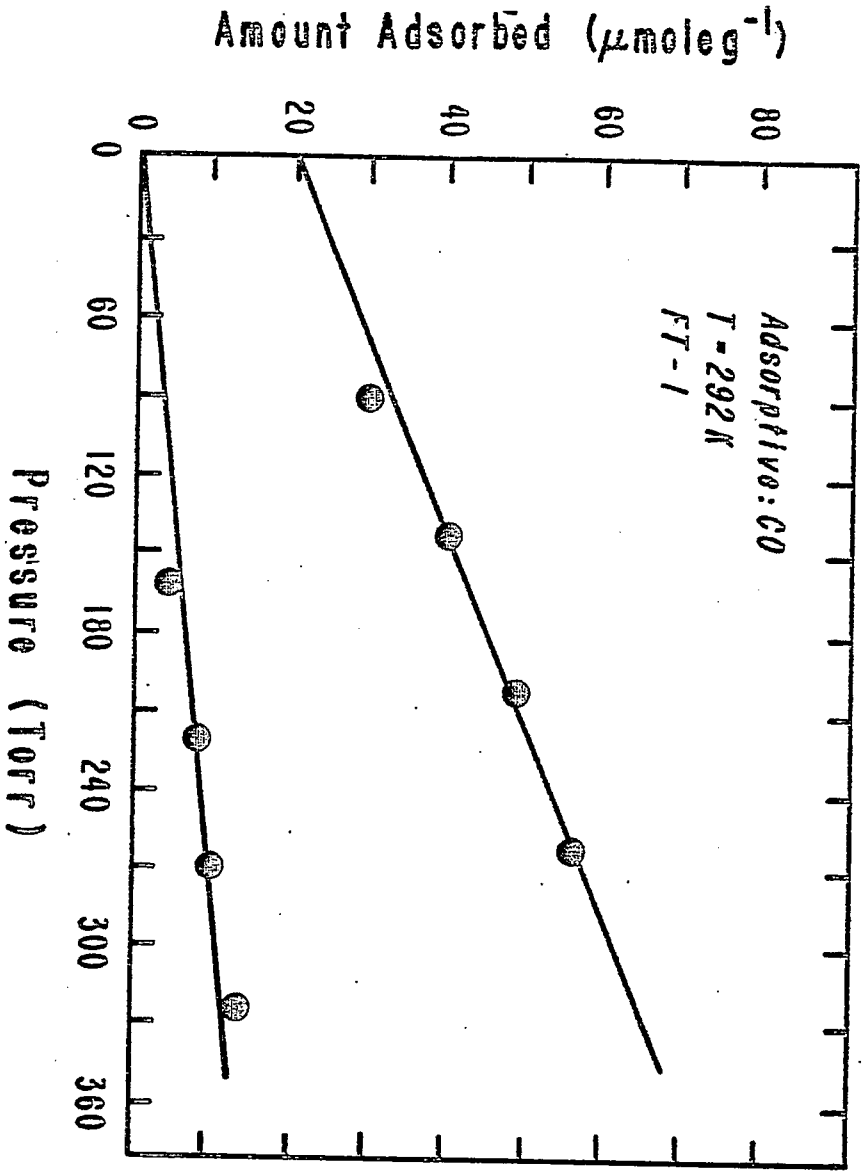
Amount Adsorbed (μmoleg⁻¹)
0
20
40
60
80
Pressure (Torr)
0
60
120
180
240
300
360
Adsorptive: CO
T = 292 K
FT-1

Figure 32

Carbon Monoxide Chemisorption Isotherm;

Temperature = 292 K;

Catalyst FT-2

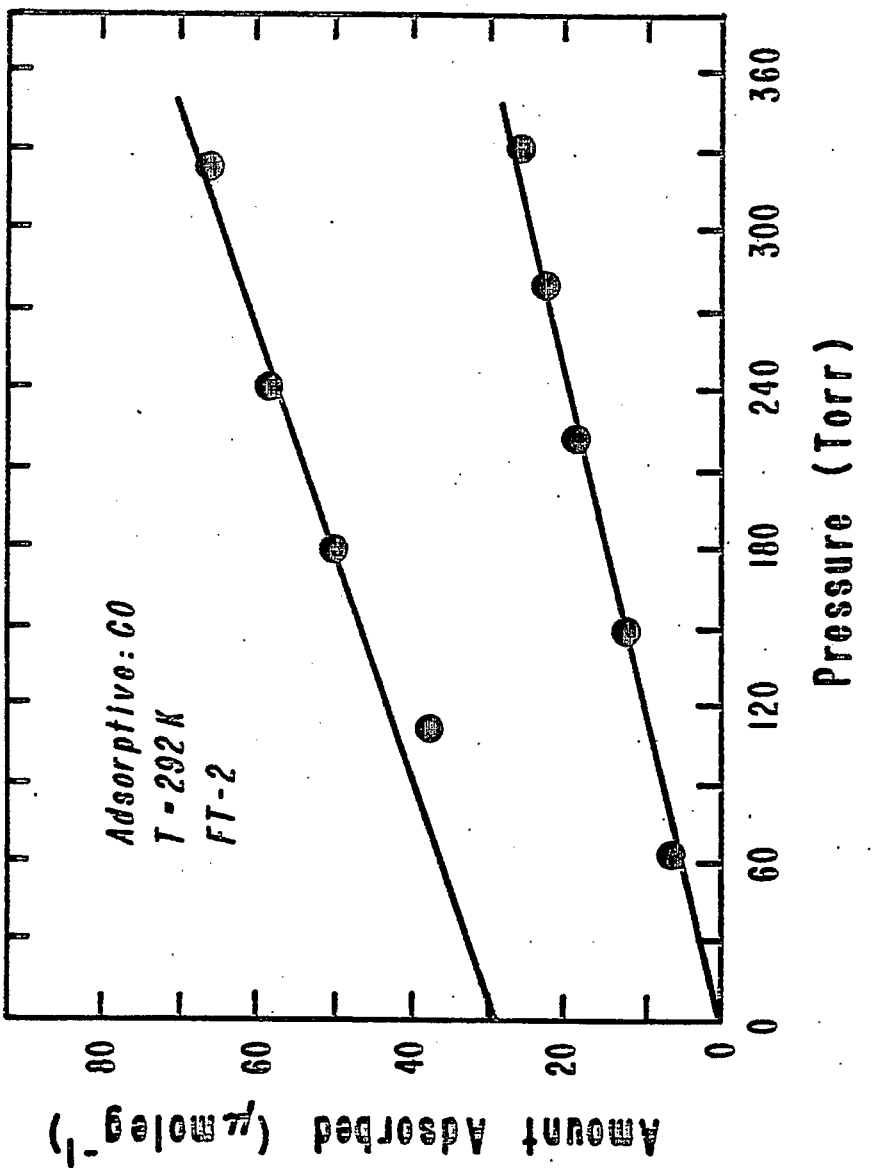
Adsorptive: CO
T - 292 K
FT-2
Amount Adsorbed (μmole g⁻¹)
Pressure (Torr)
0
20
40
60
80
0
60
120
180
240
300
360

Figure 33

Carbon Monoxide Chemisorption Isotherm;

Temperature = 292 K;

Catalyst FT-3

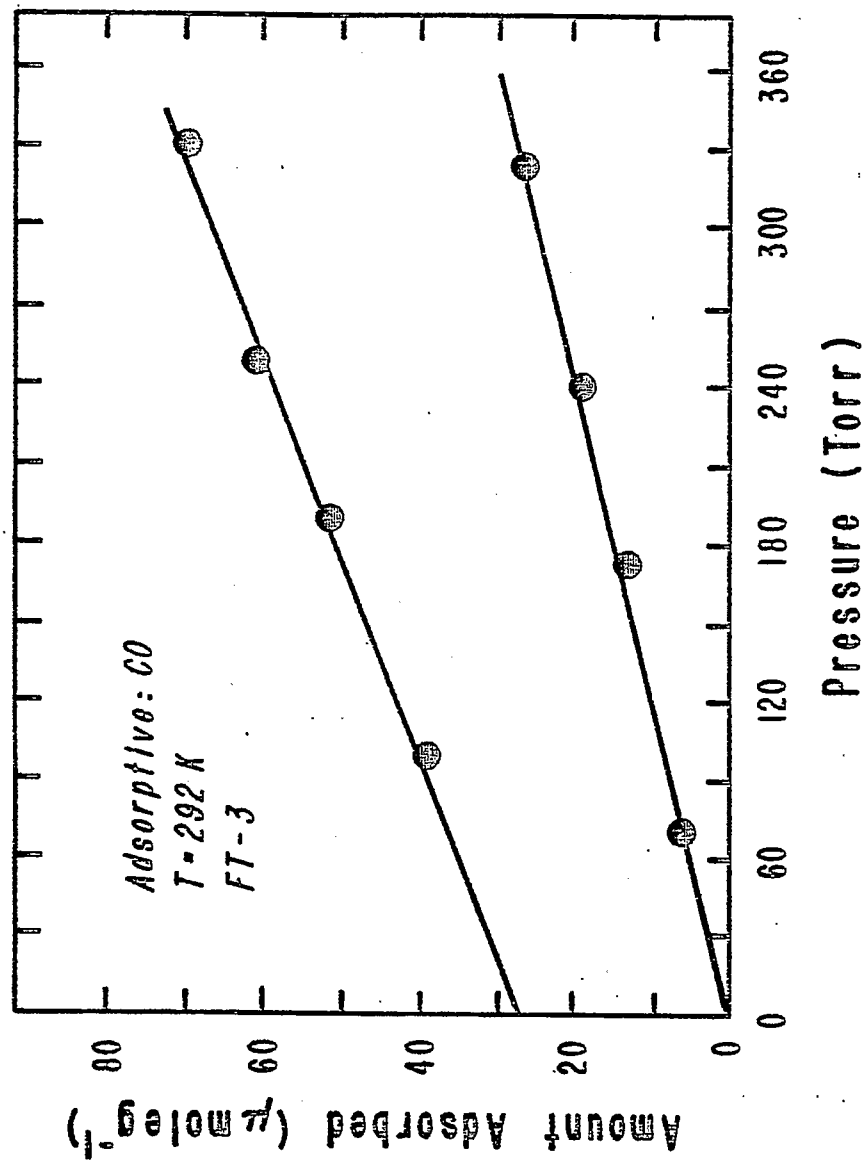
Amount Adsorbed (μmoleg⁻¹)
Pressure (Torr)
Adsorptive: CO
T = 292 K
FT-3
0
20
40
60
80
0
60
120
180
240
300
360

Figure 34

Carbon Monoxide Chemisorption Isotherm;

Temperature = 292 K;

Catalyst FT-4

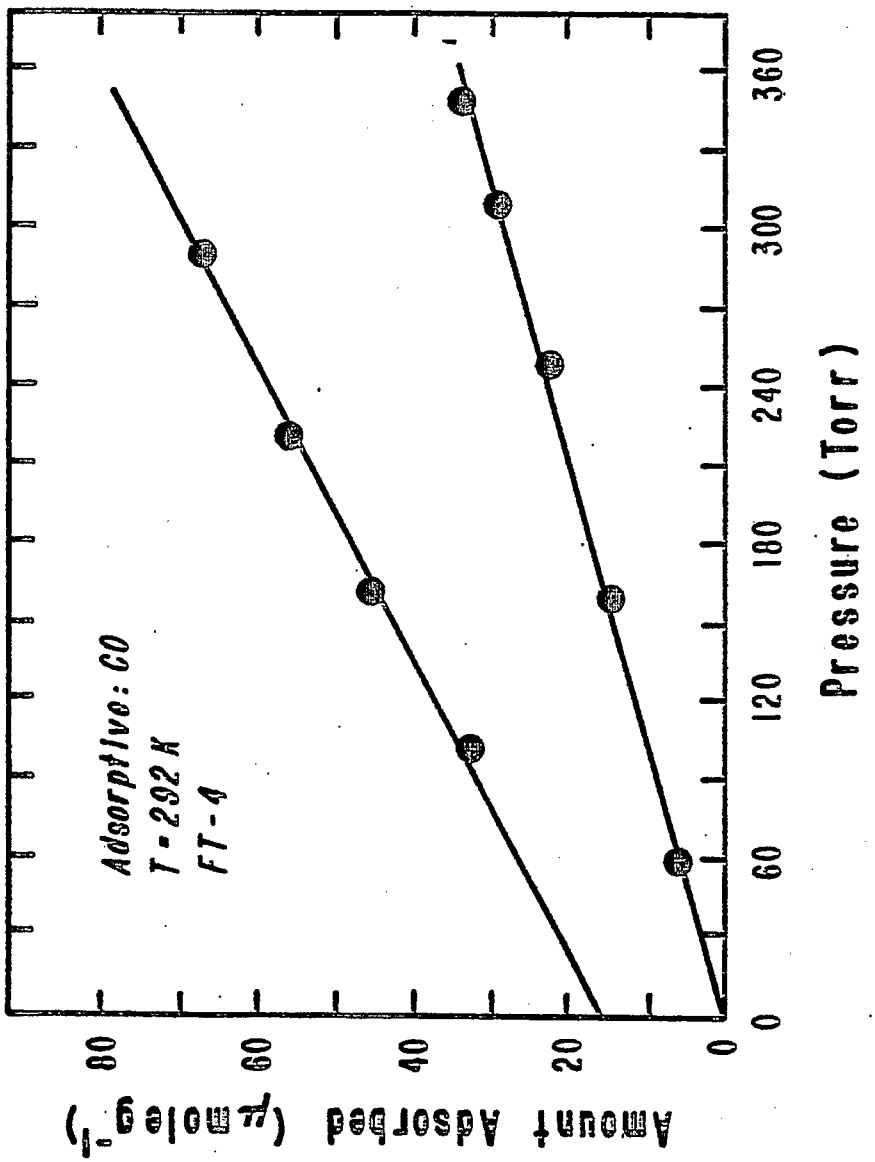
Adsorptive: CO
T - 292 K
FT - 4
Amount Adsorbed (μmole g⁻¹)
Pressure (Torr)
0
20
40
60
80
0
60
120
180
240
300
360

Figure 35

Carbon Monoxide Chemisorption Isotherm;

Temperature = 292 K;

Catalyst FT-5

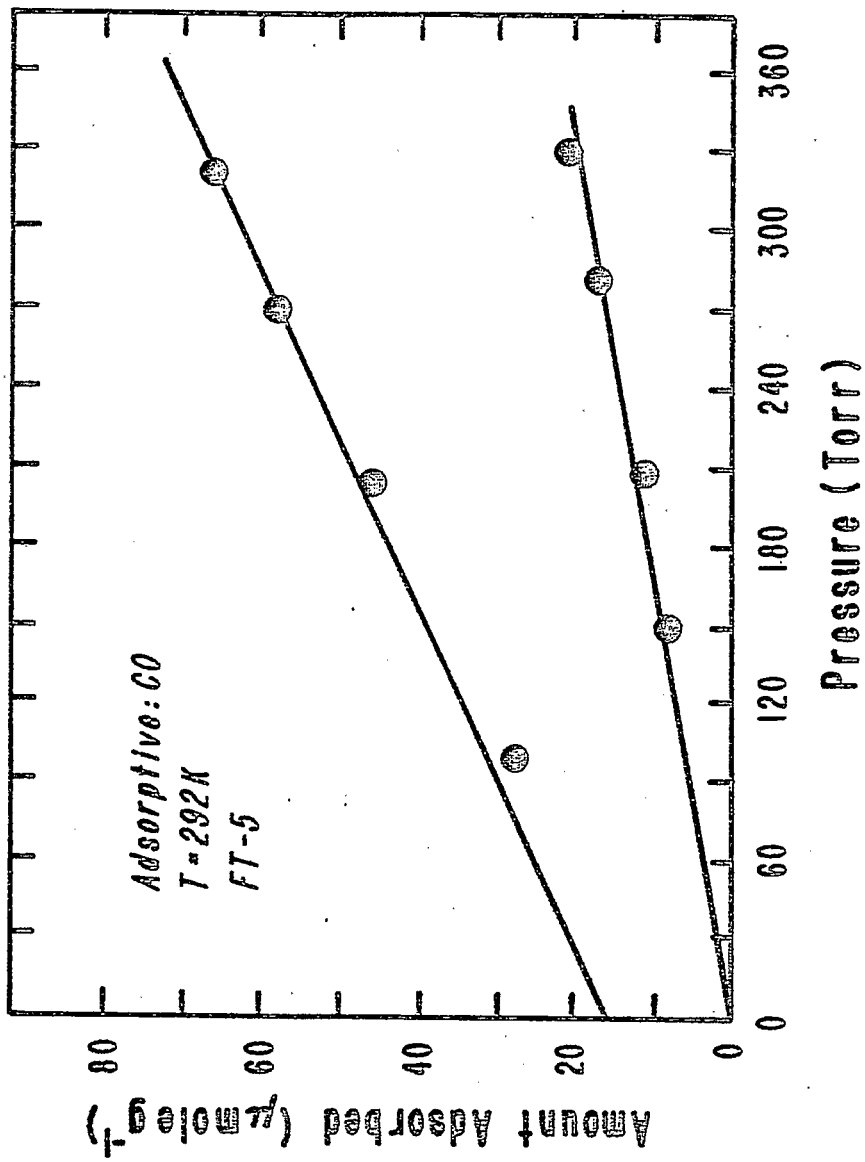
Adsorptive: CO
T = 292K
FT-5
Amount Adsorbed (μmole g⁻¹)
Pressure (Torr)
0
20
40
60
80
0
60
120
180
240
300
360

FT series catalyst was nil at 292 K. Therefore, the carbon monoxide uptakes for catalysts FT-1, FT-2, FT-3, FT-4, and FT-5 at 292 K were 20.4 μ mole g^{-1}, 29.2 μ mole g^{-1}, 27.2 μ mole g^{-1}, 16.0 μ mole g^{-1}, and 16.0 μ mole g^{-1}, respectively. The carbon monoxide uptakes were considerably larger than the hydrogen uptakes for these catalysts.

The data for the hydrogen and carbon monoxide uptakes for the FT series catalysts are summarized in Table 21. The higher the manganese content of the catalyst was, the lower the hydrogen uptake was except for the case of catalyst FT-2. The carbon monoxide uptake for the FT series catalysts was in the range of 16 - 30 μ mole g^{-1}. The carbon monoxide to hydrogen ratio for the iron-manganese catalysts was generally higher than that for the pure iron catalysts except for the case of catalyst FT-2.

TABLE 21
HYDROGEN AND CARBON MONOXIDE CHEMISORPTION DATA FOR Fe-Mn CATALYSTS AT 292 K

Catalyst	Mn/100 Fe	H_2 Uptake (μ mole g^{-1})	CO Uptake (μ mole g^{-1})	CO/H
FT-1	0	1.5	20.4	6.8
FT-2	2.5	7.6	29.2	1.9
FT-3	5.1	0.5	27.2	27.2
FT-4	8.2	0.35	16.0	22.9
FT-5	11.8	0.30	16.0	26.9

The summary of specific activity based on the turnover frequency (TOF) for the FT series iron-manganese catalysts is prestented in Table 22. Turnover frequencies were calculated based on the carbon monoxide uptakes at 292 K for these catalysts and the assumption of an adsorption stoichiometry of Fe/CO = 1. The details of the calculations for the turnover frequencies are listed in Appendix D. Generally, at 483 K the pure iron catalyst (FT-1) gave a

TABLE 22
COMPARISON OF SPECIFIC ACTIVITY FOR FT SERIES Fe-Mn PRECIPITATED CATALYSTS[a]

Catalyst:	FT-1	FT-2	FT-3	FT-4	FT-5
Mn/100 Fe:	0	2.5	5.1	8.2	11.8
Temperature (K):	483	493	504	503	504
	Turnover Frequency ($s^{-1} \times 10^3$)				
CO	40.3	19.2	25.9	47.2	39.1
CO_2	4.6	2.8	5.0	10.1	7.7
C_1	12.6	4.3	5.1	9.0	7.5
C_2	2.8	1.5	1.8	3.5	2.8
C_3	2.0	1.1	1.4	2.5	2.1
C_4	1.3	0.7	0.9	1.4	1.3
C_5^+	1.0	0.5	0.8	1.3	1.1
ROH	0.6	0.3	0.3	0.7	0.6

[a]Operating Conditions: $H_2/CO = 2/1$; P = 1465 kPa; Space Velocity = 1.0 $cm^3 g^{-1} s^{-1}$; Time On Stream: 12 hours.

relatively higher carbon monoxide turnover frequency, that is, 40.3 x $10^{-3}s^{-1}$, than the iron-manganese catalysts in the temperature range 493 - 504 K except for the case of catalyst FT-4 [i.e., $(TOF)_{CO}$ = 47.2 x $10^{-3}s^{-1}$]. The turnover frequency for these iron-manganest catalysts at the temperatures ranging from 483 K to 504 K was in the range of 19 - 48 x $10^{-3}s^{-1}$. In addition, for each of the FT series catalysts, the turnover frequency for either carbon dioxide or methane was higher than those for C_2, C_3, C_4, and C_5^+ hydrocarbons and alcohols.

DISCUSSION

Coprecipitation for Iron-Manganese Catalysts

The coprecipitation technique was used for the preparation of the iron-manganese catalysts in this investigation. The data for the catalyst compositions in Table 1 indicated that the coprecipitation technique was capable of providing reproducible catalyts with the desired compositions. Generally, the preparation procedures for FT series catalysts are more reproducible than those for YST series catalysts because the deviation from the actual catalyst composition for FT series catalysts, that is, about 5%, was less than that for YST series catalysts. Thus it was concluded that the procedure in which concentrated ammonium hydroxide is added to the homogeneous mixture of iron nitrate and manganese nitrate was the more reliable method in terms of the reproducibility.

The major phase in the bulk structure of the iron-manganese catalysts was identified as hematite (α-Fe_2O_3). The catalyst was calcined in an oven at 573 K for 17 hours before the x-ray diffraction test. Hofer[43] reported that the dehydration of hydrous ferric oxide at the temperatures of 473 to 673 K resulted in hematite. The crystal phase of the precipitated iron-manganese catalyst after the calcination at 675 K and 723 K was reported to be hematite.[23,25] Wang, et al.[44] also identified the fresh catalyst diffraction pattern for a silica-supported iron catalyst as hematite with an average particle

size of 24 nm. Van Dijk, et al.[23] reported that an average diameter of 21 - 25 nm could be estimated for the α-Fe_2O_3 particles in an iron-manganese catalyst. Both pure iron catalysts, that is, YST-1 and FT-1, had an average particle size of 23.9 nm. The similarity for these iron catalysts in terms of the bulk phase and the particle size indicates that these iron catalysts are very much the same. The manganese oxide phase was not identified for the iron-manganese catalysts used in this study due to the low manganese concentration in the catalyst; however, Mn_2O_3 was the crystal phase in the iron-manganese catalysts (Fe/Mn = 100/108 and Fe/Mn = 100/133) according to the data obtained by Maiti, et al.[25] The x-ray diffraction patterns for the reduced iron-manganese catalysts obtained by Jensen and Maiti, et al. all indicated that α-Fe phase and MnO phase were present in the catalyst.[18,25] The particle size of hematite for the calcined iron-manganese catalyst in this study generally became smaller (15 - 24 nm) as the manganese concentration of the catalyst increased. No reasonable explanation in terms of the structural information can be offered; however, the manganese may affect the formation of the hematite particles.

Catalyst Stability Tests for the Iron-Manganese Catalysts

In the long-term catalyst stability test for the pure iron catalyst (YST-1), a period of 12 hours was needed to approach constant carbon monoxide conversion. This gradual approach to the stationary state could be associated with the formation of iron carbide on the catalyst surface.[45] Amelse, et al.[46] reported that a reduced silica-supported iron catalyst gained activity as the carburization took

place under the Fischer-Tropsch synthesis conditions. Raupp, et al.[47-49] also concluded that the extent of iron carbide formation correlated with an increase in the catalyst activity for a magnesium oxide supported iron catalyst. Jensen[18] found from the x-ray diffraction pattern that there were some forms of Hagg carbide (possibly Fe_2C) in addition to α-Fe in the used iron-manganese catalysts after the Fischer-Tropsch synthesis. Reymond, et al.[50] showed that a reduced iron catalyst transformed from a bulk α-Fe structure to a $Fe_{20}C_0$ structure after 10 hours on stream at the Fischer-Tropsch synthesis conditions. Maiti, et al.[25] also found that Fe_5C_2, α-Fe, and Mno were present in the bulk structure of an unsupported iron-manganese catalyst after the Fischer-Tropsch process. Therefore, the increase in carbon monoxide conversion for catalyst YST-1 during the initial 12 hour period was probably a result of iron carbide formation on the catalyst surface. After 12 hours on stream the carbon monoxide conversion stabilized at 5 percent through the end of the run. The stabilization of the activity can be viewed as the establishment of a quasi-steady state with respect to the formation of the coke precursor and the hydrogenation of the coke precursor on the catalyst surface.[51] Many researchers have proposed a mechanism in which three reactions involving the surface carbide, C*, are possible:[52-60]

$$C^* + \text{iron} \longrightarrow \text{carbides} \qquad (19)$$

$$C^* + x\,H^* \longrightarrow CH_x^* \qquad (20)$$

$$C^* + y\,C^* \longrightarrow \text{inactive carbon} \qquad (21)$$

Reaction (19) implies bulk diffusion of carbon into metallic iron. There are at least three forms of carbon in an active iron catalyst according to this theory; namely, bulk carbide, inactive, and surface carbidic carbon. Therefore, the absence of catalyst deactivation for catalyst YST-1 during the course of the stability test up to 35 hours on stream can be attributed to the absence of an inactive carbon overlayer on the surface.[61-63] Van Diji, et al.[23] reported that their iron manganese catalyst (Fe/Mn: 154/100, atomic ratio) deactivated after approximately 2 hours on stream at 513 K and atmospheric pressure at Fischer-Tropsch synthesis conditions. Dry[33] concluded that the formation of carbon on the catalyst surface was dependent on gas composition, pressure, and temperature. The conditions in the work of van Dijk and co-workers might favor the formation of inactive carbon, consequently, the catalyst was rapidly deactivated. Because the experimental conditions for catalyst YST-1 were different from those in the work of van Dijk and co-workers, that is, a temperature of 473 K and a pressure of 1465 kPa, it is possible that the formation of inactive carbon on the surface of catalyst YST-1 was very minimal up to the end of the run.

The product distribution as a function of the time on stream for catalyst YST-1 also indicated that a period of 12 hours was needed to stabilize the catalyst. No satisfactory explanation can be offered for the variation of the product distributions during the stabilization period; however, these phenomena could be a function of the carbon monoxide conversion. Kikuchi, et al.[85] reported that the yields of C_2-C_4 hydrocarbons were a function of the carbon monoxide for a lamellar compound of graphite intercalated by ferric chloride in

the carbon monoxide hydrogenation at the conditions which were a temperature of 673 K, a H_2/CO ratio of 3, a space velocity of 0.7 $cm^3 g^{-1}s^{-1}$, and a total pressure of 2020 kPa. Ott, et al.[65] concluded that their pure iron powder catalyst for the carbon monoxide hydrogenation accepted carbon into the bulk during the initial 24 hours on stream, a-ong with a slow buildup of carbon on the surface at the conditions which were a temperature of 573 K, a pressure of 101 kPa, and a carbon monoxide conversion of less than 3 percent. They reported that the carbide formation resulted in a temporary increase in hydrocarbon synthesis activity as well as changes in the olefin-to-paraffin selectivity. This result may also indicate that the product distribution was affected by the variation of the carbon monoxide conversion in the hydrogenation of carbon monoxide. Arcuri, et al.[66] reported that the olefin-to-paraffin selectivity decreased with increasing carbon monoxide conversion for a silica supported iron catalyst in the carbon monoxide hydrogenation at the conditions which were a total pressure of 1414 kPa, a H_2/CO ratio of 3, and a carbon monoxide conversion range of 1 - 8 percent. This phenomena may also indicate that the product distribution was a function of the carbon monoxide conversion. In this study the product distribution and olefin selectivity ratios for catalyst YST-1 (pure iron) stabilized when the carbon monoxide conversion reached a constant level of 5 percent at 12 hours on stream. Therefore, the product distribution for catalyst YST-1 could also be a function of the carbon monoxide conversion.

The long-term stability test for catalyst YST-2 (3.6 Mn/100 Fe), 39 hours on stream, indicated a similar result as that for

catalyst YST-1. A period of 10 hours was needed to stabilize the activity, the product distribution, and the olefin selectivity and no indication of catalyst deactivation was detected. The same reasons for catalyst YST-1 can also be applied for catalyst YST-2 to explain the variation in the catalyst activity and product distribution during the course of the experiment

The carbon monoxide conversion declined initially from 7.3 to 5.5 percent in a period of 15 hours for catalyst YST-3 (3.5 Mn/100 Fe). The decrease in activity could be due to the formation of an inactive carbon overlayer on the surface.[51] Subsequently, the carbon monoxide conversion stabilized at a level of 5.3 percent up to the end of the run. The fact that the product distribution for catalyst YST-3 reached the stationary state after 12 hours on stream may suggest that the product distribution was still a function of the carbon monoxide conversion. It is possible that the inactive carbon overlayer on the surface of catalyst YST-3 did not affect the production of the carbon products in the carbon monoxide hydrogenation. The behavior of catalyst YST-4 (3.5 Mn/100 Fe) in terms of carbon monoxide conversion and the product distribution was similar to that of catalyst YST-3. The decline in the catalyst activity initially for catalyst YST-4 could be attributed to the formation of the inactive surface carbon overlayer and the product distribution could also be a function of the carbon monoxide conversion.

The nature of the catalyst also plays an important role in determining the product distribution for the carbon monoxide hydrogenation. It is clearly indicated in Table 7 that the presence of manganese in the iron catalyst promoted the olefin selectivity ratio

for the C_2-C_4 hydrocarbon fraction. The olefin-to-paraffin ratios for catalysts YST-2 (3.6 Mn/100 Fe), YST-3 (3.5 Mn/100 Fe), and YST-4 (3.5 Mn/100 Fe), that is, 2.9, 2.7, and 2.6, respectively, were all larger than that for the pure iron catalyst, YST-1, 1.4. The significance of the manganese promotion for the production of C_2-C_4 olefins is in agreement with the previous investigations.[15-17] The carbon dioxide yield for catalyst YST-3, that is, 16.2 percent of the total products, was higher than the carbon dioxide yields for catalysts and YST-2 and YST-4. Madon, et al.[67] proposed that the presence of Fe_3O_4 in a commercial iron catalyst (100 Fe:2.8 Cu:1 K_2CO_3) was responsible for the conversion of carbon monoxide to carbon dioxide via the water-gas-shift reaction in the carbon monoxide hydrogenation at the conditions which were a pressure of 1000 kPa, a H_2/CO ratio of 1.5, a gas hourly space velocity of 250 h^{-1}, and a temperature range of 500 - 520 K. Catalyst YST-3 was very similar to catalysts YST-2 and YST-4 in terms of the catalyst bulk compositions. The higher carbon dioxide yield for catalyst YST-3 could also be due to the higher presence of Fe_3O_4 in the catalyst. This observation indicated that the nature of the catalyst was also important in determining the product distribution for the carbon monoxide hydrogenation. Generally, catalyst YST-2 showed a higher C_2-C_4 hydrocarbon yield of 49.5 percent, a higher olefin-to-paraffin ratio in the C_2-C_4 hydrocarbon fraction, and higher olefin selectivity ratios for C_2, C_3, and C_4 than the other three catalysts. In addition, catalyst YST-2 exhibited a very stable behavior in terms of the catalyst activity and product distribution during the reaction compared to the other three YST catalysts. Therefore, in this study, catalyst YST-2 was considered to

be more selective for the production of C_2-C_4 olefins in the carbon monoxide hydrogenation.

Catalyst Reduction Study

The TGA curves in Figure 16 indicate that the final catalyst weight loss after hydrogen reduction of catalyst YST-2 (3.6 Mn/100 Fe) was 41 percent of the initial catalyst weight and the final catalyst weight after oxidation air corresponded to a weight loss of 22 percent of the initial catalyst weight. It is obvious that the oxidation of the reduced catalyst resulted in a value of the final weight which was approximately equal to the catalyst weight at 573 K in flowing hydrogen. This observation probably indicates that the iron oxide formed by the catalyst oxidation at the temperatures above 673 K is the same as that at 573 K under the hydrogen reduction. Maiti, et al.[25] proposed that the course of the reduction of the coprecipitated oxide mass could be represented as follows:

$$Fe_{2-y}Mn_yO_3 \xrightarrow{< 573\ K} Fe_{3-y}Mn_yO_4 \xrightarrow{> 573\ K} Fe, \quad MnO$$

$(y < 0.1)$

For pure iron oxide the following reduction scheme could be used:

$$\alpha\text{-}Fe_2O_3 \xrightarrow{< 573\ K} Fe_3O_4 \xrightarrow{> 573\ K} Fe\ .$$

Since there were only 3.6 parts of Mn per 100 parts of Fe in the YST-2 catalyst, the reduction scheme for pure iron oxide can be used for the explanation of the TGA curves. The theoretical value for the

weight gain from iron metal to magnetite (Fe_3O_4) as a result of iron oxidation ($3\ Fe \rightarrow Fe_3O_4$) is $(4 \times 16)/(3 \times 56)$, that is, 38.1 percent. According to the data in Figure 16, the weight gain due to the oxidation of reduced iron was $0.19/(1 - 0.41)$, that is, 32.2 percent. Though these two values are not very close, the error between these values is about 16 percent. The possible error could be due to the instrumental operation. Therefore, the speculation is that after the oxidation of the reduced catalyst YST-2 could be in the form of Fe_3O_4. According to the reduction scheme proposed by Maiti, et al.[25] the possible phase for catalyst YST-2 under reducation at 573 K could be Fe_3O_4. The possible oxide form obtained from the oxidation of the reduced catalyst YST-2 at the temperatures above 673 K could also be the magnetite, that is, Fe_3O_4, based on the TGA curves in this study.

The final weight losses under the flowing helium for catalysts YST-1 through YST-4 were 20.0, 13.0, 15.0, and 21.0 percent of the initial catalyst weight (Figure 18). Helium is inert and no reaction occurred between the catalyst and helium even at a temperature of 773 K. Therefore, the final weight loss in helium for these iron-manganese catalysts can be attributed to the total amount of the moisture evaporated from the catalysts. The final weight losses for catalysts YST-1 through YST-4 under hydrogen reduction were 43.0, 41.0, 40.0, and 43.0 percent (of the initial catalyst weight), respectively, according to Figure 17. Since the Mn concentration in the catalyst is very small the oxide form in the calcined catalyst can be assumed as hematite, that is, α-Fe_2O_3. In addition, the phase in the reduced catalyst under flowing hydrogen at 773 K can be considered as pure α-Fe according to the work by Jensen.[18] The complete

reduction of hematite to metallic iron could be represented as follows:

$$Fe_2O_3 + 3\,H_2 \longrightarrow 2\,Fe + 3\,H_2O \ . \qquad (22)$$

Therefore, according to the theoretical calculations the weight loss of hematite for the complete reduction is equal to (16 x 3)/(55.8 x 2 + 16 x 3), that is, 30.0 percent. The following equation was used for the calculation of the iron oxide weight loss for these iron-manganese catalysts:

$$\text{Iron oxide weight loss (\%)} = 1 - \frac{(1 - \text{weight loss under } H_2)}{(1 - \text{weight loss under He})} \times 100 \ . \qquad (23)$$

For catalysts YST-1 through YST-4 the weight losses of iron oxide in the catalyst under hydrogen reduction are computed to be 28.8, 32.0, 29.4, and 27.7 percent, resepctively. Generally, these values are in the range of 30 $\pm$ 2 percent. Therefore, the iron oxide in these iron-manganese catalysts was obviously near complete reduction of hematite to metallic iron under hydrogen pretreatment in this study. The catalyst reduction with flowing hydrogen at 673 K should be sufficient to reduce the iron-manganese catalyst and to activate the catalyst for the Fischer-Tropsch synthesis.

Figure 19 indicates that the final catalyst weight loss for a pure manganese oxide catalyst in helium was only 2.5 percent of the initial catalyst weight and that in hydrogen was 10.0 percent. Maiti, et al.[25] reported that the manganese oxide was a type of Mn_2O_3

according to the x-ray diffraction pattern. They also indicated that the final phase of manganese oxide after the hydrogen reduction was a form of MnO. Therefore, the following equation can be used to represent the transformation:

$$Mn_2O_3 + H_2 \longrightarrow 2\,MnO + H_2O \quad . \qquad (24)$$

Based on the theoretical calculation the total weight loss of Mn_2O_3 in the catalyst is equal to 16/(54.9 x 2 + 3 x 16), that is, 10.1 percent of the initial weight. The following equation can be used to calculate the weight loss of manganese oxide for the pure manganese oxide catalyst:

$$Mn_2O_3 \text{ weight loss (\%)} = 1 - \frac{(1 - \text{weight loss under } H_2)}{(1 - \text{weight loss under He})} \times 100 \quad . \qquad (25)$$

The value for the weight loss of Mn_2O_3 according to the TGA data is 7.7 percent. The MnO phase could be the final form of the manganese oxide in the catalyst under the hydrogen reduction. The presence of MnO in the reduced iron-manganese catalysts was also reported in the literature.[18,23,25]

Influence of Catalyst Bed Dilution

A bench-scale fixed-bed reactor was used in this investigation. Due to the nature of highly exothermic reactions and the characteristics of the poor heat transfer in the catalyst bed, the carbon monoxide conversion for the synthesis has been unusually maintained below 10 percent to minimize the heat effect in the

fixed-bed reactor. If the excess reaction heats can not be efficiently removed from the fixed-bed reactor, these heat effects may cause some hot spots in the reactor and subsequently the desired product yield and the product distribution may also shift. Up to now, only a few articles have been published dealing with the effects of the catalyst dilution;[35,36] however, no paper on the catalyst dilution effects for the Fischer-Tropsch synthesis has been reported.

In this investigation the effects of the catalyst bed dilution in the reactor were obvious. Figure 20 indicates that for a dense-packed fixed-bed reactor a temperature rise of 7 K was observed at a carbon monoxide conversion of 6.7 percent. Figure 25 shows that the temperature rise in the reactor was only 3 K for a diluted fixed-bed reactor with a volumetric ratio of Denstone 57/catalyst of 4/1 at a carbon monoxide conversion of 8.9 percent. The heat effect cannot be eliminated completely with the catalyst bed dilution only; however, the effects on the reduction of the temperature rise are very significant, that is, more than 50 percent. Tai[19] reported that a volumetric ratio of Denstone 57/catalyst of 4/1 was sufficient to decrease the temperature rise in the fixed-bed reactor for the Fischer-Tropsch synthesis. These observations all illustrated the effectiveness of the catalyst bed dilution on the reduction of the temperature rise in the fixed-bed reactor.

The influence of the dilution of the catalyst bed on the product distribution and the olefin selectivity is presented in Table 8. It is evident that the dense-packed catalyst bed resulted in a relatively lower C_2-C_4 olefin yield than other cases of catalyst dilution. Higher yields for carbon dioxide and methane, that is,

15.9 and 22.5 percent, respectively, were also obtained as a result of the dense-packed catalyst bed for the synthesis. The higher heat effects in the catalyst bed for the case of no dilution was probably responsible for higher rates of water-gas shift reaction and the hydrogenation of the primary products. Therefore, a higher CO_2 yield and a lower C_2-C_4 olefin selectivity ratio were observed. A few articles reported that the presence of Fe_3O_4 in the catalyst was responsible for the conversion of carbon monoxide to carbon dioxide.[67,68] Though there was no proof for the presence of Fe_3O_4 in the iron-manganese catalysts during the synthesis in this investigation, the speculation was that higher temperature rise in the dense-packed catalyst bed may increase the formation of magnetite and the carbon dioxide yield in the synthesis.

Two experiments were conducted for a dilution ratio of 4/1 with two different catalyst weights, that is, 4.8 g and 8.0 g. The product distribution and yields for these two tests were almost identical under the same operating conditions. These data clearly indicate that the reproducibility of the catalyst performance is very good (i.e., the difference was 5 percent or less). It is possible that the good reproducibility of the catalyst was attributed to the minimal heat effects influenced by the catalyst bed dilution with a ratio of inert/catalyst of 4/1. The effects of the catalyst bed dilution with a ratio of 4/1 can be presented as follows:

(1) Higher selectivity for C_2-C_4 olefins and lower temperature rise in the catalyst bed;

(2) Good reproducibility for the catalyst performance for the Fischer-Tropsch synthesis.

Influence of Catalyst Pretreatment

The effects of the catalyst pretreatment on the catalyst activity and the product distribution over catalyst YST-2 (3.6 Mn/100 Fe) have been investigated with hydrogen, carbon monoxide, and synthesis gases. Table 9 shows the data on the carbon monoxide conversion and the product distribution as a function of time on stream with the hydrogen reduction at 673 K for 8 hours. The carbon monoxide conversion increased gradually with the time on stream. This result also illustrates that the catalyst gained activity as the carburization took place under the Fischer-Tropsch synthesis conditions.[46-49] The data at 11.5 hours were approximately in a stationary state because the results from the previous stability tests indicated that a period of about 12 hours was needed to reach the constant catalyst activity. When the carbon monoxide conversion increased to 7.2 percent at 13.5 hours on stream, the product distribution was different from that at 3.5 percent carbon monoxide conversion. In addition, the data for the carbon monoxide conversion and the product distribution at 12.6 hours on stream with the hydrogen reduction for 20 hours were very close to those at 13.5 hours with the hydrogen reduction for 8 hours. These results clearly illustrated that the product distribution was a function of the carbon monoxide conversion and the good reproducibility for the catalyst in the carbon monoxide hydrogenation can be obtained by using the hydrogen reduction for only 8 hours instead of 20 hours.

Table 10 lists the results for the catalyst activity and the product distribution as a function of time on stream with the carbon monoxide pretreatment at 673 K for 8 hours. Initially, the catalyst

exhibited a very high activity as indicated by a carbon monoxide conversion of 21.9 percent at 0.5 hours on stream. Since the carbon monoxide gas was used for the catalyst pretreatment, the catalyst was actually activated under the carburization conditions.[46,54] Therefore, some carbidic carbons possibly covered the catalyst surface in addition to the formation of the bulk iron carbides.[50,52,54,56,57] When the catalyst was tested in the carbon monoxide hydrogenation these surface carbidic carbons could be readily converted to the carbon products and subsequently a high carbon monoxide conversion was observed. As the reaction time increased the catalyst activity declined. The decrease in the catalyst activity was probably due to an inactive carbon sublayer on the catalyst surface in the carbon monoxide hydrogenation.[51] The data for the product distribution in this experiment also indicated that the product distribution was a function of the carbon monoxide conversion. The results from the test at 12.3 hours on stream with the carbon monoxide pretreatment for 20 hours were similar to those with the carbon monoxide pretreatment for 8 hours. This good reproducibility proves again that a pretreatment period of 8 hours is sufficient to activate the catalyst for the hydrogenation of carbon monoxide.

The product distribution and the olefin selectivity versus time on stream for the catalyst pretreatment in synthesis gases atmospheres, 1 H_2/1 CO, 2 H_2/1 CO, and 3 H_2/1 CO, are presented in Tables 11, 12, and 13, respectively. The catalyst initially exhibited a high activity, that is, a carbon monoxide conversion of 12.1 percent (1 H_2/1 CO pretreatment). The carbon monoxide conversions for the pretreatment by 2 H_2/1 CO and 3 H_2/1 CO synthesis

gases were also relatively high, that is, 10.5 and 8.7 percent, respectively. This observation was also probably as a result of the formation of active carbidic carbons on the catalyst surface which occurred during the pretreatment with the synthesis gas.[50,52,54,56,57] The results from these experiments also indicated a decline in the catalyst activity as the time on stream increased. An inactive carbon sublayer on the catalyst surface was possibly responsible for this phenomena.[51] The data for the product distribution from these experiments all illustrated that the product distribution was a function of the carbon monoxide conversion.

Table 14 lists the summary for the influence of catalyst pretreatment on the catalyst activity and product distribution at 12 hours on stream under a standard set of operating conditions in the hydrogenation of carbon monoxide over catalyst YST-2 (3.6 Mn/100 Fe). At 483 K the hydrogen pretreatment resulted in lower catalyst activity, that is, a carbon monoxide conversion of 3.5 percent, compared to the carbon monoxide conversions with other methods (e.g., 8.4 percent carbon monoxide conversion with the carbon monoxide pretreatment). The difference in catalyst activity was probably attributed to the extent of the bulk carbide formation and the concentration of the surface active carbon sublayer.[47,49,50,54] The pretreated catalyst with the hydrogen reduction began the carburization only when it was under the carbon monoxide hydrogenation conditions but the catalysts with the carbon monoxide pretreatment (or the synthesis gas pretreatment) became carburized at the beginning of the pretreatment. Reymond, et al.[50] reported that an unreduced α-Fe_2O_3 in the carbon monoxide hydrogenation conditions (atmospheric pressure, H_2/CO =

9/1, 523 K, and a flow of 60 cm^3 min^{-1}) after 1.5 hours on stream showed a pattern of the bulk iron carbide and the formation of surface active carbon. Therefore, it was possible that the extent of the bulk iron carbide and the active surface carbon sublayer for the catalyst with the hydrogen reduction was relativley less than that for the catalyst pretreated with carbon monoxide or synthesis gas even though the catalyst was in the carbon monoxide hydrogenation conditions for 12 hours. The observation of a relatively less active catalyst with the hydrogen reduction was probably attributed to the effects of the catalyst carburization during the pretreatment. However, a decline in the carbon monoxide conversion was observed for all of the catalysts except for the case of hydrogen reduction. The formation of an inactive carbon sublayer was possibly responsible for this result.[51] The influence of the catalyst pretreatment on the product distribution is also shown in Table 14. The product distribution varied case by case; however, the carbon monoxide conversion probably affected the variation. Since different methods of catalyst pretreatment caused different levels of carbon monoxide conversion at 12 hours on stream, the product distribution would be different as a result of the pretreatment effect. Therefore, the product distribution could be a function of the carbon monoxide conversion which may also be influenced by the catalyst pretreatment in the carbon monoxide hydrogenation.

Generally speaking, the catalyst pretreated with hydrogen showed a more stable performance than other catalysts with carbon monoxide or synthesis gas pretreatment because the catalyst activity increased gradually to a stationary state while other catalysts

exhibited a decline in catalyst activity initially. The total amount of carbon dioxide and methane yields for this hydrogen reduced catalyst, that is, 28.1 percent, was generally lower than those for the other catalysts (e.g., 37.5 percent for a catalyst with 2 H_2/1 CO pretreatment). In addition, the C_2-C_4 yield for this hydrogen reduced catalyst, that is, 49.8 percent, was higher than those for the other catalysts (e.g., 44.6 percent for a catalyst with 2 H_2/1 CO pretreatment). Though an olefin-to-paraffin ratio in C_2-C_4 of 2.4 for the hydrogen reduced catalyst was only moderate compared to other cases, the olefin content in the C_2-C_4 hydrocarbons was 70 percent. However, the synthesis gas pretreatment generally gave higher olefin-to-paraffin selectivity ratios for C_2, C_3, and C_4 at 12 hours on stream; 1.3 - 1.4, 10.5 - 12.6, and 8.6 - 13.0, respectively. The speculation was that the hydrogenation rates of the primary products for the catalysts pretreated by the synthesis gas may be less than that for the catalyst pretreated by either hydrogen or carbon monoxide.

Influence of Manganese

Tables 15 through 19 show the activity and the product distribution as a function of time on stream for catalysts FT-1 through FT-5. The carbon monoxide conversion for catalyst FT-1 (pure iron) at 483 K after 3 hours on stream was 9.7 percent; however, it declined slightly to 8.5 percent at 13.5 hours on stream. This small decrease in catalyst activity was probably due to the formation of inactive carbon sublayer on the surface during the carbon monoxide hydrogenation.[51] The product distribution for catalyst FT-1 varied during the course of the experiment. A period of 12 hours on stream should be

sufficient for the stabilization of the catalyst activity and the product distribution based on the conclusions of the stability study. The carbon monoxide conversion at 13.5 hours on stream was 8.5 percent. The carbon monoxide conversion at 7.7 hours on stream was 8.4 percent. The product distribution and olefin selectivity ratios for C_2, C_3, and C_4 for thest two cases were very similar. Therefore, this fact illustrated that the product distribution could also be a function of the carbon monoxide. Generally, for catalysts FT-2 through FT-5 the catalyst activity gained as the time on stream increased. The product distribution also showed a changing pattern during the course of the experiment. After a period of 12 hours on stream the catalyst activity and the product distribution generally reached a stationary state. In Table 16 the data for the carbon monoxide conversion and the product distribution at 12.5 hours and 17.5 hours were very similar. This similariy indicated that a period of 12 hours was sufficient for the stabilization of the catalyst activity and the product distribution again. The product distribution for these iron-manganese catalysts was also a function of the carbon monoxide conversion from the illustration of data in Tables 15 through 19.

Table 20 lists the comparison of the catalyst activity and the product distribution for these FT catalysts in the carbon monoxide hydrogenation conditions at 12 hours on stream. Generally, the pure iron catalyst, catalyst FT-1, was more active than other FT series catalysts in terms of the carbon monoxide conversion. For instance, the carbon monoxide conversion for catalyst FT-1 was 8.5 percent at 483 K but that for catalyst FT-2 was only 6.2 percent even

at 493 K. The olefin-to-paraffin ratio of C_2-C_4 fraction for pure iron catalyst was much less than those for the other manganese promoted catalysts. For example, the C_2-C_4 yield and the olefin-to-paraffin ratio in C_2-C_4 hydrocarbon fraction for catalyst FT-1 were 45.7 percent and 1.6 with a conversion of 8.5 percent; however, the yield and the ratio were 46.1 percent and 4.7 for catalyst FT-2 (2.5 Mn/100 Fe). The olefin selectivity ratios for C_2, C_3, and C_4 for catalyst FT-2 were also higher than those for catalyst FT-1. The influence of manganese on the C_2-C_4 olefin production was significant. Catalyst FT-2 was considered to be a more selective catalyst for the light olefin production than the other FT catalysts based on the following reasons:

(1) the catalyst activity for catalyst FT-2, that is, a carbon monoxide conversion of 6.2 percent at 493 K, was less than that for catalyst FT-1; however, it was moderate compared to those for the other iron-manganese catalysts (e.g., 6.9 percent carbon monoxide conversion for catalyst FT-3 at 504 K);

(2) the C_2-C_4 hydrocarbon yield for catalyst FT-2, that is, 46.1 percent, was generally higher than those for the other FT catalysts, 42 - 43 percent;

(3) the olefin-to-paraffin ratio in C_2-C_4 hydrocarbon fraction for catalyst FT-2, that is, 4.7, was moderate compared to those for the iron-manganese catalysts but it was much higher than that for the pure iron catalyst.

This conclusion is very similar to that in the previous study which stated that a catalyst composed of 2.2 parts of Mn per 100 parts of

Fe was very selective for the C_2-C_4 olefin production in the carbon monoxide hydrogenation.[17,21]

Table 21 lists the amounts of hydrogen and carbon monoxide adsorbed by the FT series catalysts at 292 K. Generally, the carbon monoxide uptake for these catalysts was in the range of 16 - 30 μ mole g^{-1}. The hydrogen uptake generally decreased as the presence of manganese in the catalyst increased except for catalyst FT-2. The amount of carbon monoxide adsorbed by the catalyst was much higher than that of hydrogen. Chemisorption measurements of hydrogen and carbon monoxide over metallic and nonmetallic catalysts have been described extensively in the literature.[69-73] Studies on iron surfaces in the ultra high vacuum system have been relatively few in number due to the difficulty in removing impurities such as oxygen to obtain a clean, well-defined surface.[74] A few articles reported the chemisorption of hydrogen and carbon monoxide over iron,[3,75-80] but the interpretation for these results are often difficult. Therefore, the interpretation of the data on the chemisorption of hydrogen and carbon monoxide in this study is only speculative with regard to the correlation between the catalyst activity and the product distribution, influenced by the effects of manganese, and the hydrogen and carbon monoxide uptakes for these iron-manganese catalysts. The data on specific activity for the FT series iron-manganese catalysts are presented in Table 22. These data were obtained based on the carbon monoxide chemisorption data and assuming an adsorption stoichiometry of Fe/CO = 1. Since the hydrogen uptake at 292 K for these catalysts was relatively low, the hydrogen chemisroption data at 292 K may not be good for the calculations of specific activity. The

adsorption stoichiometry of carbon monoxide on iron surface might be expected to vary between 1 and 2;[69,71,72,75,77,80] however, the assumption of the Fe/CO adsorption stoichiometry of 1/1 in this investigation resulted in reasonable data on turnover frequency for these FT series iron-manganese catalysts. Generally, the range of the furnover frequency for carbon monoxide was 19 - 48 s^{-1} in the temperature range 483 - 504 K. Arakawa and his co-workers[68] reported that the turnover frequency of carbon monoxide was 50.0 x $10^{-3}s^{-1}$ for an alumina supported iron catalyst in the carbon monoxide hydrogenation at the conditions which were a temperature of 533 K, a H_2/CO ratio of 3, and a space velocity of 1.7 $cm^3g^{-1}s^{-1}$ (based on hydrogen adsorption data). Though the FT series iron-manganese catalysts were unsupported and the reaction conditions in this study were different from those in the work of Arakawa and co-workers, the range of turnover frequency for carbon monoxide indicated the data were relatively reasonable based on the Fe/CO adsorption stoichiometry of 1/1.

The decline in the catalyst activity for the carbon monoxide hydrogenation with the increase of manganese presence could be attributed to the ensemble effect and the electronic effect. Ponec, et al.[81] reported that the activity toward the higher hydrocarbon synthesis in the carbon monoxide hydrogenation decreased with the increasing Cu content of the Ni-Cu alloy catalysts. They proposed that it was because of the decrease in the number of ensenbles (of Ni atoms) which could dissociate carbon monoxide. Recently, Barrault, et al.[24,26] also found that the catalyst activity for the supported iron catalysts in the carbon monoxide hydrogenation decreased with the increasing Mn content. They further reported that an ensemble effect,

that is, the interdispersion of iron atoms with manganese oxide, was responsible for the variation of the catalyst activity. Similarly, the variation of the catalyst activity in this study may be also due to the ensemble effect. Since the pattern of α-Fe and MnO were reported to be the main phases in the reduced iron-manganese catalysts,[18] the interdispersion of active iron atoms with manganese oxide could possibly decrease the number of ensembles of iron atoms which can dissociate carbon monoxide and initiate the hydrocarbon synthesis in the carbon monoxide hydrogenation.[46,65,61] In addition, the electronic effect of MnO on iron atoms could also be the cause for the variation of catalyst activity. Dry and co-workers[76,82,83] studied the effects of potassium for the fused iron catalysts in carbon monoxide hydrogenation. Generally, they found that promotion with K_2O increased the heat of carbon monoxide adsorption at low coverage while it decreased the initial heats of hydrogen adsorption. Subsequently, they reported that the coverage of the surface by hydrogen would be expected to be lower and presumably the amount of hydrogen capable of being adsorbed owuld be lower in the presence of carbon monoxide. They reported that the reaction rate in the carbon monoxide hydrogenation was observed to be only first-order dependence on the hydrogen partial pressure. Therefore, they concluded that alkali promotion could result in a decrease in activity for the fused iron catalyst in the carbon monoxide hydrogenation. Benziger, et al.[84] found that the potassium promotion significantly strengthened the adsorption of carbon monoxide but weakened the adsorption of hydrogen. Many authors[3,68] reported that the activity of the iron catalyst declined with further addition of potassium after a maximum

of the synthesis rate was obtained at approximately 0.5 parts of K_2O per 100 parts by weight of Fe. All of these conclusions illustrated the electronic effects of potassium on the adsorption of hydrogen and carbon monoxide which correlate with the catalyst activity. The chemisorption data in Table 21 generally indicate that the presence of manganese in the catalyst for these FT series catalysts was responsible for the increase in the amount of carbon monoxide adsorption per hydrogen atom adsorbed by the catalyst as shown by the CO/H ratio except for catalyst FT-2. If the manganese oxide could exhibit the similar electronic effects as that for potassium oxide, the decline in the catalyst activity due to the manganese presence would be easily understood in the same way. Vannice[77] reported that the carbon monoxide hydrogenation reaction was also an order of 1.1 in the hydrogen partial pressure and an order of -0.1 in the carbon monoxide partial pressure over an alumina supported iron catalyst. Therefore, the rate of the synthesis reaction could be presumably dependent upon the hydrogen partial pressure and then a decrease of the hydrogen coverage would lead to a lower catalyst activity. As for catalyst FT-2 (2.5 Mn/100 Fe) the CO/H ratio decreased as the manganese content increased in the catalyst; however, the decline in activity was also observed. This result indicates that the ensemble effect of manganese oxide might play a more important role for the decline in activity. Generally, the ensemble effect and the electronic effect of manganese oxide on the iron atoms in the catalyst could explain the variation of the catalyst activity.

In this research the manganese presence in the catalyst also enhanced the olefin content in the C_2-C_4 hydrocarbon fraction. The

electronic effect of manganese oxide on iron atoms and the influence of iron crystallite size may be responsible for the increase in the olefin content. The observation that the promotion of potassium oxide in the iron catalyst caused an increase in higher molecular weight of the products and the olefin-to-paraffin ratio was reported by several researchers.[68,76,82,83] They concluded that the enhancement in the olefin-to-paraffin ratio and the decrease in the methane formation were attributed to the increase of carbon monoxide adsorption and the decrease of hydrogen adsorption on the reduced catalyst with the potassium addition. Dry, et al.[76] reported that the promotion of potassium oxide altered the electronic state of the iron atoms by the transfer of electrons from potassium oxide to the metal and increasing electron density on the iron atoms also strengthened the Fe-C bond which increased the probability of chain growth. Therefore, an increase in the heavier hydrocarbon production was expected. The chemisorption data in Table 21 generally indicate that for these FT catalysts the manganese presence in the catalyst was responsible for the increase in the amount of carbon monoxide adsorption per hydrogen atom adsorbed by the catalyst as shown by the CO/H ratio except for catalyst FT-2 (2.5 Mn/100 Fe). If it could be assumed that the electronic effect of the manganese oxide in the FT catalysts would be similar to that of potassium oxide in the iron catalysts, then the observation in this study that the methane yield decreased and the C_2-C_4 olefin content increased may also be due to the effect of manganese oxide on the suppression in the relative concentration of hydrogen and carbon monoxide for the iron atoms. For catalyst FT-2 the decrease in methane yield and the increase in C_2-C_4

olefin content were also observed. Jung, et al.[85] indicated that the iron metal with a smaller particle size caused an increase in C_2-C_3 olefin content in the carbon monoxide hydrogenation over a series of carbon supported iron catalysts at the conditions of 101 kPa, 3 H_2/ 1 CO, and a carbon monoxide conversion range of 2.5 - 5 percent. Table 2 indicates that the particle size of α-Fe_2O_3 decreased as the manganese presence in the catalyst increased. If it could be assumed that the particle size of α-Fe in the reduced catalyst also became smaller as the manganese presence in the catalyst increased, then the effect of particle size would be primarily responsible for the increase in C_2-C_4 olefin content and the decrease in methane yield. The increase in C_5^+ yield with the addition of manganese for these iron-manganese catalysts might also be attributed to the electronic effect of manganese oxide on iron atoms which is similar to that of potassium oxide for the fused iron catalysts.

CONCLUSIONS

The hydrogenation of carbon monoxide for the production of C_2-C_4 olefins has been investigated over precipitated iron-manganese catalysts. The following conclusions are drawn from the results of this investigation:

(1) The coprecipitation catalyst preparation procedure, in which concentrated ammonium hydroxide as added to a homogeneous mixture of iron and manganese nitrates, was reproducible in terms of preparing iron-manganese catalysts of the same manganese/iron atomic ratio.

(2) The major bulk phase for the calcined iron-manganese catalysts was hematite (α-Fe_2O_3). The average particle size of hematite decreased as the manganese concentration in the catalyst increased. No manganese oxide phase was identified in the catalyst. The average particle sizes of hematite for these iron-manganese catalysts were generally in the range of 15 - 24 nm.

(3) In the long-term tests under the Fischer-Tropsch synthesis conditions for the iron-manganese catalysts, no sign of catalyst deactivation was detected for up to 40 hours on stream. Generally, a period of 12 hours was needed to stabilize the activity, as measured by the conversion of carbon monoxide, the olefin selectivity, as reflected by the olefin/paraffin ratio of the C_2-C_4 hydrocarbon fraction, and the olefin/paraffin ratio of individual C_2, C_3,

and C_4 hydrocarbons, and the product distribution, as reflected by the yields of methane, C_2-C_4 hydrocarbons, C_5^+ hydrocarbons, alcohols, and carbon dioxide, for these catalysts.

(4) The thermogravimetric analysis (TGA) for the iron-manganese catalysts indicated that a catalyst reduction in flowing hydrogen at 673 K and at the ambient pressure for 8 hours was sufficient to reduce the catalyst and to activate it for carbon monoxide hydrogenation.

(5) A volumetric ratio of Denstone 57/catalyst of 4/1 for the catalyst bed dilution in the fixed-bed reactor decreased the heat effects in the catalyst bed. Generally, this dilution ratio also resulted in higher yield for C_2-C_4 hydrocarbons, higher olefin content in the C_2-C_4 hydrocarbon fraction, and lower yields for carbon and methane. The good reproducibility for the catalyst activity and the product distribution was also observed with this dilution ratio of 4/1.

(6) The catalyst pretreatment study with hydrogen, carbon monoxide, and synthesis gas indicated that the hydrogen reduction at 673 K for 8 hours generally resulted in a more stable catalyst activity for the carbon monoxide hydrogenation. Higher yield for C_2-C_4 hydrocarbons and lower production of carbon dioxide and methane were also attributed to the hydrogen pretreatment.

(7) The presence of manganese in the iron catalysts generally decreased the catalyst activity in terms of the carbon monoxide conversion. The C_2-C_4 content in the C_2-C_4 hydrocarbon fraction greatly enhanced as the manganese presence in the catalysts increased. An iron-manganese catalyst with an atomic ratio of Mn/Fe of 2.5/100

was selective for the production of C_2-C_4 olefins in the carbon monoxide hydrogenation.

(8) In the selective chemisorption study the carbon monoxide uptake for these iron-manganese catalysts was higher than the hydrogen uptake. In addition, the increase of the manganese presence in the catalyst generally resulted in higher carbon monoxide uptake per hydrogen atom adsorbed by the catalyst.

(9) The decrease in the catalyst activity for the Fischer-Tropsch synthesis with the manganese concentration in the iron catalyst could be attributed to the ensemble effect or the electronic effect of manganese oxide on iron atoms. The increase in the olefin content in the C_2-C_4 hydrocarbon fraction could also be due to the electronic effect of manganese oxide on iron atoms or the decrease of the particle size of α-Fe.

REFERENCES

1. Fischer, F. and Tropsch, H., Brennst.-Chem., (1923), 4, 276.

2. Storch, H. H., Golumbi, N. and Anderson, R. B., The Fischer-Tropsch and Related Syntheses, John Wiley and Sons, Inc., New York, 1951.

3. Anderson, R. B., Catalysis, Vol. 4, Ch. 1-3, (P. H. Emmett, Ed.), Reinhold, New York (1956).

4. Dry, M. E., "The Fischer-Tropsch Synthesis," Catalysis, Vol. 1, (Anderson, J. R. and Boudart, M. Ed.), Springer-Verlag, New York, 1981, Ch. 4.

5. Dry, M. E., "Sasol's Fischer-Tropsch Experience," Hydrocarbon Processing, (1982), 61 (8), 121.

6. Waddams, A. L., Chemicals from Petroleum, 3rd ed., John Wiley and Sons, Inc., New York, 1973.

7. Frohning, C. D. and Cornils, B., "Chemical Feedstocks from Coal," Hydrocarbon Processing, (1974), 53 (11), 143.

8. Bussemeier, B., Frohning, C. D. and Cornils, B., "Lower Olefins via Fischer-Tropsch," Hydrocarbon Processing, (1976), 55 (11), 101.

9. Zaman Khan, M. K., Yang, C. H. and Oblad, A. G., "The Synthesis of Light Hydrocarbons from CO and Hydrogen Mixtures over Selected Metal Catalysts," Paper presented in Fuel Chemistry Division, 173rd ACS National Meeting, New Orleans, March, 1977.

10. Kolbel, H. and Tillmetz, K. D., German Patent 2507647.

11. Kolbel, H., Ralek, M. and Tillmetz, K. D., "Feedstock for Chemical Industry by Selective Fischer-Tropsch Synthesis," Proc. 15th Intersociety Energy Conversion Engineering Conference, Society of Automot, Engineers, San Diego, California, 1978.

12. Dent, A. L. and Lin, M., "Cobalt-Based Catalysts for the Production of C_2-C_4 Hydrocarbons from Syn-Gas," Paper presented in Petroleum Chemistry Division, 175th ACS National Meeting, Anaheim, March, 1978.

13. Rao, V. U. S. and Bormley, R. J., "Make Olefins from Syn Gas," Hydrocarbon Processing, (1980), 59 (11), 139.

14. Murchison, C. B. and Murdick, D. A., "Use Syngas for Olefin Feedstock," Hydrocarbon Processing, (1981), 60 (1), 159.

15. Yang, C. H. and Oblad, A. G., "Catalytic Synthesis of Light Olefinic Hydrocarbons from CO and Hydrogen over Some Iron Catalysts," Paper presented in Petroleum Chemistry Division, 175th ACS National Meeting, Anaheim, March, 1978.

16. Yang, C. H., "Catalytic Synthesis of Light Hydrocarbons from Carbon Monoxide/Hydrogen over Metal Catalysts," Ph.D. Dissertation, University of Utah, Salt Lake City, Utah, 1979.

17. Tsai, Y. S., "The Hydrogenation of Carbon Monoxide over Unsupported Manganese/Iron Catalysts to Produce Low-Molecular Weight Olefins," M.S. Thesis, University of Utah, Salt Lake City, Utah, 1980.

18. Jensen, K. B., "Characterization of Iron-Manganese Oxide Carbon Monoxide Hydrogenation Catalysts," Ph.D. Dissertation, University of Utah, Salt Lake City, Utah, 1982.

19. Tai, W. P., "The Hydrogenation of Carbon Monoxide over Coprecipitated Iron-Manganese Catalysts in a Pseudo Slurry Reactor," Ph.D. Dissertation, University of Utah, Salt Lake City, Utah, 1983.

20. Kim, C. S., "Carbon Monoxide Hydrogenation over Raney Iron Catalysts," Ph.D. Dissertation, University of Utah, Salt Lake City, Utah, 1983.

21. Tsai, Y. S., Hanson, F. V., Oblad, A. G. and Yang, C. H., "The Hydrogenation of Carbon Monoxide over Unsupported Iron-Manganese Catalysts for the Production of Low-Molecular Weight Olefins," Paper presented in Fuel Chemistry Division, 176th ACS National Meeting, Houston, March, 1980.

22. Chen, K. R., "The Hydrogenation of Carbon Monoxide over Raney Iron-Manganese Catalysts," M.S. Thesis, University of Utah, Salt Lake City, Utah, 1984.

23. Van Dijk, W. L., Niemantsverdriet, J. W., Van Der Kraan, A. M. and Van Der Baan, H. S., "Effects of Manganese Oxide and Sulphate on the Olefin Selectivity of Iron Catalysts in the Fischer-Tropsch Reaction," Applied Catalysis (1982), 2, 273-288.

24. Barrault, J., Forquy, C. and Perrichon, V., "Effects of Manganese Oxide and Sulphate on Olefin Selectivity of Iron Supported Catalysts in the Fischer-Tropsch Reaction," Applied Catalysis, (1983), 5, 119-125.

25. Barrault, J., "Selective Hydrogenation of Carbon Monoxide on Supported Iron or Cobalt Catalysts; Effects of Manganese Oxide and (or) Chloride," in "Metal-Support and Metal-Additive Effects in Catalysis," Imelik, B. et al. Ed., Elsevier Scientific Publishing Company, Amsterdam, 1982, 225-231.

27. Satterfield, C. N., Huff, G. A., Jr. and Longwell, J. P.," Product Distribution from Iron Catalysts in Fischer-Tropsch Slurry Reactors," Ind. Eng. Chem., Proc. Des. Dev., (1982), 21 (3), 465-470.

28. Satterfield, C. N. and Stenger, H. G., "Fischer-Tropsch Synthesis on a Precipitated Mn/Fe Catalyst in a Well-Mixed Slurry Reactor," Ind. Eng. Chem., Proc. Des. Dev., (1984), 23 (1), 26-29.

29. Deckwer, W. D., Serpemen, Y., Ralek, M. and Sc-midt, B., "Fischer-Tropsch Synthesis in the Slurry Phase on Mn/Fe Catalysts," Ind. Eng. Chem., Proc. Des. Dev., (1982), 21 (2), 222.

30. Vannice, M. A., "The Catalytic Synthesis of Hydrocarbons from Carbon Monoxide and Hydrogen," Catal. Rev. - Sci. Eng., 14 (2), Marcel-Dekker, 1976, 153-191.

31. Kolbel, H. and Ralek, M., "The Fischer-Tropsch Synthesis in the Liquid Phase," Catal. Rev. - Sci. Eng., 21 (2), Marcel-Dekker, 1980, 225-274.

32. Anderson, R. B., "Nitrided Iron Catalysts for the Fischer-Tropsch Synthesis in the Eighties," Catal. Rev. - Sci. Eng., 21 (1), Marcel-Dekker, 1980, 53-71.

33. Dry, M. E., "Advances in Fischer-Tropsch Chemistry," Ind. Eng. Chem., Prod. Res. Dev., (1976), 15 (4), 282.

34. Baird, M. J., Schehl, R. R. and Haynes, W. P., "Fischer-Tropsch Processes Investigated at the Pittsburgh Energy Tec-nology Center Since 1944," Ind. Eng. Chem., Prod. Res. Dev., (1980), 19 (2), 175-191.

35. Caldwell, A. D. and Calderbank, P. H., "Catalyst Dilution - A Means of Temperature Control in Packed Tubular Reactors," Reaction Engineering, (1969), 14 (9), 1199-1201.

36. Van Den Bleek, C. M., Van Der Wiele, K. and Van Den Berg, P. J., "The Effects of Dilution on the Degree of Conversion in Fixed-Bed Catalyst Reactors," Chem. Eng. Sci., (1969), 24, 681-694.

37. Yokoyama, A., Komiyama, H., Inoue, H., Masumoto, T. and Kimura, H. M., "The Hydrogenation of Carbon Monoxide by Amorphous Ribbons," J. of Catalysis, (1981), 68, 355-361.

38. Borghard, W. G. and Bennett, C. O., "Evaluation of Commercial Catalysts for the Fischer-Tropsch Reaction," Ind. Eng. Chem., Prod. Res. Dev., (1979), 18 (1), 18.

39. Atwood, H. E. and Bennett, C. O., "Kinetics of the Fischer-Tropsch Reaction over Iron," Ind. Eng. Chem., Proc. Des. Dev., (1979), 18 (1), 163.

40. Kolbel, H. and Tillmetz, K. D., "Model Studies of the Interaction of CO and H_2 on Transition Metals, II. On the Role of Chemisorption Complex in Primary Reactions," J. Catalysis, (1974), 34, 307.

41. Sorum, C. H. and Legowski, J. J., Introduction to Semi-Micro Qualitative Analysis, 5th ed., Prentice-Hall, Inc., 1977.

42. Hanson, F. V., "The Reaction Between H_2 and O_2 over Supported Platinum Catalysts," Ph.D. Dissertation, Stanford University, Stanford, California, 1976.

43. Hofer, L. J. E., Catalysis, Vol. 4, Ch. 4, (P. H. Emmett, Ed.), Reinhold, New York (1956).

44. Wang, C. J. and Ekerdt, J. G., "Study of Fischer-Tropsch Synthesis over Fe/SiO_2: Reactive Scavenging with Pyridine and Cyclohexene," J. of Catalysis, (1983), 80, 172-187.

45. Biloen, P. and Sachtler, W. M. H., "Mechanism of Hydrocarbon Synthesis over Fischer-Tropsch Catalysts," Advances in Catalysis, 30, Academic Press, 1981, 165-216.

46. Amelse, J. A., Butt, J. B. and Schwartz, L. H., "Carburization of Supported Iron Synthesis Catalysts," J. of Phy. Chem., (1978), 82 (5), 558.

47. Raupp, G. B. and Delgass, W. N., "Mossbauer Investigation of Supported Fe and FeNi Catalysts: I. Effects of Petroleum Pretreatment on Particle Size," J. of Catalysis, (1979), 58, 337-347.

48. Raupp, G. B. and Delgass, W. N., "Mossbauer Investigation of Supported Fe and FeNi Catalysts: II. Carbides Formed by Fischer-Tropsch Synthesis," J. of Catalysis, (1979), 58, 348-360.

49. Raupp, G. B. and Delgass, W. N., "Mossbauer Investigation of Supported Catalysts: III. In-Situ Kinetics and Spectroscopy during Fischer-Tropsch Synthesis," J. of Catalysis, (1979), 58, 361-369.

50. Reymond, J. P., Meriaudean, P. and Teichner, S. J., "Changes in the Surface Structure and Composition of an Iron Catalyst of Reduced or Unreduced Fe_2O_3 during the Reaction of Carbon Monoxide and Hydrogen," J. of Catalysis, (1982), 75, 39-48.

51. Butt, J. B., Schwartz, L. H., Baerns, M. and Malessa, R., "Comparison of Activity and Selectivity Maintenance for Supported Fe and FeCO Fischer-Tropsch Catalysts," Ind. Eng. Chem., Prod. Res. Dev., (1984), 23 (1), 51-56.

52. Rofer-DePoorter, C. K., "A Comprehensive Mechanism for the Fischer-Tropsch Synthesis," Chem. Rev., (1981), 81 (5), 447-474.

53. Ponec, V., "Some Aspects of the Mechanism of Methanation and Fischer-Tropsch Synthesis," Catal. Rev. - Sci. Eng., 18 (1), Marcel-Dekker, 1978, 151-171.

54. Matsumoto, H. and Bennett, C. O., "The Transient Method Applied to the Methanation and Fischer-Tropsch Reactions over a Fused Iron Catalyst," J. of Catalysis, (1978), 53, 331-344.

55. Reymond, J. P., Meriaudean, P., Pommier, B. and Bennett, C. O., "Further Results on the Reaction of H_2/CO on Fused Iron by Transient Method," J. of Catalysis, (1980), 64, 163-172.

56. Bianchi, D., Tau, L. M. and Bennett, C. O., "Nature of Surface Species on Supported Iron during CO/H_2 Reaction," J. of Catalysis, (1983), 84, 358-374.

57. Kieffer, E. P. and van der Baan, H. S., "Reactivity of Carbonaceous Species Deposited on Precipitated Iron Catalyst by Carbon Monoxide and Synthesis Gas," Applied Catalysis, (1982), 3, 245.

58. Niemantsverdriet, J. W. and van der Kraan, A. M., "On the Time-Dependent Behavior of Iron Catalysts in Fischer-Tropsch Synthesis," J. of Catalysis, (1981), 72, 385-388.

59. Unmuth, E. E., Schwartz, L. H. and Butt, J. B., "Iron Alloy Fischer-Tropsch Catalysts; II. Carburization Studies of the Fe-Ni System," J. of Catalysis, (1980), 63, 404-414.

60. Erley, W., McBreen, P. H. and Ibach, H., "Evidence for CH_x Surface Species after the Hydrogenation of CO over an Fe(110) Single Crystal Surface," J. of Catalysis, (1983), 84, 229-234.

61. Ponec, V. and van Barneveld, W. A., "The Role of Chemisorption in Fischer-Tropsch Synthesis," Ind. Eng. Chem., Prod. Res. Dev., (1979), 18 (4), 268-271.

62. Dwyer, D. J. and Somorjai, G. A., "Hydrogenation of CO and CO_2 over Iron Foils; Correlation of Rate, Product Distribution and Surface Compositions," J. of Catalysis, (1978), 52, 291-301

63. Niemantsverdriet, J. W., van der Kraan, A. M., van Dijk, W. L. and van der Baan, H. S., "Behavior of Metallic Iron Catalysts during Fischer-Tropsch Synthesis studied with Mossbauer Spectroscopy, X-ray Diffraction, Carbon Content Determination and Reaction Kinetic Measurements," J. of Phy. Chem., (1980), 84 (25), 3363-3370.

64. Kikuchi, E., Ino, T. and Morita, Y., "Catalytic Synthesis of Hydrocarbons from Carbon Monoxide and Hydrogen on Lamellar -Compound of Graphite Intercalated by Ferric Chloride," J. of Catalysis, (1979), 57, 27-34.

65. Ott, G. L., Fleisch, T. and Delgass, W. N., "Carbon Deposition and Activity Changes over FeRu Alloys during Fischer-Tropsch Synthesis," J. of Catalysis, (1980), 65, 253-262.

66. Arcuri, K. B., Schwartz, L. H., Piotrowski, R. D. and Butt, J. B., "Iron Alloy Fischer-Tropsch Catalysts; IV. Reaction and Selectivity Studies of the FeCO System," J. of Catalysis, (1984), 85, 349-361.

67. Madon, R. J. and Taylor, W. F., "Fischer-Tropsch Synthesis on a Precipitated Iron Catalyst," J. of Catalysis, (1981), 69, 32.

68. Arakawa, H. and Bell, A. T., "Effects of Potassium Promotion on the Activity and Selectivity of Iron Fischer-Tropsch Catalysts," Ind. Eng. Chem., Proc. Des. Dev., (1983), 22 (1), 97-103.

69. Anderson, J. R., Structure of Metallic Catalysts, Academic Press, New York, 1975, Ch. 6.

70. Thomas, J. M. and Thomas, W. J., Introduction to the Principles of Heterogeneous Catalysis, Academic Press, New York, 1967.

71. Hayward, D. O. and Trapnell, B. M. W., Chemisorption, 2nd ed., Butterworth & Co., London, 1964.

72. Satterfield, C. N., Heterogeneous Catalysis in Practice, McGraw-Hill Book Company, New York, 1980.

73. Hightower, J. W. (Coordinator), A Five-Day Intensive Short Course on the Use of Heterogeneous Catalysts, Rice University, Houston, 1975,

74. Vannice, M. A., "Catalytic Activation of Carbon Monoxide on Metal Surfaces," Catalysis, Vol. 3, (Anderson, J. R. and Boudart, M. Ed.), Springer-Verlag, New York, 1982, Ch. 3.

75. Parkash, S., Kretschmer, H. O1 and Chakrabartty, S. K., "Sorptive and Activity Behavior of Iron Minerals for Hydrocarbon Synthesis," Fuel Processing Technology, (1981), 4, 31-41.

76. Dry, M. E., Shingles, T., Boshoff, L. J. and Oosthuizen, G. L., "Heats of Chemisorption on Promoted Iron Surfaces and the Role of Alkali in Fischer-Tropsch Synthesis," J. of Catalysis, (1969), 15, 190.

77. Vannice, M. A., "The Catalytic Synthesis of Hydrocarbons from H_2/CO Mixtures over Group VIII Metals; I. The Specific Activities and Product Distribution of Supported Metals," J. of Catalysis, (1975), 37, 449-461.

78. Subramanyam, K. and Rao, M. R. A., "Adsorption of Hydrogen and Carbon Monoxide and Their Mixtures on Iron Fischer-Tropsch Catalysts; I. Synthesis Experiments and Adsorption Studies with Hydrogen and Carbon Monoxide on Promoted and Unpromoted Iron Catalysts," J. Res. Inst. Catalysis, Hokkaido University, (1970), 18 (3), 115-123.

79. Subramanyam, K. and Rao, M. R. A., "Adsorption of Hydrogen and Carbon Monoxide and Their Mixtures on Iron Fischer-Tropsch Catalysts; II. Adsorption from Mixtures of Hydrogen and Carbon Monoxide on Promoted and Unpromoted Iron Catalysts," J. Res. Inst. Catalysis, Hokkaido University, (1970), 18 (3), 124-141.

80. Vannice, M. A. and Garten, R. L., "The Synthesis of Hydrocarbons from CO and H_2 over Well-Characterized Supported PtFe Catalysts," J. of Molecular Catalysis, (1976), 1, 201-222.

81. Ponec, V. and van Barneveld, W. A., "Influence of Alloying on the Selectivity in Fischer-Tropsch Synthesis by Nickel-Copper Alloys," J. of Catalysis, (1978), 51, 426-430.

82. Dry, M. E. and Oosthuzen, G. J., "The Correlation Between Catalyst Surface Basicity and Hydrocarbon Selectivity in the Fischer-Tropsch Synthesis," J. of Catalysis, (1968), 14, 18-24.

83. Dry, M. E., Shingles, T. and Boshoff, L. J., "Rate of the Fischer-Tropsch Reaction over Iron Catalysts," J. of Catalysis, (1972), 25, 99-104.

84. Benziger, J. and Madix, R. J., "The Effects of Carbon, Oxygen, Sulfur and Potassium Adlayers on CO and H_2 Adsorption on Fe(100)," Surface Science, (1980), 94, 119-153.

85. Jung, H. J., Walker, P. L., Jr. and Vannice, M. A., "CO Hydrogenation over Well-Dispersed Carbon-Supported Iron Catalysts," J. of Catalysis, (1982), 75, 416-422.

86. Dietz, W. A., "Response Factors for Gas Chromotographic Analyses," J. of Gas Chromatography, (1967), 5 (2), 68-71.

U.S. GOVERNMENT PRINTING OFFICE: 1986-631-076/20042